THE UNIVERSITY of EDINBURGH

MEng Mechanical Engineering

Levitation Design of a Hyperloop Pod

by

Paul Dewhurst

2024

Declaration

This project report is submitted in partial fulfilment of the requirements for the degree of MEng Mechanical Engineering. I declare that this thesis was composed by myself, and that it has not been submitted, in whole or in part, for any other degree or professional qualification.

Paul Dewhurst

This thesis was conducted under the supervision of Prof Markus Mueller.

Personal Statement

I lead the development of a novel levitation system for a Hyperloop pod, a venture that propelled our team into uncharted territories. Diverging from HYPED's focus on conventional suspension mechanisms, I was tasked with leading the inception, design, and execution of a cutting-edge levitation module.

Approaching this challenge, I initiated a comprehensive analysis of existing pod designs and levitation technologies, identifying solutions that align with scalability and low power consumption requirements. Collaborative discussions with Prof. Markus Mueller provided a framework for refining theoretical models and strategies for validation. My leadership involved managing a team dedicated to simulations, CAD design, and the integration of a cohesive system, with valuable input from the propulsion head, technical directors, and controls group.

The project's theoretical foundation was based on established models, adapted to our design needs. This adaptation required validation through experimental testing, for which I designed and constructed a test rig, conducting risk assessments and managing material procurement independently. The challenges of navigating risk assessment approvals and managing workload were met with strategic planning and resilience, leading to the successful validation of our design.

This experience has significantly honed my software skills, leadership capabilities, and analytical thinking. It underscored the importance of balancing theoretical predictions with experimental data in design iteration, shaping my approach to engineering problem-solving.

Reflecting on this journey, the project stands as a testament to the collaborative effort and innovation at the heart of HYPED's pursuit of advanced transportation technologies. It has been a pivotal chapter in my academic and professional development, laying the groundwork for future advancements in levitation technology.

Abstract

This thesis investigates the design of a levitation system for a Hyperloop pod, undertaken in collaboration with the HYPED society at the University of Edinburgh. It critically examines various levitation techniques to select the most suitable design for the Hyperloop's high-speed requirements. Through the application of electromagnetic theory and mathematical modeling, the study ensures the selected design offers not only feasibility in levitation but also optimisation for energy efficiency. Theoretical simulations and experimental data collectively validate the practical viability of the design. This comprehensive approach ensures the levitation system is both effective and efficient, contributing to the advancement of Hyperloop technology.

Dedication

To my team members, Fadzrul, Sean, and Tyler, whose collaboration and dedication were instrumental in navigating the complexities of our project. To Tinius and Daniel for their unwavering support and guidance, and to Filip, not just a technical director but a flatmate and close friend too. To An, for her endless patience and for listening to my countless rants about the project. A thanks to Vai, Marco, Rory, and all their sub team members for their contributions.

My deepest gratitude to Markus, my supervisor, for his guidance and support through the challenges.

To the University staff - Tom, Calum, Andrew and Chris for there continued support in the labs.

To all at HYPED, for being willing to take on the additional challenge within each sub team in order to facilitate the design.

To my father, whose resilience and courage through his battle with cancer have been a beacon of strength for me throughout this year. And to rest of my family and friends, who have provided unwavering support through it all - thank you.

Summary of Resources

MEng budget provided by the School of Engineering of £150 has been supplemented by HYPED's budget. A deal was agreed with HYPED to cover the entire cost of the test setup in exchange for the MEng budget. Total spent on the test setup is approximately £220. Of this £98 was used to order components while the other £122 was given to HYPED in exchange for copper wire and Bosch material owned by the society. Additionally a load cell was borrowed from the school and returned after use.

An allotted 3 hours of technician time for MEng projects was utilised in order to aid in experimental setup (load cell) and meetings to discuss procedure.

Contents

List of Figures

Abbreviations

EHW European Hyperloop Week.

FEMM Finite Element Method Magnetics.

HEMS Hybrid Electromagnetic Suspension.

Note: Author abbreviations are shown in their corresponding reference entry.

Nomenclature

aiaostyle

A Cross-sectional area of the coil.

B Magnetic flux density.

E Electric field strength.

EMF Electromotive force.

ϵ_0 Permittivity of free space.

F Lorentz force acting on charged particles in an electromagnetic field.

F_{mag} Magnetic force in electromagnetic suspension.

g Gap between the coil and the levitated object.

H Magnetic field strength.

I Electric current.

J Current density.

L Inductance of an electromagnet.

μ_0 Permeability of free space.

N Number of turns in the coil of an electromagnet.

Φ Magnetic flux.

q Charge of a particle in an electromagnetic field.

RN Reluctance Networks, a method for analyzing magnetic circuits.

S Total reluctance of a magnetic path.

v Velocity of a charged particle in an electromagnetic field.

nounits

Word Count Summary

Chapter	Word Count
Introduction	619
Literature Review	2139
Initial Design	2346
Mathematical Modelling & Simulations	1356
Experimental Design	512
Results & Analysis	1897
Final Design	646
Conclusion	395
Total	9910

Summary of word counts by chapter.

Chapter 1

Introduction

1.1 Context & Motivation

In a rapidly evolving world, the demand for transformative transportation solutions becomes increasingly critical. The pressing challenge of sustainability looms large as traditional modes of transport, notorious for their substantial carbon footprints, continue to exacerbate climate change and environmental degradation. To address this, a shift towards more sustainable transportation solutions is imperative.

Innovative solutions could include further development of high-speed rail, or the emergence of the hyperloop concept, involving pods travelling along vacuum tubes at high speeds [7]. HYPED, the University of Edinburgh's Hyperloop society, was formed in 2015 and has co-founded the European Hyperloop Week (EHW), a significant international event bringing together student teams to advance hyperloop technology [8]. In July 2024, the fourth edition of EHW will take place in Zurich, featuring HYPED's pod.

1.2 Aims & Objectives

The aim of this project is to design a levitation system which can be integrated into the pod. Previously a standard suspension has been used and a levitation method has never been implemented for the past pods. HYPED wants to include a levitation system that is power efficient and scales well for real world applications.

The following objectives have been set for this project:

- **Achieve a design that is power efficient by optimising layout and parameters.** This depends on both the method of levitation and design parameters such as nominal air gap.
- **Develop a mathematical model to describe the system.** Force estimates need to be accurate for both safety and to ensure the design will indeed levitate.
- **Perform simulations and adapt the design accordingly.** Another method for force estimations to ensure safety and functionality.
- **Develop a test to gather experimental data that can be used to validate the design.** The forces obtained both from the mathematical model and the simulations should align with experimental data to ensure it is valid.
- **Achieve a final design for the Levitation Module.** This would be a design that is ready for manufacturing.
- **Achieve a final report detailing my project and progress to these objectives.**

1.3 Project Planning

1.3.1 HYPED Society Structure

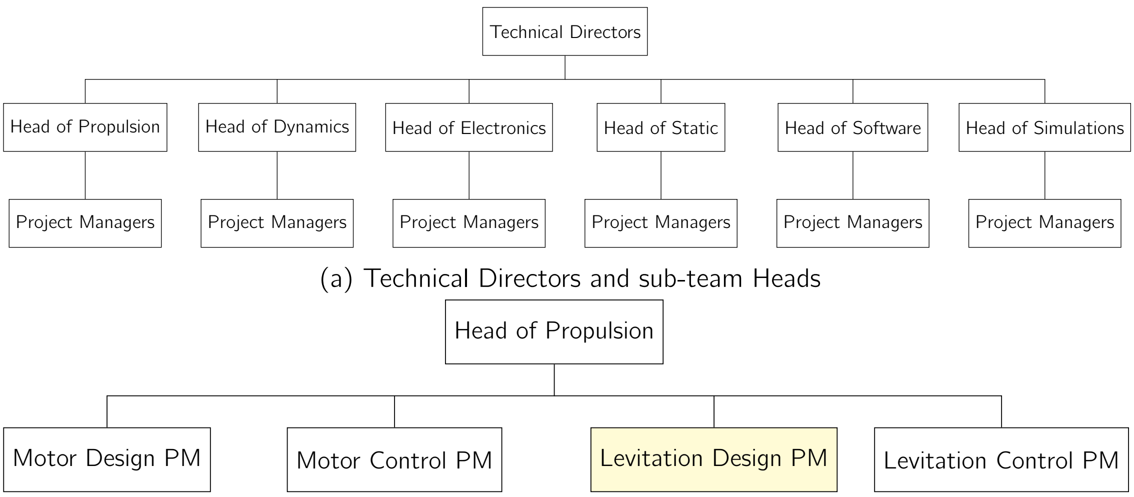

(a) Technical Directors and sub-team Heads

(b) Propulsion sub-team

Figure 1.1: HYPED Society Structure

The HYPED society has a hierarchical structure, at the top are the technical directors, with the Heads of each team underneath. Each Team Head has project mangers which in turn has standard members working for them. Each project manager is responsible for a project. This project is an overview of Levitation Design (ie simulations for air-gap and design layout).

1.3.2 Project Split

The task of designing the levitation system for HYPED is a large undertaking requiring knowledge from multiple disciplines from software to structural. It was crucial to divide the workload effectively among team members.
Figure 1.2 shows the division of levitation system responsibilities among society managers, each leading a student team to fulfill specific tasks. The three main parts of the levitation system are: physical design, control systems, and electronic hardware.

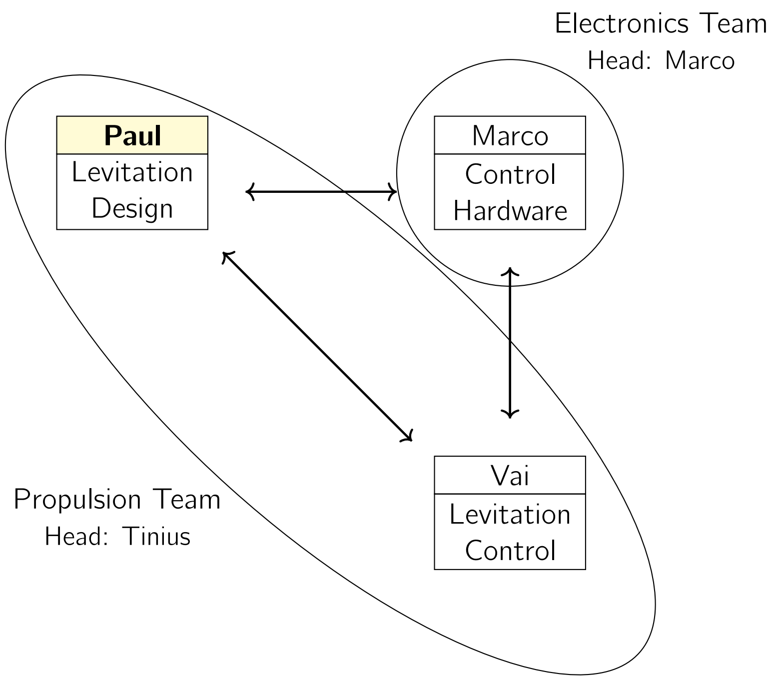

Figure 1.2: Levitation Development Team Split

1.3.3 Timeline

The timeline (figure 1.3) shows the expected schedule for the project. Though everything was finished before the deadline for the thesis submission, there were large delays especially with testing. This mainly involved getting a Risk Assessment approved for use of string permanent magnets. It should be noted due to the tight deadlines within HYPED and how it would affect the entire society this project has been in the works since early July.

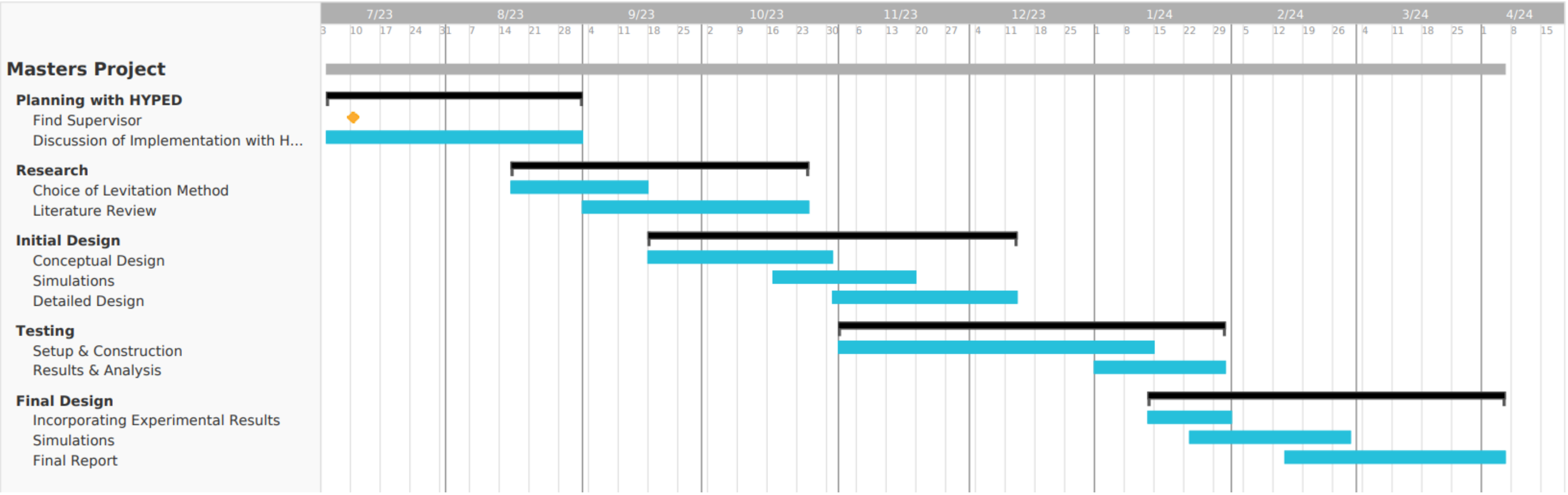

Figure 1.3: Gantt Chart for Project

Chapter 2

Literature Review

2.1 Electromagnetism

Electromagnetism forms the theoretical backbone of various levitation techniques used in modern engineering. This section outlines the core principles of electrodynamics and their application to levitation methods, emphasising the equations that govern these phenomena [9].

2.1.1 Definitions

Magnetic Flux (Φ) is the measure of the quantity of magnetism, considering the strength and extent of a magnetic field. The flux through a surface is proportional to the number of magnetic field lines passing through that surface, measured in Weber (Wb) [10].

MagnetoMotive Force (MMF) is the force that drives magnetic flux through a magnetic circuit. It is analogous to electromotive force in an electrical circuit, causing the flow of magnetic flux [11].

Flux Density (B) represents the amount of magnetic flux through a unit area perpendicular to the direction of magnetic flow, measured in Tesla (T) [12].

Magnetic Field Strength (H) is a measure of the magnetizing force required to create a certain magnetic field in a material, measured in A/m (Ampere per meter) [13].

Permeability (μ) is the measure of a material's ability to support the formation of a magnetic field within itself, hence the ease with which a material can be magnetised [14].

Inductance (L) quantifies the magnetic response of an electrical conductor to the change in electric current flowing through it, measured in Henry (H) [15].

Self-Inductance is the property of a circuit, often a coil, by which a change in current induces an electromotive force (EMF) within the same circuit [16].

Mutual Inductance occurs when a change in current in one circuit induces an electromotive force in a neighboring circuit [3].

2.1.2 The Importance of Flux

Magnetic flux plays a pivotal role in the operation of electrical machines and devices. It is fundamental in the conversion of electrical energy to mechanical energy and vice versa, influencing the design and efficiency of these devices. Understanding flux patterns allows for the optimisation of machine design to enhance performance and reliability [17].

2.1.3 Inductance

Inductance is essential for the functionality of transformers, motors, and generators. It affects the rate of current change in a circuit, making it instrumental in filtering noise, stabilising current flow, and controlling AC motor speeds. The design and manipulation of inductance are crucial for developing efficient electronic devices and power systems.

2.1.4 Maxwell's Equations

Maxwell's equations describe the fundamentals of electricity and magnetism, essential for understanding electromagnetic levitation [9].

- **Gauss's Law for Electricity** states that the electric flux out of any closed surface is proportional to the enclosed electric charge, providing insight into electric field distribution around charges. In levitation, this helps in designing the distribution of electric charges on surfaces to create desired levitational forces.

$$\nabla \cdot \mathbf{E} = \frac{\rho}{\epsilon_0} \tag{2.1}$$

- **Gauss's Law for Magnetism** asserts the non-existence of magnetic monopoles; magnetic field lines are always closed loops. This principle is crucial for understanding the magnetic field configuration around magnets used in magnetic levitation systems.

$$\nabla \cdot \mathbf{B} = 0 \tag{2.2}$$

- **Faraday's Law of Induction** shows how a changing magnetic field induces an electromotive force (EMF) in a closed circuit. This is fundamental for EDS, where moving conductors through magnetic fields generate currents that oppose the original magnetic field, creating levitation.

$$\nabla \times \mathbf{E} = -\frac{\partial \mathbf{B}}{\partial t} \tag{2.3}$$

- **Ampère's Law with Maxwell's Addition** relates magnetic fields to the currents that produce them, including the contribution from a changing electric field. This underpins the design of electromagnets in EMS systems, dictating the magnetic field generated for levitating objects.

$$\nabla \times \mathbf{B} = \mu_0 \mathbf{J} + \mu_0 \epsilon_0 \frac{\partial \mathbf{E}}{\partial t} \tag{2.4}$$

Lorentz Force Law

The Lorentz Force Law is pivotal for directly calculating the force acting on charged particles in an electromagnetic field, a principle exploited in magnetically levitated transport systems.

$$\mathbf{F} = q(\mathbf{E} + \mathbf{v} \times \mathbf{B}) \tag{2.5}$$

This equation highlights how both electric and magnetic fields contribute to the force on a particle, with implications for both the stabilization and propulsion of levitated objects.

2.2 Methods of Levitation

This section provides an overview of various levitation methods, highlighting their principles, advantages, and applications. Understanding these methods is crucial for designing efficient levitation systems for transportation technologies.

2.2.1 Degrees of freedom

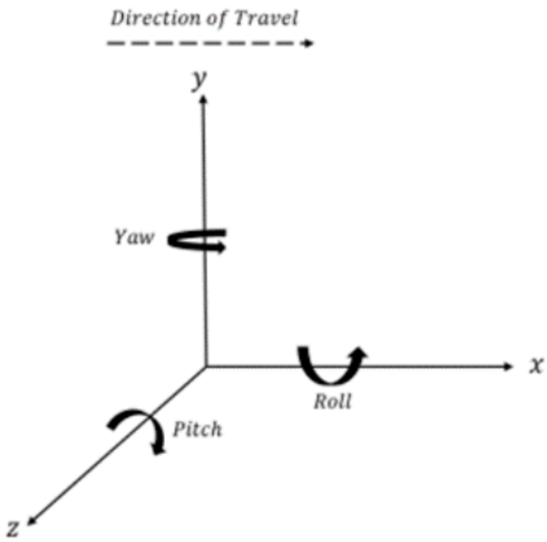

Figure 2.1: Degrees of freedom [1]

Any form of levitation has to successfully address a method where all degrees of freedom are considered. Looking at a standard 6-degree-of-freedom in figure 2.1, the only degree of freedom the pod should be able to move in is the x direction along the track (controlled by the motor and brakes). The levitation system will control the remaining five degrees of freedom.

2.2.2 Electromagnetic Suspension (EMS)

Electromagnetic Suspension uses electromagnets to levitate an object by the attractive force between the electromagnets and the ferromagnetic material (figure 2.2). The system requires active control to maintain stable levitation. The force formula used to maintain a stable air-gap is below and can be derived from Reluctance Networks [2; 16]. It should be noted that the greater the force desired (weight of the pod) the more power required by the system.

$$F_{\text{mag}} = \frac{\mu_0 \cdot N^2 \cdot I^2 \cdot A}{2 \cdot g^2} \tag{2.6}$$

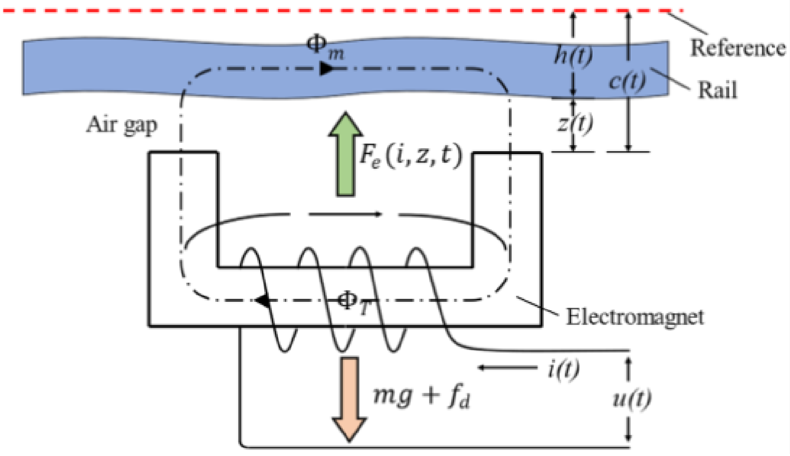

Figure 2.2: EMS Configuration [2]

2.2.3 Electrodynamic Suspension (EDS)

Electrodynamic Suspension leverages the repulsive forces generated by induced currents in conductive tracks as a moving magnet passes over them. This is through Lenz's law, which account for an opposite field being produced in the conductor causing a repulsive force. It is inherently stable at high speeds but requires motion to initiate levitation [3; 18]. This can be achieved using a halbach array, though the construction of one is difficult due to the orientation and position of the magnets. An example of this configuration of magnetic poles and their placement can be seen in figure 2.3. Drag to lift ratios are an important consideration for finding optimal speeds depending on the loading.

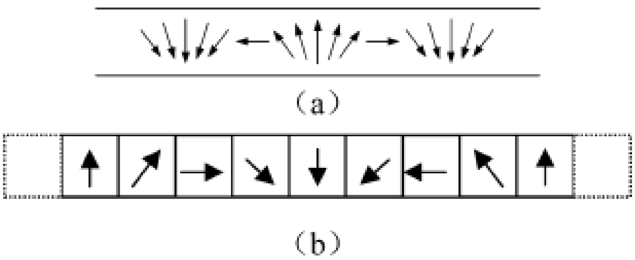

Figure 2.3: Halbach Array Pole orientation for EDS [3]

2.2.4 Hybrid Electromagnetic Suspension (HEMS)

A hybrid approach to the EMS system allowing for lower power requirements for continued running [19]. It is significantly harder to model compared to the standard EMS system providing difficulties with controls.

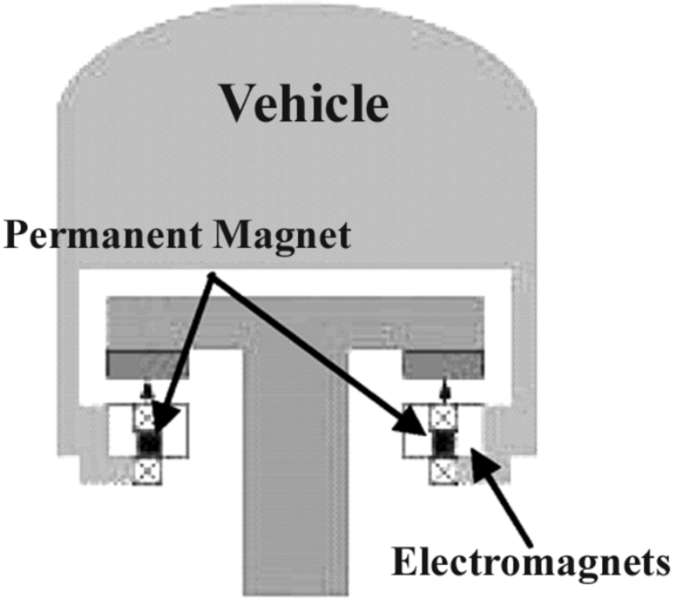

Figure 2.4: Possible HEMS configuration [4]

2.2.5 Superconducting Magnetic Levitation

Superconductos have the ability to expel magnetic fields (Meissner effect) and pin magnetic field lines (flux pinning), allowing for stable, passive levitation without energy input once cooled below their critical temperature [20; 21].

Superconductors can be utilised in the same manner as other conductors for levitation techniques. This means they can be used for both EMS and EDS. Using High Temperature Superconducting (HTS) coils and use the same principle as an EMS system as shown in figure 2.5. The lack of electrical resistance allows for power efficient designs.

HYPED currently does not have the capability to maintain the cool temperatures required for superconductors. Even high temperature superconductors need cooling to at least 80K and thus requiring liquid nitrogen [22].

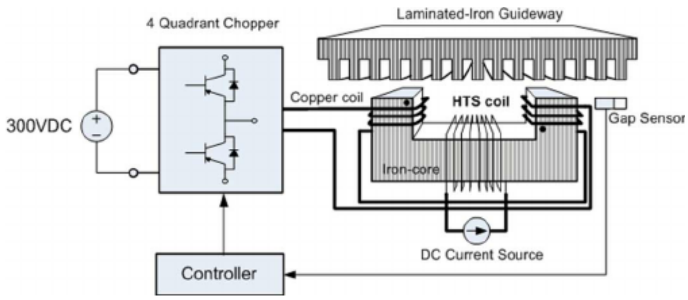

Figure 2.5: EMS with HTS Coil [5]

2.3 Methods of Mathematical Modelling

In the design and analysis of levitation systems for transportation technologies, mathematical modelling plays a pivotal role. It allows for the prediction of system behavior under various conditions, aiding in the optimisation of design parameters for improved performance and efficiency [23]. This section elaborates on the mathematical modelling involved in the project, highlighting the equations and their applications.

2.3.1 Reluctance Networks (RN)

Reluctance networks are a fundamental concept in the study of magnetic circuits, serving as the magnetic equivalent of electrical circuits. These networks allow for the analysis and design of magnetic systems by utilising the analogy between magnetic and electrical quantities [24]. In electrical circuits, resistance opposes the flow of electric current; similarly, in magnetic circuits, reluctance opposes the flow of magnetic flux.

Reluctance is defined as the opposition to the establishment of magnetic flux in a magnetic circuit and is dependent on the material properties and geometry of the circuit. The total reluctance of a magnetic path can be calculated using the formula $S = \frac{l}{\mu A}$, where l is the length of the path, μ is the permeability of the material, and A is the cross-sectional area. Magnetic circuits can be analysed using Ohm's law for magnetic circuits, where the MMF across a magnetic element is equal to the product of the magnetic flux (Φ) and the reluctance (S) of the element: $MMF = \Phi S$.

Reluctance networks enable the modeling of complex magnetic systems, including transformers, inductors, and motors, by simplifying them into networks of reluctances. This approach is particularly useful in the design and optimisation of magnetic devices, allowing engineers to predict the performance of a device under various conditions and to identify efficient paths for magnetic flux.

2.3.2 Examples of RN

Two reluctance network examples,

1. U-bar with a coil.

2. U-bar with a permanent magnet.

1 (U-bar with a coil)

First the conversion to the equivalent circuit using Ampere's Law which is given by:

$$\oint \mathbf{H} \cdot d\mathbf{l} = NI \tag{2.7}$$

The integral can be expressed as a sum:

$$\sum_{\mathrm{l}}^{\mathrm{n}} \mathbf{H}_{\mathrm{n}} \mathbf{l}_{\mathrm{n}} = NI \tag{2.8}$$

Looking at figure 2.6, the flux path has been divided into sections (AB, BC, etc). A constant flux Φ flows around the loop so the magnetic field strength is constant along each section (for AB this can be called H_1).

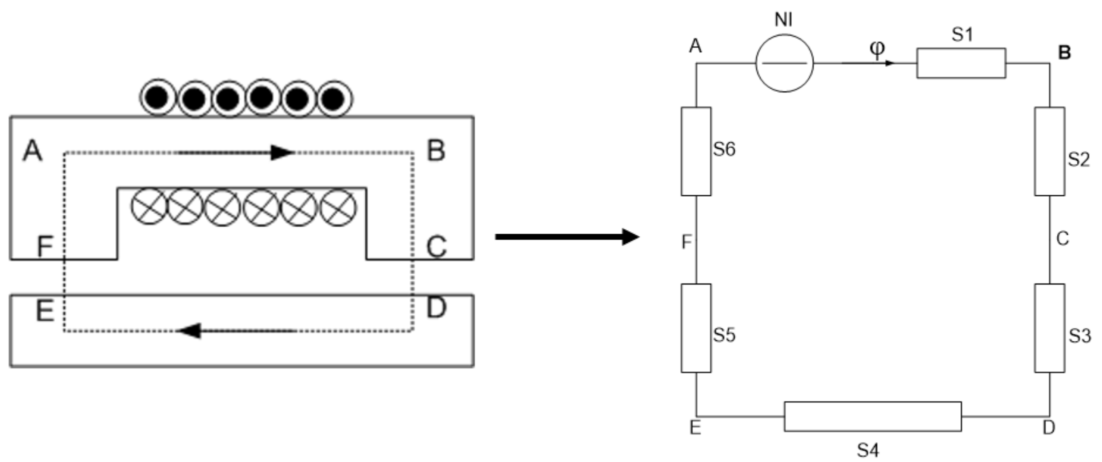

Figure 2.6: U bar with coil RN [6]

$$H_1L_1 + H_2L_2 + H_3L_3 + H_4L_4 + H_5L_5 + H_6L_6 = NI \tag{2.9}$$

Substituting in equation 2.11 into 2.10 for H:

$$B = \mu_0\mu_r H \tag{2.10}$$

To get

$$\frac{B_1}{\mu_0\mu_r}L_1 + \frac{B_2}{\mu_0\mu_r}L_2 + \frac{B_3}{\mu_0\mu_r}L_3 + \frac{B_4}{\mu_0\mu_r}L_4 + \frac{B_5}{\mu_0\mu_r}L_5 + \frac{B_6}{\mu_0\mu_r}L_6 = NI \tag{2.11}$$

$$B = \frac{\Phi}{A} \tag{2.12}$$

$$\Phi[S_1 + S_2 + S_3 + S_4 + S_5 + S_6] = NI \tag{2.13}$$

Now the system is a sum of reluctance which translates to the circuit equivalent shown in figure 2.6. This can be further simplified using assumptions about permeability. Further equations can be used to calculate inductance, voltage and force values.

U-bar with a permanent magnet

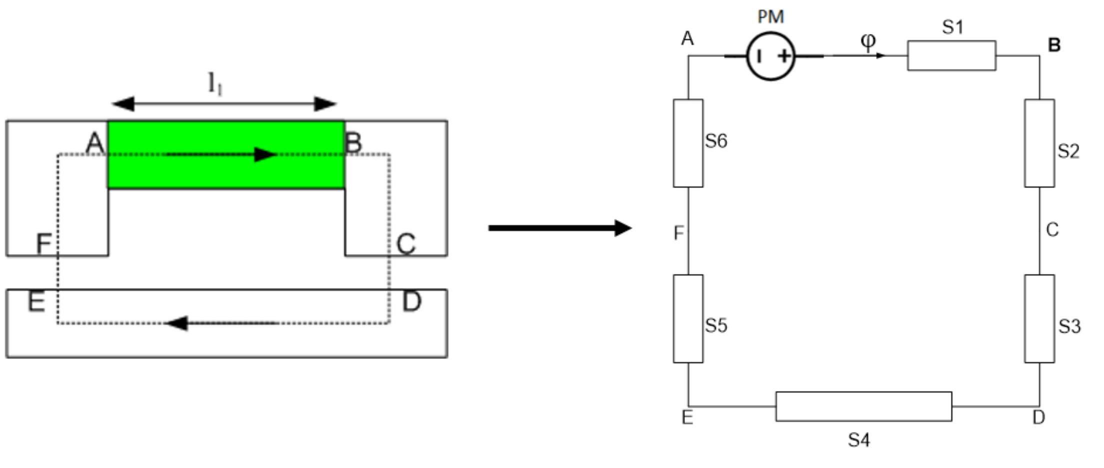

Figure 2.7: U bar with Permanent Magnet RN [6]

For a permanent magnet there is a similar process. Looking at figure 2.7 the diagram is labeled in a similar way to before. The main difference for the calculations is the expression is no longer involves a number of turns multiplied by the current to express the MMF. For a permanent magnet the expression is in 2.14.

$$MMF = B_{rem}\frac{l_1}{\mu_0} \tag{2.14}$$

Ampere' Law changes like so,

$$\oint \mathbf{H} \cdot d\mathbf{l} = B_{rem}\frac{l_1}{\mu_0} \tag{2.15}$$

Then by redoing the same steps with a different value on the right side:

$$\Phi[S_1 + S_2 + S_3 + S_4 + S_5 + S_6] = B_{rem}\frac{l_1}{\mu_0} \tag{2.16}$$

Simplifications can be made, and additional calculations can be performed to determine inductance, voltage, and force values. These aspects will be thoroughly examined for the selected levitation method.

2.3.3 Voltage and Current Dynamics

The voltage ($u(t)$) applied to the electromagnet's coil and the resulting current (i) are governed by the electromagnet's inductance (L) and resistance (R), encapsulated in the differential equation:

$$u(t) = Ri + \frac{d\psi}{dt} \tag{2.17}$$

$$\psi = LI \tag{2.18}$$

$$u(t) = RI + = L\frac{dI}{dt} + I\frac{dL}{dt} \tag{2.19}$$

This relationship is crucial for understanding how changes in the applied voltage or the coil's characteristics affect the current, and thereby, the levitation force.

2.3.4 Electromagnetic Force

The electromagnetic force (F) generated by the electromagnet and acting on the levitated object is a key component of the system. This force can be described by:

$$F = \frac{\mu_0 N^2 I^2 A}{2g^2} \tag{2.20}$$

where μ_0 is the permeability of free space, N is the number of turns in the coil, I is the current through the coil, A is the cross-sectional area of the coil, and g is the gap between the coil and the levitated object. This equation underscores the direct relationship between the force and the current, as well as the inverse square relationship with the gap, highlighting the critical parameters for controlling levitation.

2.3.5 System Dynamics

The dynamics of the levitation system are captured through a set of differential equations, reflecting the relationships between electromagnetic forces, motion, and system responses. A simplified model might consider the electromagnet's force (F) as a function of current (i) and distance (x) from the levitated object to the electromagnet, leading to an equation of motion for the levitated object. This equation can be represented as:

$$\ddot{x} + b\dot{x} + kx = F(i, x) \tag{2.21}$$

where b represents damping coefficients, and k denotes stiffness coefficients, illustrating the system's resistance to motion and its propensity to return to an equilibrium position, respectively.

Chapter 3

Initial Design

3.1 Levitation Method

3.1.1 Hybrid Electromagnetic Suspension (HEMS)

Though the use of superconductors would provide the best results (Table 3.1), due to limitations in cost and implementation, HEMS was chosen as the levitation method. This hybrid approach allows for an energy efficient design that scales well.

Criterion	**EMS**	**EDS**	**HEMS**	**Superconductors**
Power Efficiency	Low	Moderate	**High**	High
Control Complexity	Moderate	Moderate	High	Moderate
Scalability	High	Moderate	**High**	High
Manufacturability	High	Low	Moderate	Low
Cost	Moderate	High	High	Very High
Maintenance Requirements	Low	Moderate	Moderate	High

Table 3.1: Comparison of Levitation Methods for the Hyperloop Pod

The electromagnet component works by creating a counter flux to oppose that of the permanent magnet. For a complete understanding, examine the flux lines produced by both an electromagnet and a permanent magnet in figure 3.1.

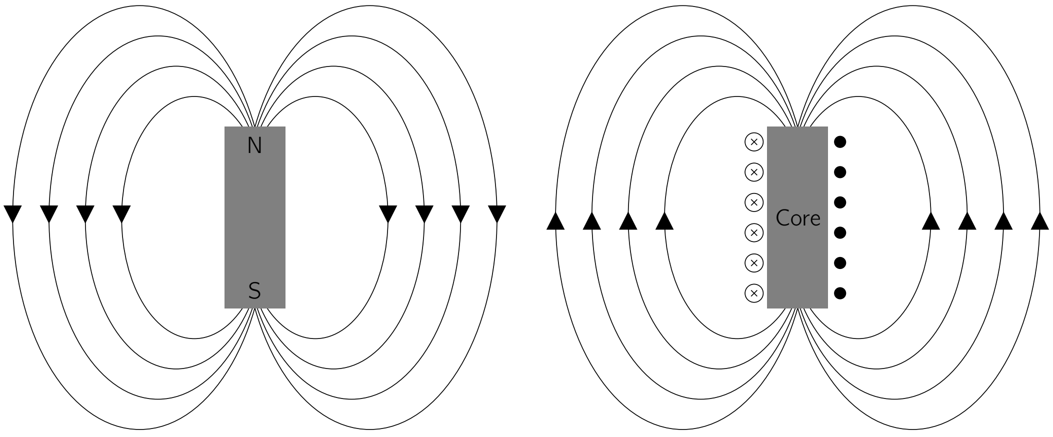

(a) Permanent Magnet (b) Electromagnet

Figure 3.1: Flux line diagrams

As can be seen they are both very similar but for the electromagnet this depends on the direction of the current. Reversing the current means the flux lines will go in the opposite direction. Using this principle and winding a coil around a permanent magnet, the force the permanent magnets exerts can be reduced by flowing a current in one direction, or the force can be increased by the current flowing in the other direction. This is key for controlling the hybrid system in order to balance forces.

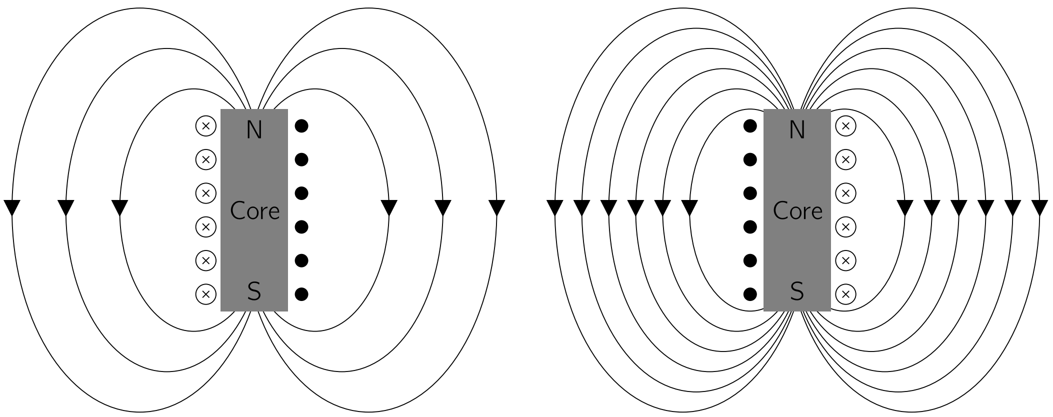

(a) Decreased Field strength due to current (b) Increased Field strength due to current

Figure 3.2: Lateral Movement

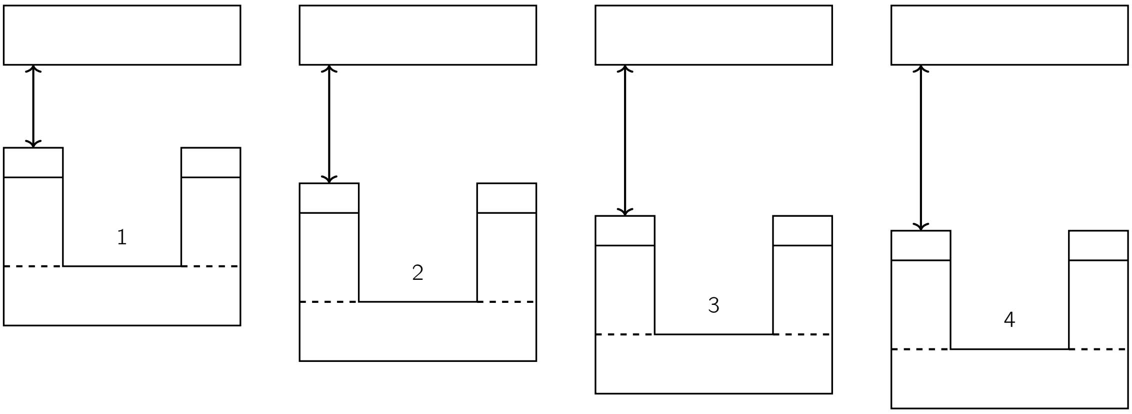

Figure 3.3: Levitation Unit movement

Figure 3.3 illustrates the four key stages of a magnetic levitation system's operation within a HEMS system:

1. **Startup:** The system initiates with a high starting current, positioning the levitation module at its closest to the magnets, requiring significant power to overcome gravity.

2. **Levitation Distance Achievement:** The module reaches the desired levitation height, balancing the magnetic force against the gravitational pull with optimized current flow.

3. **Equilibrium Point:** Here, the magnetic force exactly counters the weight of the pod, maintaining stable levitation without additional power adjustment. Here is where a zero current mode would aim to balance to maximise power efficiency by minimising nominal current.

4. **Overshoot and Fall:** Beyond this equilibrium, the system cannot increase the magnetic strength due to current for this controls system only flowing in one direction, leading to inevitable descent as the magnetic force weakens with distance. Updating the system to change the direction of the current would allow optimisation of this step.

So for the HEMS module, it will first start in a position where the force of attraction to the track is greater than the weight. The by applying a current to weaken this attraction and the force of attraction is less than the weight and so the the pod will begin to drop. Once the pod reaches a specified distance, the current will decrease until the weight of the pod and the magnet attraction balances and so the pod will levitate.

3.1.2 Implementation

Each levitation module will have a HEMS and EMS component (figure 3.4). This ensures control over the 5 degrees of freedom by each each aiming for a specified displacement. This exact displacement needs to be calculated for in the design phase.

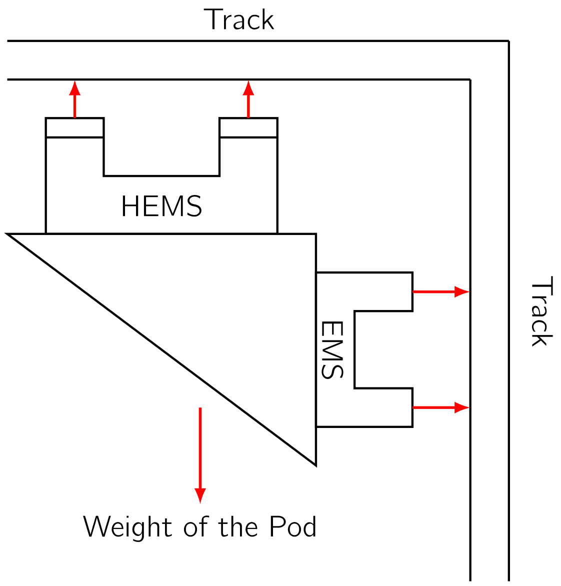

Figure 3.4: Levitation Module Components

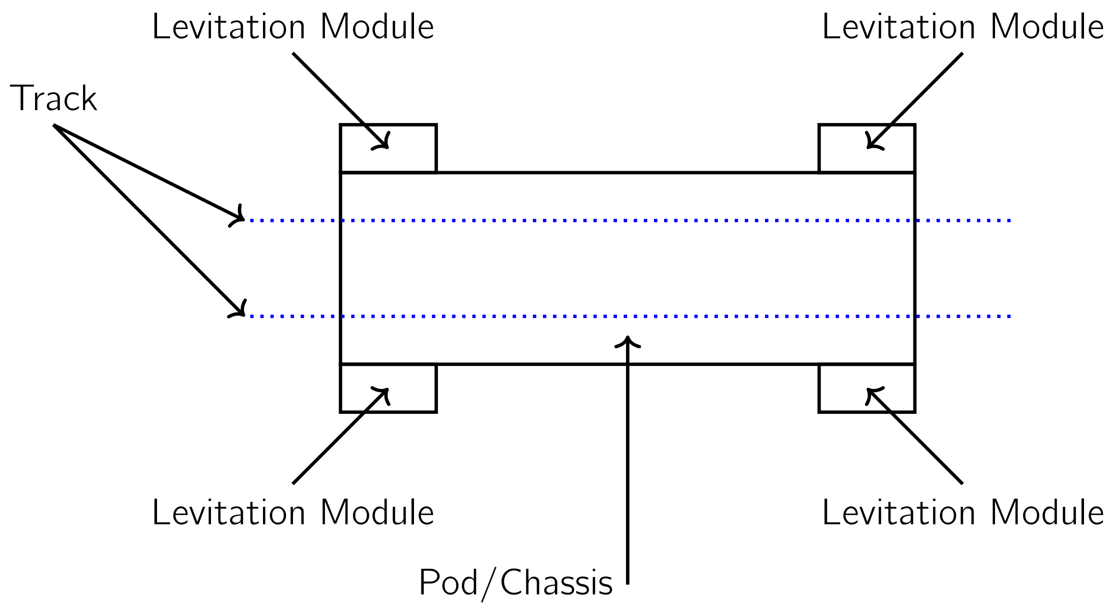

Figure 3.5: Placement of levitation modules

Four levitation modules will be created that will go at the 4 corners of each pod as seen in figure 3.5. Each will have there own independent HEMS system for vertical control.

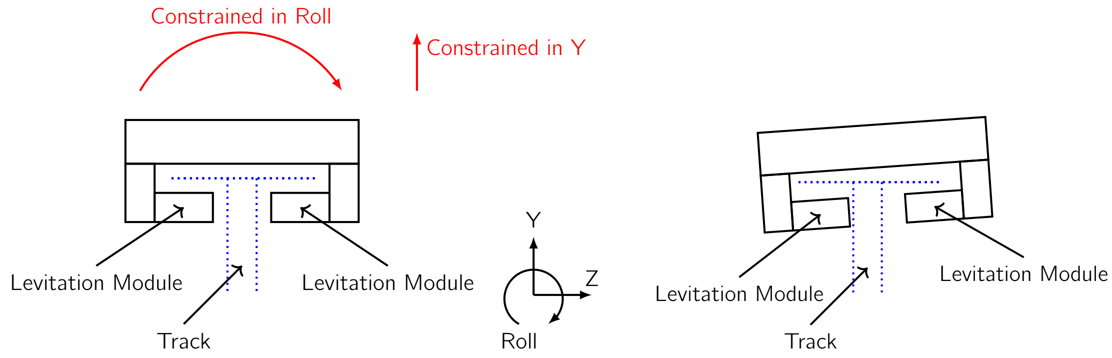

(a) Levitation Module Placement (b) Movement to be corrected

Figure 3.6: Front view of the pod

This ensures the degrees of freedom for the Y, Roll and Pitch are constrained (figures 3.6 & 3.7). This still leaves two degrees of freedom (Z & Yaw), thus on the sides of each Levitation module will be an EMS system. The EMS system will control lateral movement as seen in figure (3.8).

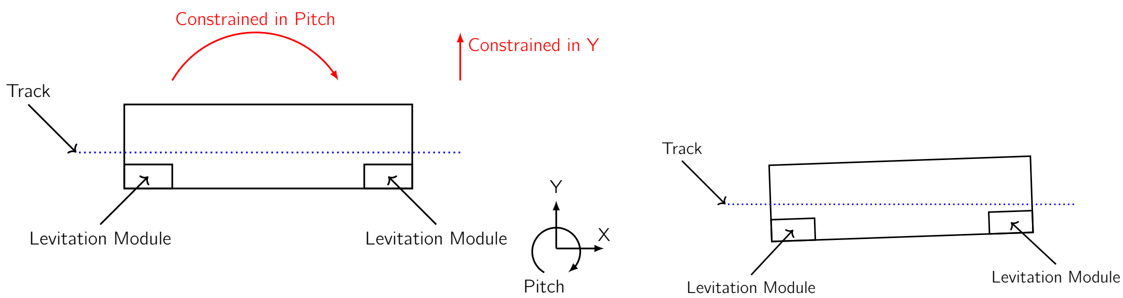

(a) Levitation Module Placement (b) Movement to be corrected

Figure 3.7: Side View of the pod

The HEMS module will start attached to the top of the track and then once a current runs through the coils this will counter the magnetic field causing the attractive force to weaken. The current will allow the control of the attraction to the track. A HEMS module will compromise of a U bar with magnets on top. Then a set of coils wrapping around which will allow for the control. Figure 3.9 shows the cross section of an example HEMS component with the side boxes denoting the placement of the coils.

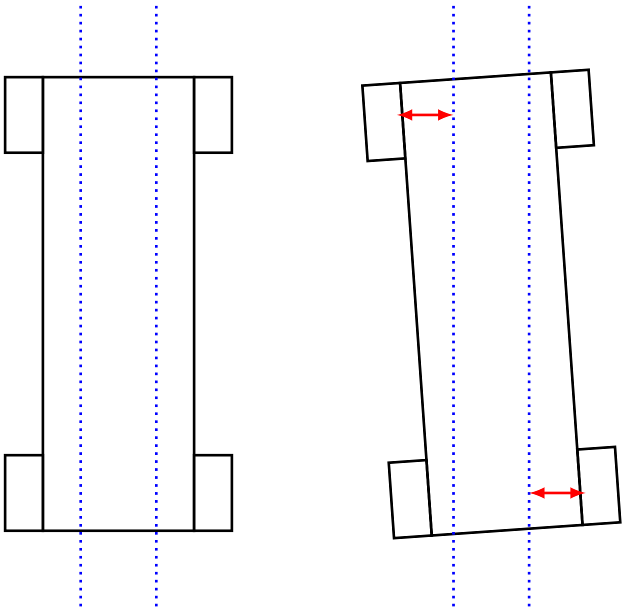

(a) Desired lateral location (b) Yaw Control (c) Z Control

Figure 3.8: Lateral Movement

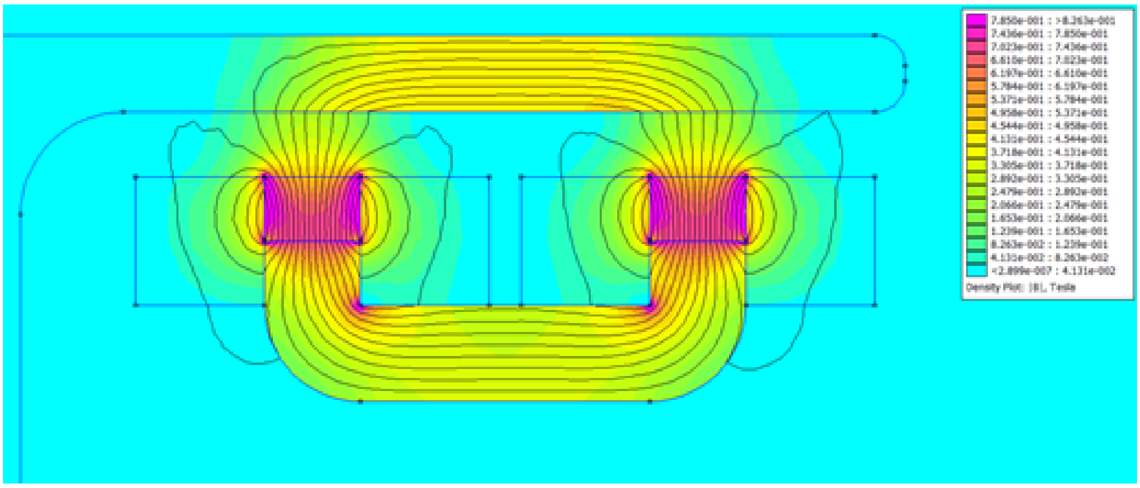

Figure 3.9: HEMS Layout for Simulation

Each Levitation module with have a target air-gap for both the HEMS and EMS components and this ensures control all over the 5 degrees of freedom and thus allowing the pod to still move in the x direction.

3.1.3 Future Improvements

One of the primary advantages of a HEMS levitation module is its exploitation of the zero current air gap. This feature capitalises on the point at which the force exerted by permanent magnets perfectly counterbalances the weight of the pod. A comparison of the current variation between the standard system and the HEMS illustrates this advantage (figure 3.10). Initially, both systems demand a high current, influenced by the proximity of the permanent magnet to the track, the closer the magnet, the higher the required current for creating the counter flux. Subsequently, each system seeks an equilibrium; for a standard system, this equilibrium current might approximate 3A, whereas the zero current aims for a balance at 0A. As current fluctuates around these values, and given that power consumption is directly proportional to current, the zero current gap results in substantially lower power usage. By leveraging the inherent strength of permanent magnets, HEMS achieves efficient operation.

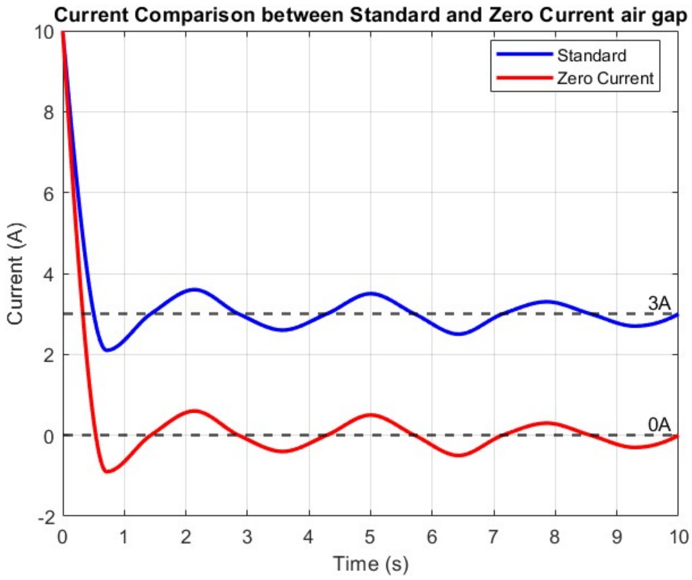

Figure 3.10: Placement of levitation modules

The pod for this year will not make use of the zero current air gap as this control algorithm is difficult to implement in the current design. Trying to balance at this point would mean a near zero current and thus optimal power usage. It will be a future improvement for the system and a task for HYPED members next year.

3.2 Integration & Constraints

3.2.1 Overview

The pod is being completely redesigned this year and thus all systems have to be checked for compatibility. This is an overview from final designs from other sections of the pod, the actual design work required using estimates of each sub system providing additional challenges.

3.2.2 Track

The pod needs to be designed to fit the track. Currently the track is made of aluminium, so modifications are mandatory for the HEMS system. Two proposed version of the track can be seen in figure 3.11, which both utilise installing L-plates in order to fit the levitation modules underneath. Concept B was chosen with the finalised version shown in figure 3.12.

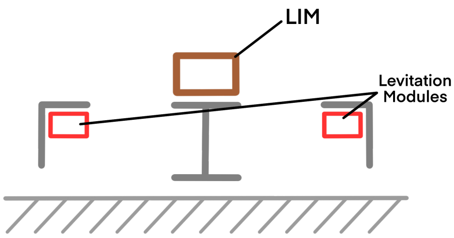

(a) Concept A

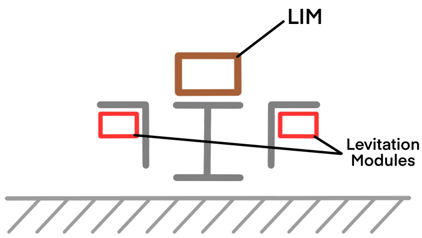

(b) Concept B

Figure 3.11: Main caption for both images.

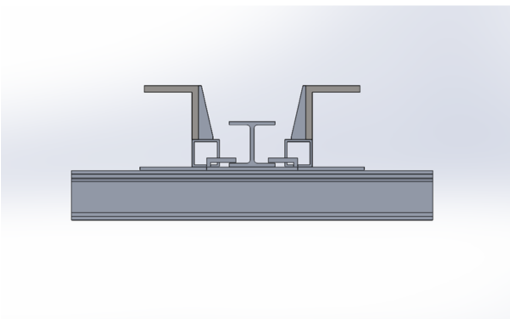

(a) Front View

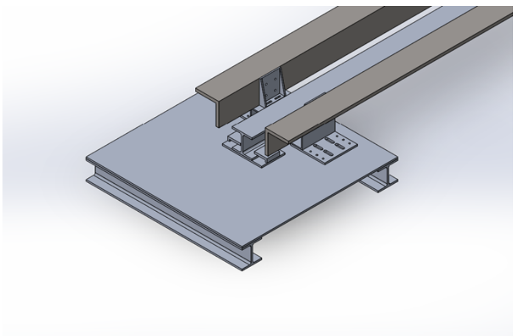

(b) Angled View

Figure 3.12: Track Final Design

The steel L-plates on the sides must fit the levitation module underneath it. The track sets the dimensions for each module with the space given in figure 3.13. The red box notes the square it must fit in.

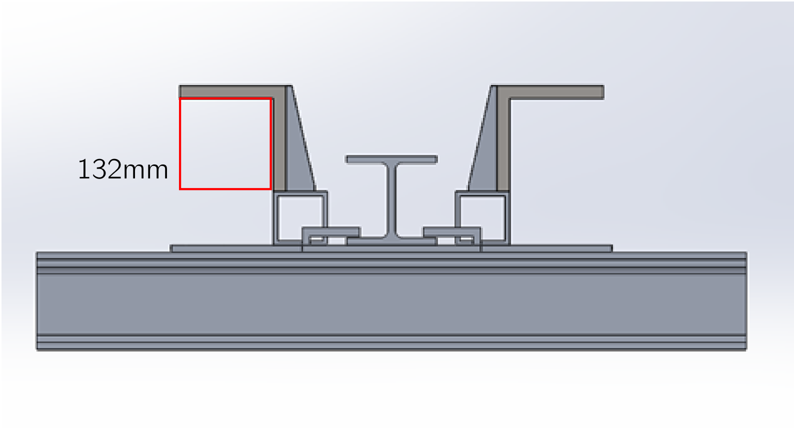

Figure 3.13: Constraints in Height & Width

3.2.3 Chassis

The chassis design can be seen in figure 3.14. This sets a constraint for the length of the module as 400mm.

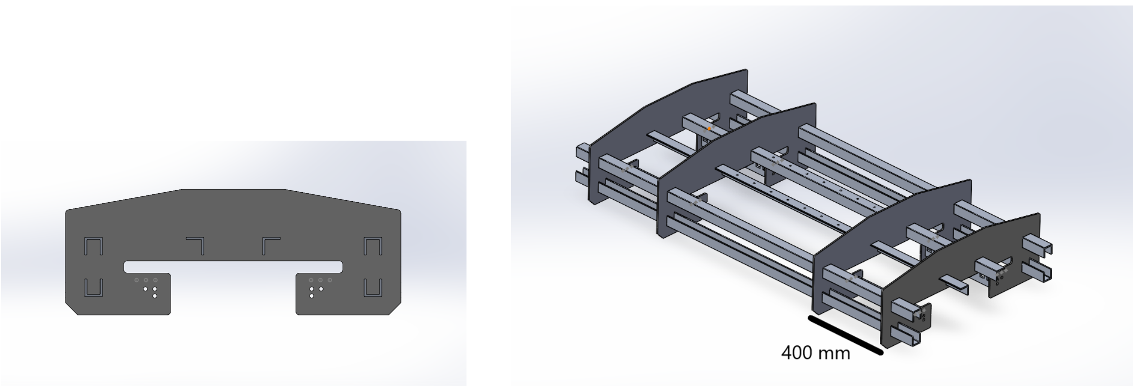

(a) Front View (b) Isometric view

Figure 3.14: Chassis CAD

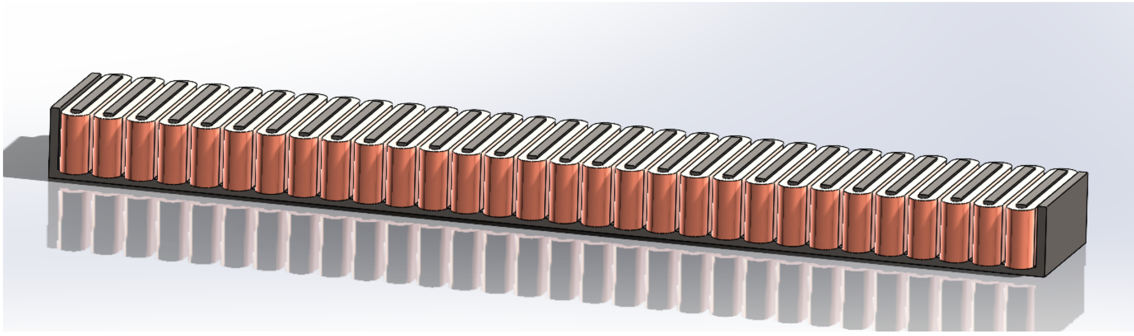

Figure 3.15: Linear Induction Motor

3.2.4 Linear Induction Motor (LIM)

The distance the linear motor is from the track directly affects its efficiency. With the linear motor being further away decreasing the efficiency and the closer it is increased. The desired air gap for the LIM is approximately 4mm away from the track. Since the pod is expected to be able to do levitating and non levitating runs this imposes the constraint on the motor team to ensure it can be adjusted by the drop distance for both.

3.2.5 Vertical Suspension

The vertical suspension constraint can be setup into 3 sections:

1 Compression and displacement

The vertical suspension acts as a constraint for the displacement of the levitation. The suspension needs to be able to compress by a certain amount depending on the displacement drop (start point to end point). The greater the displacement drop the greater the compression required.

2 Top wheels and displacement

The top wheels needs to catch the pod in the case where levitation controls fail. The height of these wheels needs to coincide with the drop off point (where magnetic attractive force at 0A is equal to the weight of the pod). This drop off point again is only specified for this year's pod and a new distance will have to be determined when trying to implement the zero current air gap.

This will be a constraint set by levitation modules for dynamics and determines where the upper wheels need to be placed.

3 Emergency Wheels

Attached to the top of the HEMS module is a set of wheels that will act as an emergency stop in the case the vertical suspension fails. Additionally this creates a constraint for the height of the emergency wheels since they only come into contact with the track when the others fail. This means the wheels have to be designed to take the full force from the magnets at a distance of 4mm.

3.2.6 Lateral Suspension

Lateral consists of the same concerns but there are zero permanent magnets. Making it simpler.

The EMS emergency wheels can make use of a similar design and also ensure the wheels do not come into contact with the track unless there is a failure in the horizontal suspension.

Since the pod will stay the same set distance away no movement needs to be taken into account so it is just the height of the wheels that need to be constrained.

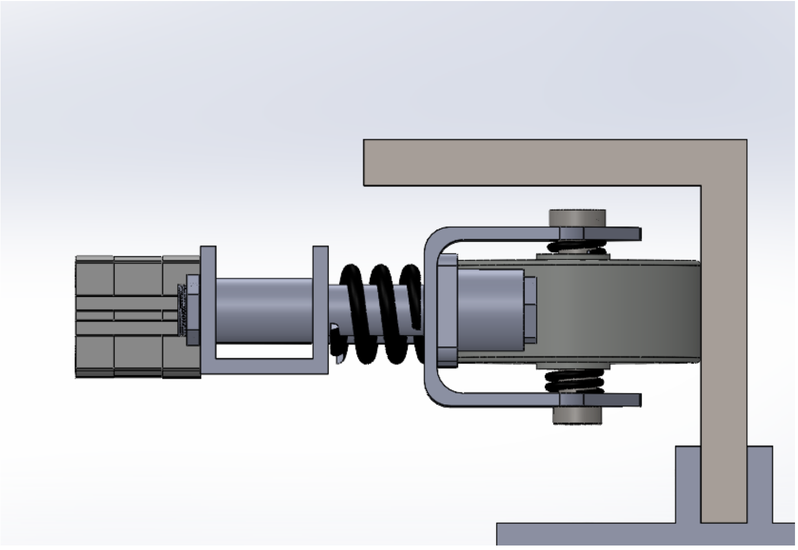

Figure 3.16: Lateral suspension

3.2.7 Current & Power

Finally the current was an important constraint to be considered based on thickness of the wires. The permanent magnets being next to the coils will require temperatures lower than 80 degrees Celsius to avoid demagnetisation. Heat from a wire will relate to the current density flowing through the wire which is simply the the current divided by the cross sectional area of the wire (Amm^{-2}). Usually $5Amm^{-2}$ is considered a safe value, though for the HEMS a current greater than this can be done for the drop and then the nominal current can $5Amm^{-2}$ or less. Below again the diagram is now labelled with starting value constraint for current density (Amm^{-2}).

This allows for customisation of the starting current in simulations based on the thickness of the wire. For example abut 4A in a 1mm diameter wire will be roughly the $5Amm^{-2}$ max for operating at. Increasing the wire's thickness will allow for a greater starting current and thus a closer starting point to the track as more of the field can be cancelled out. This would also allow for a greater drop distance as was outlined as a requirement earlier. Increasing the Cross section in order to allow for a greater current can both make it difficult to wind the coils and for it to fit within the limited space available (figure 3.17). This needs to be balanced well with the number of turns each module component needs.

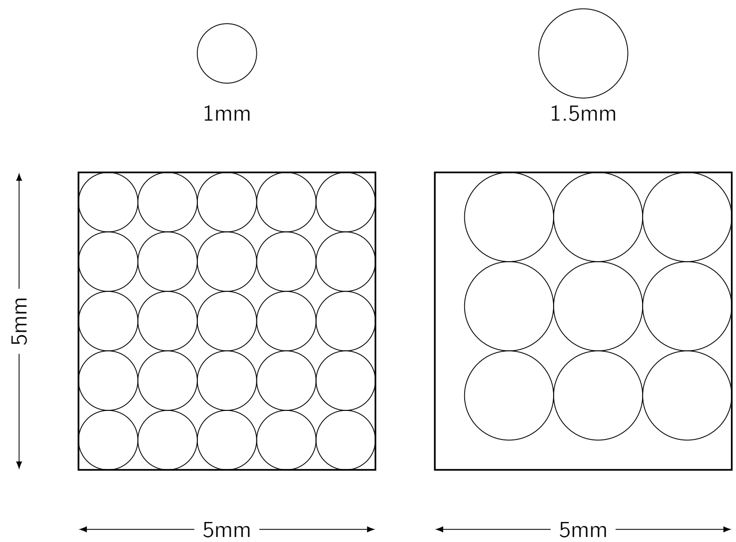

Figure 3.17: Wire Cross Sections and Spacing

The exact values to these starting point will be crucial for designing and integrating the levitation units into the pod and thus will be the main focus. Finding these values while staying within the range for each possible dimension should meet all requirements. The final step before finalising an initial design is simulations for these values. Taking note of the pods weight is critical to ensure forces can be balanced, force lines representing the pods weight (quarter of the total weight due to there being 4 modules) to find current values for the HEMS to move. Figure 3.18 shows the force lines (500N, 562.5N, 625N) for the initial design. If the displacement of the HEMS is greater than the target displacement then the force value will be need to be in the region below the force line (by changing the current) and if the displacement is less than the target displacement then it will need to be above this line.

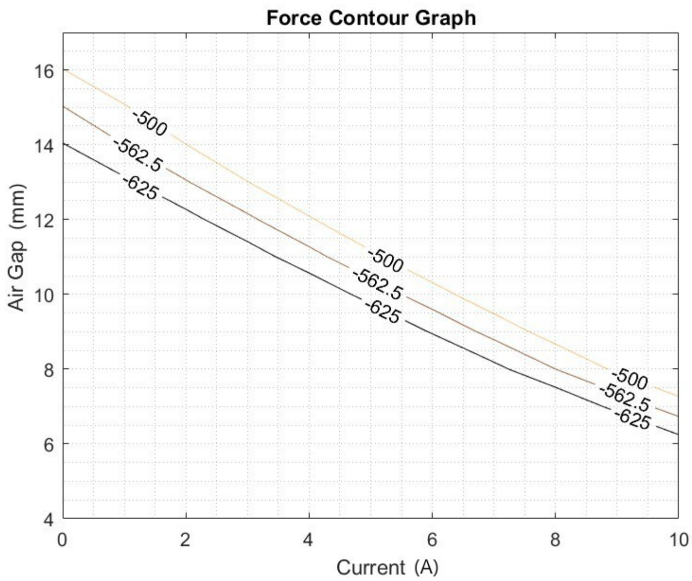

Figure 3.18: Balance force

3.2.8 First Design

An early estimate of the first design is shown in figure 3.19. A detailed view of the simulations completed is shown in the next section while also covering the theory behind them.

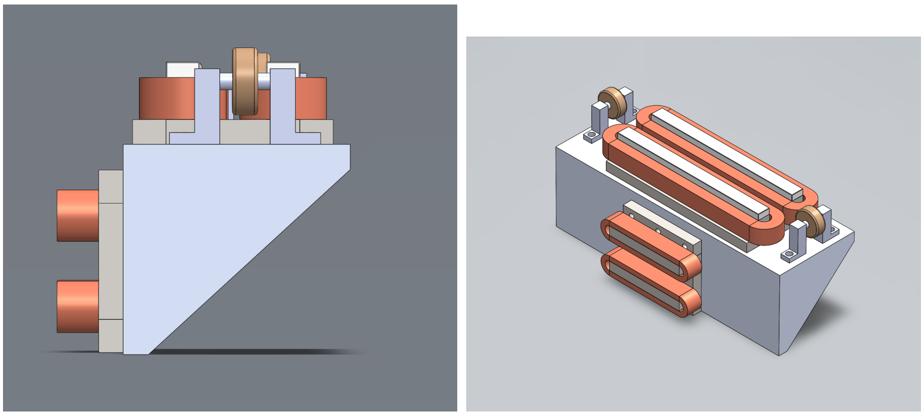

(a) Levitation Module Cross-section (b) Levitation Module Isometric View

Figure 3.19: CAD Models

Chapter 4

Mathematical Modelling & Simulations

4.1 FEMM Simulations

Finite Element Method Magnetics is a free to use software developed by researchers for accurate simulation of electromagnetic behaviour. It uses a simple 2d drawing field that can then be extended into a 3d simulation using its depth field.

4.1.1 Understanding Finite Element Methods

Finite Element Methods (FEM) are a cornerstone of computational engineering, enabling the numerical solution of physical problems that are otherwise analytically intractable. By changing a large system into smaller, manageable pieces, known as elements, FEM allows for a detailed simulation of complex behaviors across various disciplines.

FEM's versatility is demonstrated through its wide range of applications. In structural engineering, it is used to predict the response of structures under various loads, taking into account the material properties and geometry [25]. For fluid mechanics, FEM helps in analyzing flow fields around objects, predicting fluid behavior under different conditions [26]. Thermal analysis through FEM is crucial for understanding heat distribution and transfer in systems, aiding in the design of more efficient cooling strategies [27].

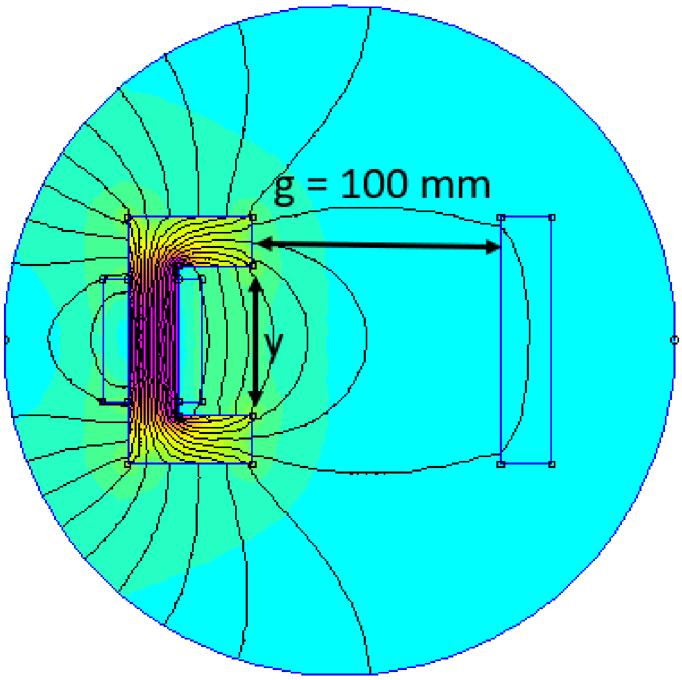

Figure 4.1: FEMM of an Electromagnet

4.1.2 Meshing

At its core, FEM is built upon the idea of breaking down a large problem into a series of smaller, simpler problems that can be solved in a systematic way.

It is broken down by meshing the system, so the domain is divided into discrete elements. The quality of the mesh directly influences the accuracy and convergence of the solution. Various techniques, such as Delaunay triangulation, are employed to ensure that the mesh efficiently captures the geometry of the domain while maintaining computational feasibility [28; 29]. The choice between finer and coarser meshes involves a trade-off between computational cost and solution accuracy.

4.1.3 Limitations

A limitation of the software is that it requires images to be drawn in 2d and thus some shapes cannot be represented. For instance consider a disk viewed from a side angle, this would be drawn as a rectangle and thus is simplified to such in FEMM. This is particularly important for the experimental results as simplifications have to be made.

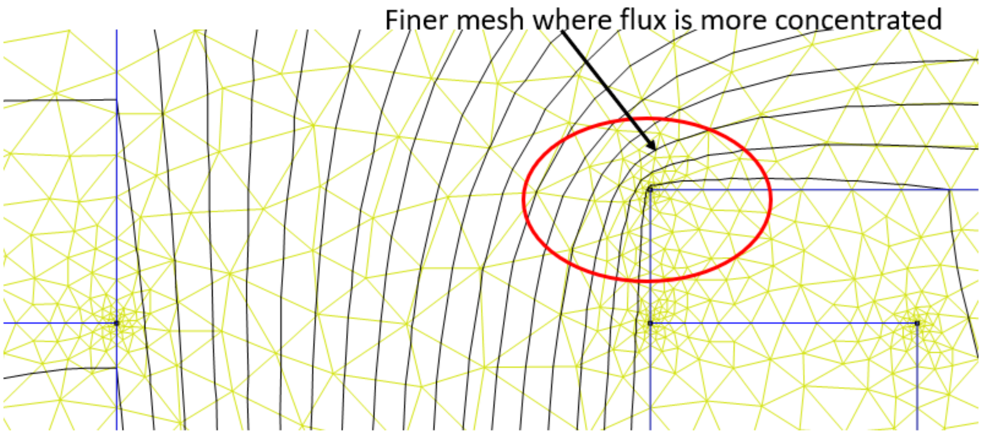

Figure 4.2: Mesh refinement

4.1.4 Iterations

Iterations were done using a varying air-gap and current. The images in figure 4.3 visually reveal the affect of an electromagnet moving further from a ferromagnetic bar.

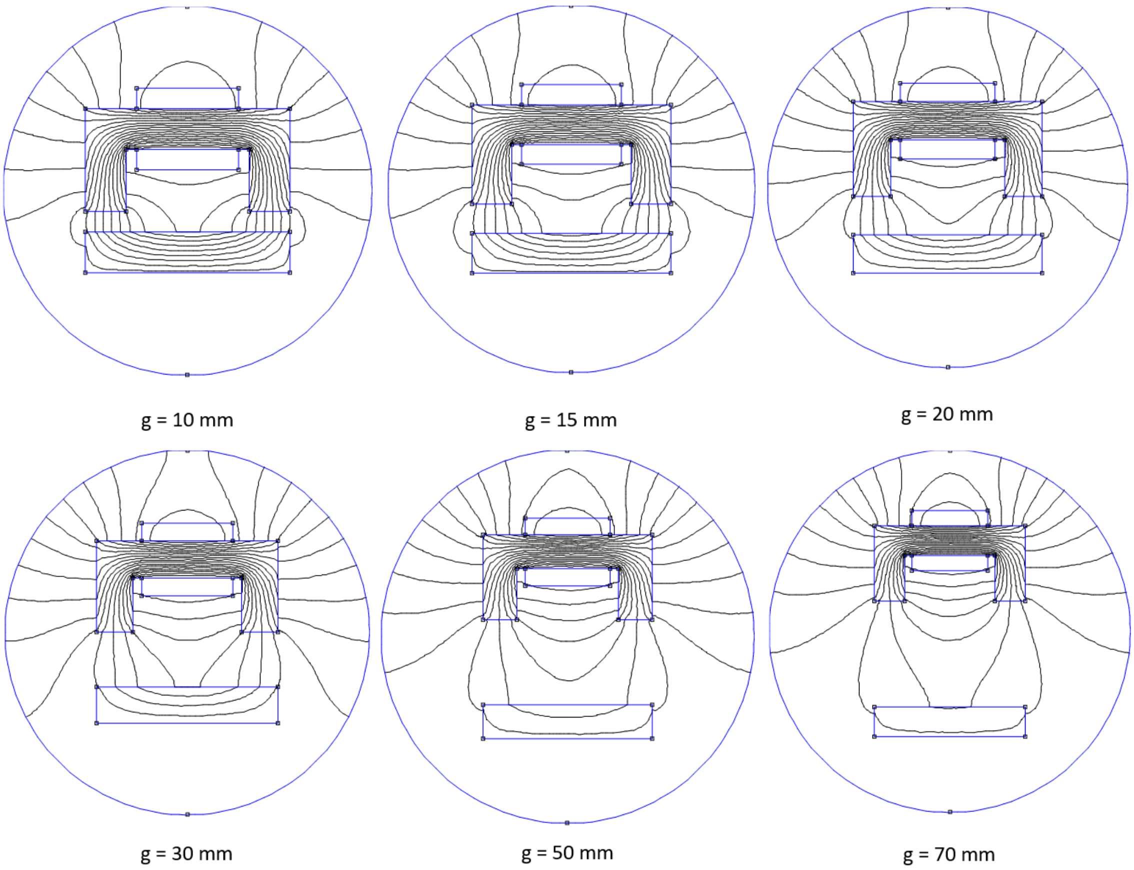

Figure 4.3: Electromagnet varying with distance

Initial simulations started with a rough estimate of the design. Magnets and other dimensions were tuned until it could hold the estimated weight of the pod (200-250kg).

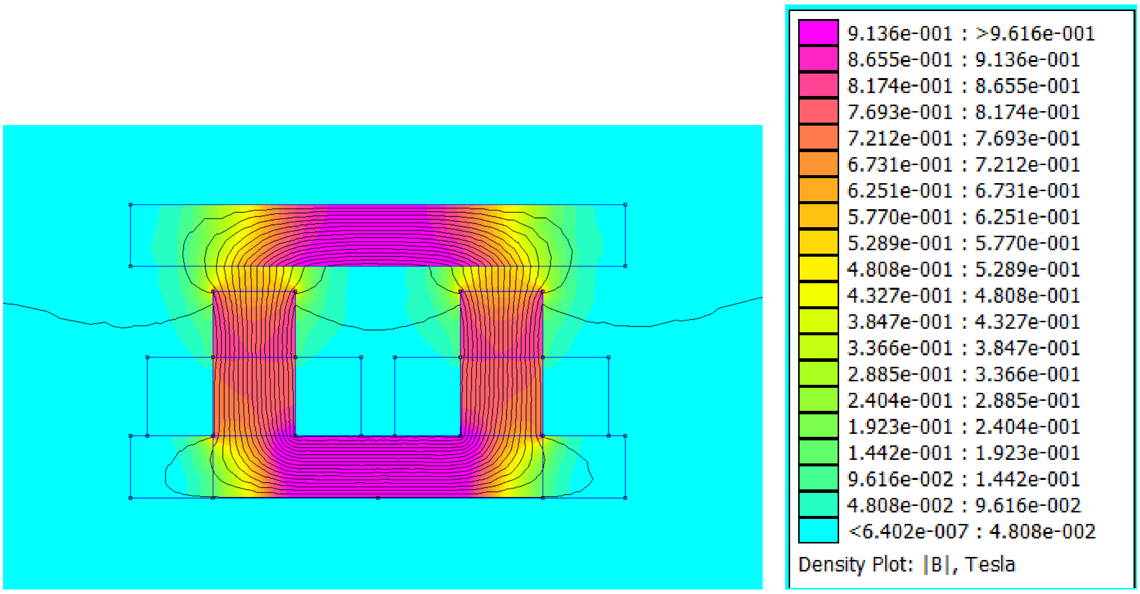

(a) FEMM (b) Flux density

Figure 4.4: HEMS FEMM Design

It is important to look at the flux density when analysing the thickness of the sections. Ideally this should be lower than 1.5 Tesla.

Iterations were done to find a suitable assembly that could be constructed that met the constraints for the size and determining the a suitable start point and drop distance for the levitation of the pod. Additionally ChatGPT was utilised to create Lua script in order to speed up the entire iteration process.

4.1.5 Initial Design

Figure 4.5 shows a constant force across the line with varying the distance and current. This is the same as shown in the Initial dsign section and it was determined from the FEMM simulations. The force shown for each line is an early estimate of the pods total weight divided by four. With the levitation system it will be crucial to keep close to this force as possible for stabilisation.

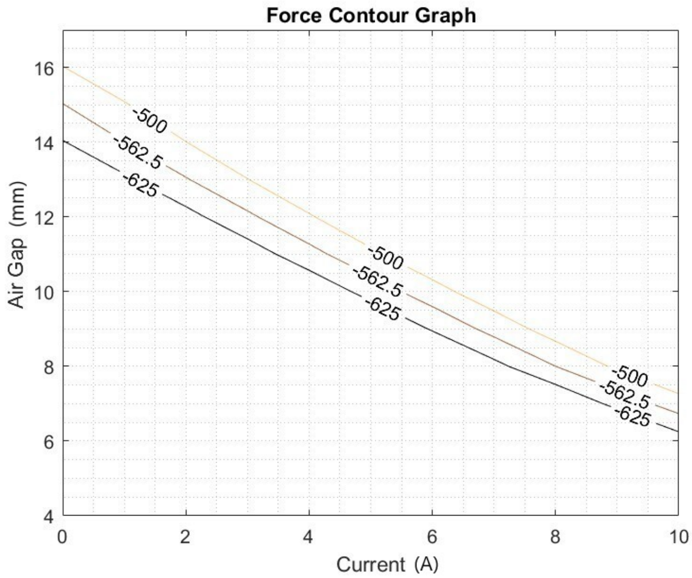

Figure 4.5: Balance Force

4.2 Reluctance Network

This is a method that can be done to mathematically model the system by constructing a magnetic circuit equivalent.

As mentioned in the literature review, the circuit will be the sum of the reluctance multiplied by the flux which will equal the MMF. Figure 4.6shows the actual layout of the system with DE & FG being the electromagnet and CD & GH being the permanent magnet.

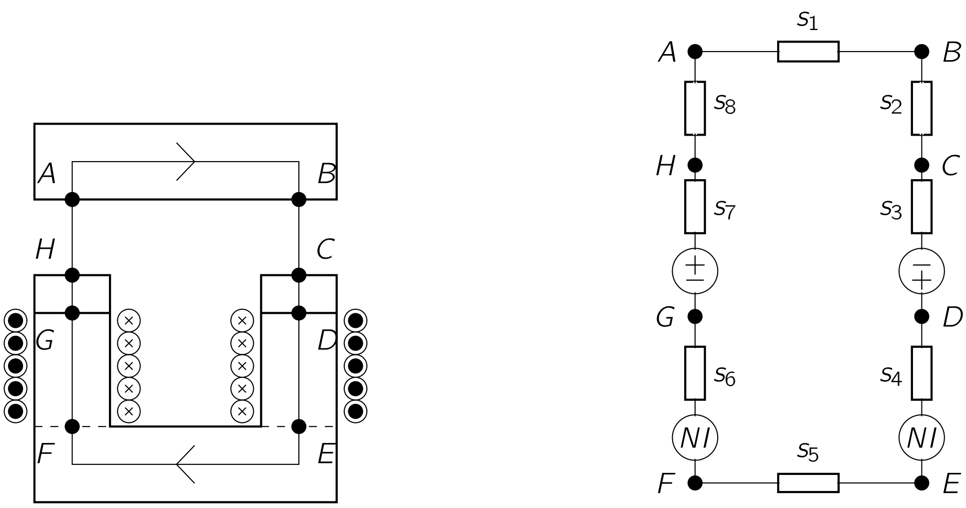

Figure 4.6: Equivalent circuit

First an expression of the MMF needs to obtained and then can be used with Amperes law. This can be understood by looking at the sources in the electrical circuit.

$$MMF = 2B_{rem}\frac{l_1}{\mu_0} + 2NI \tag{4.1}$$

And so when following the same steps from the literature review, the sum of the reluctance in the circuit can be expressed as

$$\Phi[S_1 + S_2 + S_3 + S_4 + S_5 + S_6 + S_7 + S_8] = 2B_{rem}\frac{l_1}{\mu_0} + 2NI \tag{4.2}$$

where the reluctances are:

$$s_2 = s_8 \text{ are both the Airgap } (s_{gap}), \tag{4.3}$$

$$s_3 = s_7 \text{ are the internal reluctance of the magnet } (s_{PM}), \tag{4.4}$$

$$s_4 = s_6 \text{ are both the electromagnet}, \tag{4.5}$$

$$s_1 = s_5 \text{ are both the steel component}, \tag{4.6}$$

$$\mu_0 \text{ is the permeability of free space}, \tag{4.7}$$

$$\tag{4.8}$$

$$S_1 = \frac{l_1}{\mu_0\mu_r A} \tag{4.9}$$

Now if we assume the reluctance of steel to be 0 due to it having a very high permeability (μ_r) this will make

$$s_1 = s_4 = s_5 = s_6 = 0 \tag{4.10}$$

So a simplified expression of the system can be

$$\Phi[2S_{gap} + 2S_{PM}] = 2B_{rem}\frac{l_1}{\mu_0} + 2NI \tag{4.11}$$

Subbing in the previous equation for reluctance we get

$$\Phi[2\frac{l_{gap}}{\mu_0\mu_r A} + 2\frac{l_{PM}}{\mu_0\mu_r A}] = 2B_{rem}\frac{l_1}{\mu_0} + 2NI \tag{4.12}$$

4.2.1 Magnetic Force Derivation

This formula can be rearranged for flux and substituted into the formula for magnetic force.

$$\Phi = \frac{2B_{rem}\frac{l_1}{\mu_0} + 2NI}{[2\frac{l_{gap}}{\mu_0\mu_r A} + 2\frac{l_{PM}}{\mu_0\mu_r A}]} \tag{4.13}$$

$$F_{\text{magnetic}} = \frac{B^2 \cdot A}{2 \cdot \mu_0} \tag{4.14}$$

$$B = \frac{\Phi}{A} \tag{4.15}$$

$$F_{\text{magnetic}} = \frac{\left(\frac{2B_{rem}\frac{l_1}{\mu_0}+2NI}{[2\frac{l_{gap}}{\mu_0\mu_r A}+2\frac{l_{PM}}{\mu_0\mu_r A}]}\right)^2}{2 \cdot A \cdot \mu_0} \tag{4.16}$$

$$F_{\text{magnetic}} = \frac{(2B_{rem}\frac{l_1}{\mu_0} + 2NI)^2}{2 \cdot A \cdot \mu_0 \cdot [2\frac{l_{gap}}{\mu_0\mu_r A} + 2\frac{l_{PM}}{\mu_0\mu_r A}]^2} \tag{4.17}$$

$$F_{\text{magnetic}} = \frac{(2B_{rem}\frac{l_1}{\mu_0} + 2NI)^2 \cdot A \cdot \mu_0}{2 \cdot [2\frac{l_{gap}}{\mu_r} + 2\frac{l_{PM}}{\mu_r}]^2} \tag{4.18}$$

Simplifying and making $\mu_r = 1$ for air, the expression becomes

$$F_{\text{magnetic}} = \frac{(2B_{rem}\frac{l_1}{\mu_0} + 2NI)^2 \cdot A \cdot \mu_0}{2 \cdot [2l_{gap} + 2l_{PM}]^2} \tag{4.19}$$

4.2.2 Inductance Derivation

The inductance can be calculated from the expression of Φ. This important value given to controls. Additionally l_{gap} can be expressed as x_1, while $l_1 = l_{PM}$

$$LI = N\phi \tag{4.20}$$

$$\frac{LI}{N} = \frac{2B_{rem}\frac{l_{PM}}{\mu_0} + 2NI}{[2\frac{x_1}{\mu_0\mu_r A} + 2\frac{l_{PM}}{\mu_0\mu_r A}]} \tag{4.21}$$

$$L = \frac{2B_{rem}\frac{l_1}{\mu_0}N + 2N^2 I}{I \cdot [2\frac{x_1}{\mu_0\mu_r A} + 2\frac{l_{PM}}{\mu_0\mu_r A}]} \tag{4.22}$$

4.2.3 Voltage Derivation

Another expression useful for controls is obtaining the voltage equation. This can be derived from the initial expression for voltage.

$$u(t) = Ri + \frac{d\psi}{dt} \tag{4.23}$$

$$\psi = LI \tag{4.24}$$

$$u(t) = RI + = L\frac{dI}{dt} + I\frac{dL}{dt} \tag{4.25}$$

After performing the product rule it involves finding the derivatives of the current and inductance with respect to time and then substituting them back into Equation 4.25. Once the derivative of L is determined, $\frac{di}{dt}$ will be within the formula and so can be rearranged to find it. An important note is that both the x_1 (l_{gap}) and I (current) change with time.

$$\frac{dL}{dt} = \frac{d}{dt}[\frac{2B_{rem}\frac{l_{PM}}{\mu_0}N + 2N^2 I}{I \cdot [2\frac{l_{gap}}{\mu_0\mu_r A} + 2\frac{l_{PM}}{\mu_0\mu_r A}]}] \tag{4.26}$$

$$\frac{dL}{dt} = \frac{d}{dt}[\frac{2B_{rem}l_{PM}NAI^{-1} + 2N^2\mu_0 A}{t[2x_1 + 2l_{PM}]}] \tag{4.27}$$

$$\frac{dL}{dt} = \frac{2B_{rem}l_{PM}NA\frac{d}{dt}[I^{-1}] + 2N^2\mu_0 A}{[2\frac{d}{dt}[x_1] + 2l_{PM}]} \tag{4.28}$$

$$\frac{dL}{dt} = \frac{[-4B_{rem}l_{PM}NAI^{-2}\frac{dI}{dt} + 2N^2\mu_0 A] \cdot (-2) \cdot (2)}{[2x_1 + 2l_{PM}]^2}\frac{dx_1}{dt} \tag{4.29}$$

$$\frac{dL}{dt} = \frac{[16B_{rem}l_{PM}NAI^{-2}\frac{dI}{dt} - 8N^2\mu_0 A]}{[2x_1 + 2l_{PM}]^2}\frac{dx_1}{dt} \tag{4.30}$$

Now with $\frac{dL}{dt}$, this can be substituted back into equation 4.25, along with substituting in the inductance from equation 4.22 and a full expression can be developed as seen in equation 4.32. Again simplifying r $\mu_r = 1$, $l_{gap} = x_1$, and $l_1 = l_{PM}$.

$$u(t) = RI + = \frac{2B_{rem}\frac{l_{PM}}{\mu_0}N + 2N^2 I}{I \cdot [2\frac{x_1}{\mu_0\mu_r A} + 2\frac{l_{PM}}{\mu_0\mu_r A}]}\frac{dI}{dt} + I\frac{[16B_{rem}l_{PM}NAI^{-2}\frac{dI}{dt} - 8N^2\mu_0 A]}{[2x_1 + 2l_{PM}]^2}\frac{dx_1}{dt} \tag{4.31}$$

$$u(t) = RI + = \frac{2B_{rem}l_{PM}NA + 2N^2 IA\mu_0}{I \cdot [2x_1 + 2l_{PM}]}\frac{dI}{dt} + I\frac{[16B_{rem}l_{PM}NAI^{-2}\frac{dI}{dt} - 8N^2\mu_0 A]}{[2x_1 + 2l_{PM}]^2}\frac{dx_1}{dt} \tag{4.32}$$

4.2.4 State Equations

The system can be expressed as a set of three first order differential equations. x_1 is the displacement, x_2 is the velocity, and x_3 is the current. This set of equations is useful for modelling the system as a whole which is valuable to the controls team.

$$Z = \begin{bmatrix} x_1 \\ x_2 \\ x_3 \\ \dot{x}_1 \\ \dot{x}_2 \\ \dot{x}_3 \end{bmatrix} \tag{4.33}$$

Chapter 5

Experimental Design

5.1 Test Design

5.1.1 Test structure

The experiment structure would have to mimic the design of the module. Bosch provided by HYPED was utilised to create the main test structure. The CAD and real image can be seen in figure 5.1.

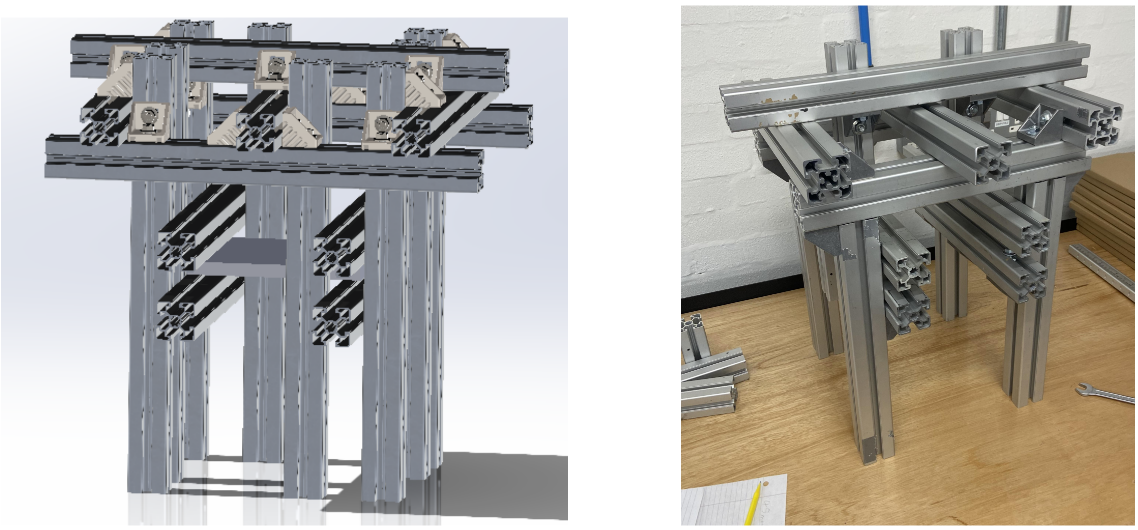

(a) CAD of Test Structure (b) Construction of Test Structure

Figure 5.1: Outer Test structure

This test structure would hold the main components: hybrid magnet, load cell and steel plate. The test structure will have the hybrid magnet fixed at the top and the load cell fixed at the bottom. The steel plate would then be attached to the bottom end of the load cell to provide a force that could be measured from the electromagnet by adjusting the air-gap and the current applied. This can be visualised in the figure 5.2.

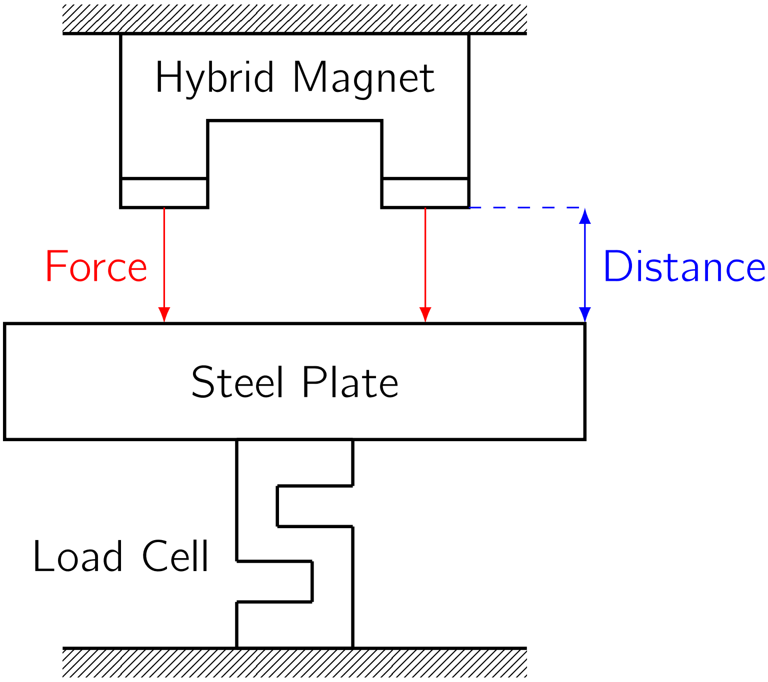

Figure 5.2: Simplified sketch of test setup

This setup was completed while also using a power supply for the coils (figure 5.3).

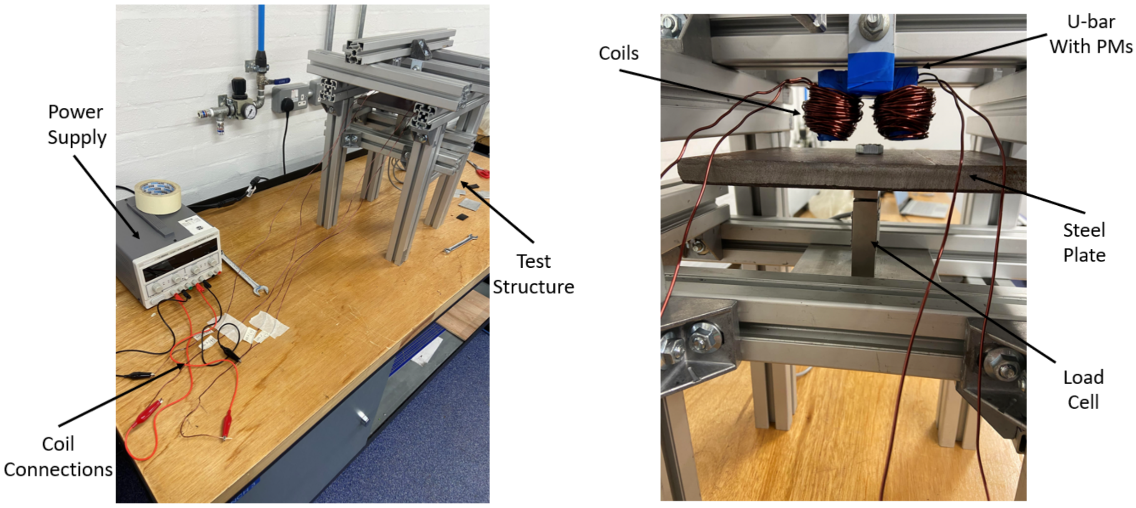

(a) Entire Test Setup

(b) View inside Test Structure

Figure 5.3: Full Test Setup

5.1.2 HEMS equivalent Hybrid Magnet

The hybrid magnet was created using a steel bar, cut into 3 pieces and welded together. This was followed by placing the permanent magnets (PMs) onto the u-bar and ensuring correct orientation (orientation must be opposite to one another for a stronger flux path). This is seen in figure 5.4a. Next the coils were wrapped around the bar (figure 5.4b), additionally using tape to ensure there are no shorts in the circuit.

(a) U-bar with PMs attached

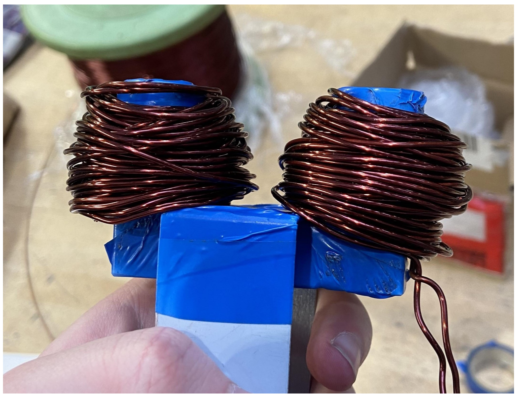

(b) Coils added

Figure 5.4: Hybrid Magnet

5.1.3 Potential Flaws

The disc shape of the magnets cannot be modelled in FEMM and instead an "equivalent representation" has to be used. This could result in an inaccuracy between experimental results and simulations.

Additionally in figure 5.4a, underneath the magnets there is an epoxy layer to ensure they stay in place though this has consequences of adding an additional reluctance / air-gap that is not taken into account in simulations.

5.2 Test Procedure

A Risk Assessment and SSOW (Appendix B) was completed both for both the construction and the testing of the module. The Hybrid magnet always remains in positions at the top of the structure. The plate the load cell was fixed to would be adjusted to create different air-gaps for taking results.

1. Load Cell is calibrated to take into account the weight of the plate ie 0N when the plate is on
2. Load Cell is positioned using the plate it is fixed to and secured by tightening bolts in the main structure.
3. Using Flex-logger record the force values being exerted on the load cell.
4. Adjust the current value through steps 0A, 0.5A, 1A, 1.5A, 2A, 2.5A and 3A.
5. Reposition the load cell and repeat steps 3 & 4.

From here the data could then be utilised in Matlab for visualisation.

Chapter 6

Results & Analysis

6.1 Theoretical Results

6.1.1 FEMM Results

Tables for the data are in Appendix A.

First an analysis of the data by looking at the change in force due to distance while the current is constant. This essentially keeps the current at 0A and moving the magnet further away and seeing the change in force values which can be seen in figure 6.1.

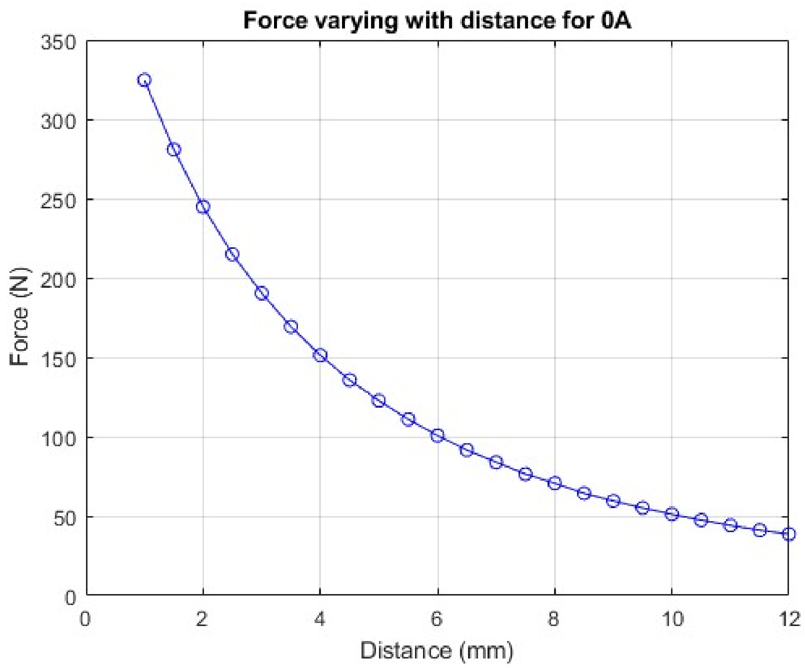

Figure 6.1: Force Variation for varying distance and constant current at 0A

As expected the force decreases the further the magnet is away from the plate. This is the same if the current is constantly 1A, 2A or 3A, which can be plotted as individual lines.

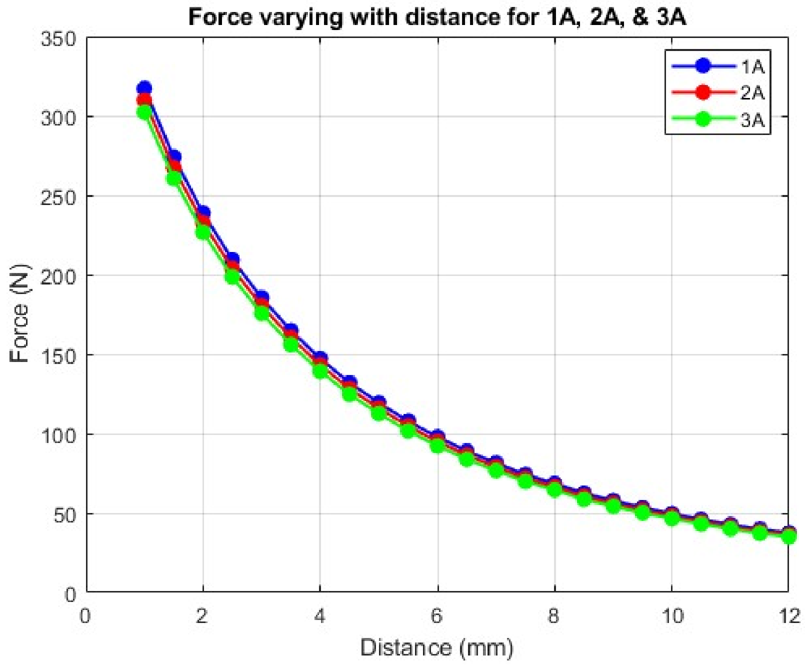

Figure 6.2: Force Variation for varying distance and constant current at 1A, 2A & 3A

This again is as expected with each line following the same trend and decreasing with distance. As anticipated, each line exhibits a consistent trend, with force values decreasing as the distance increases. Notably, the interaction between current and force aligns with expectations; at any given distance, the force at 3A is consistently lower than at 2A, this is the same relationship between 2A and 1A respectively.

The next step in the analysis is validating the current interaction for the system. Now each line can be plotted for constant distance and changing current.

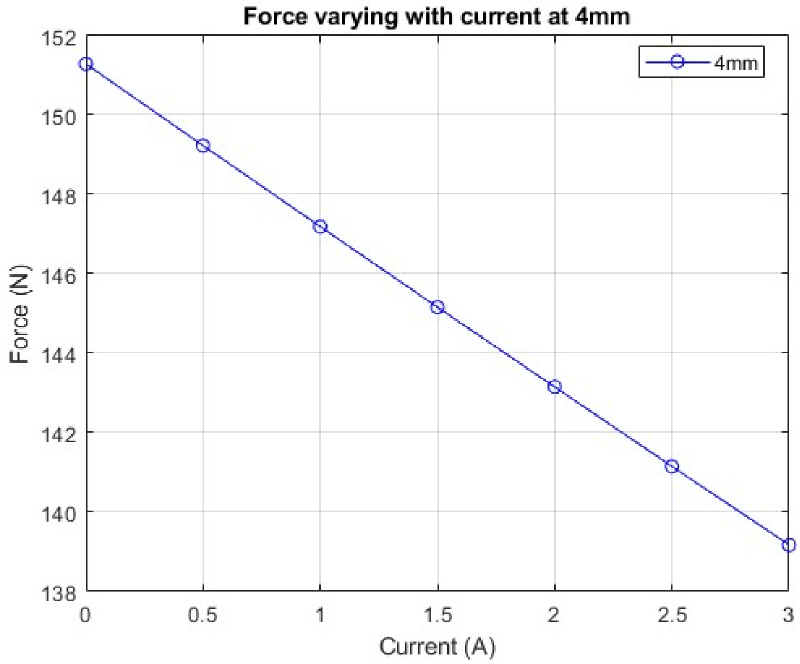

Figure 6.3: Force Variation for varying current and constant distance at 4mm

The force decreases as current increases so the system is setup correctly with current flowing in the correct direction. This can then be visualised for multiple distances, figure 6.4 shows this for 2, 4, 6, 8 and 10mm.

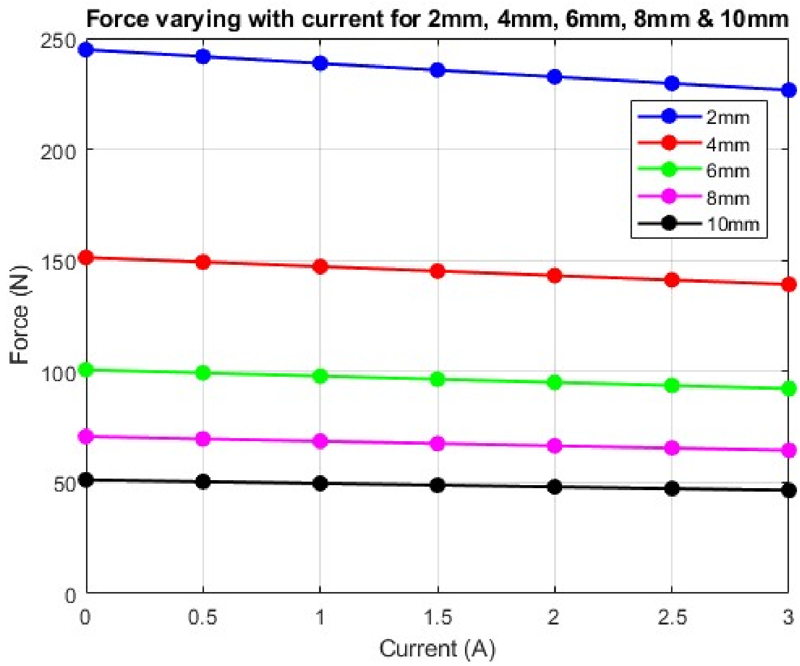

Figure 6.4: Force Variation for varying current and constant distance at 2, 4, 6, 8 & 10mm

Looking at figure 6.5, the gradient of the lines varies with the distance as well. At 2mm the gradient is larger in magnitude compared to that of 4mm. Thus a plot of all the gradients can be made against distance to see the variation in the data. The gradient would be expected to decrease as distance increases as the effect of the electromagnet decreases with distance.

Figure 6.6 plots the gradients against distance to see the effectiveness of the electromagnet component.

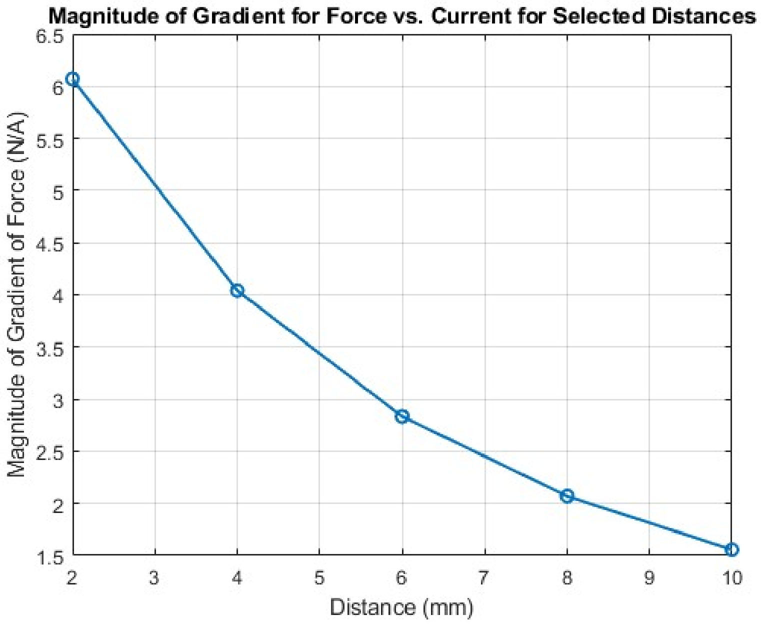

Figure 6.5: Magnitude of Gradient for Force vs Current for distance at 2, 4, 6, 8 & 10mm

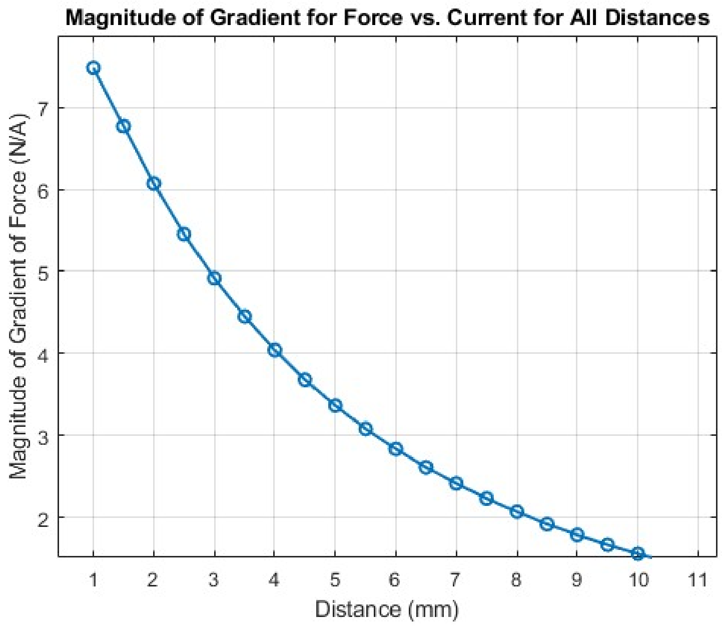

Figure 6.6: Magnitude of Gradient for Force vs Current for distance all distance

6.1.2 Reluctance Network (RN)

The mathematical model can be re-utilised for this experiment by adjusting some of the values since the equivalent circuit is the same.

This can be used to achieve the the theoretical results for the same range of values and the plots for each can be produced. The three areas to view are:

- The force against distance and constant current 0A. For comparison of the strength of the magnets.
- The force against current for specified distances. For comparison of the affect of the current and thus the effect of the electromagnet.
- The gradients for the force against current graph for the effectiveness of the electro-magnets with varying distances.

For clarification effectiveness of the electromagnet in this scenario is the counter force it can produce based on current input. It is more effective if at 1A it creates a counter force of 10N than 5N. This should directly relate to distance and so a change of gradient across the multiple currents can be observed when plotted against distance.

The force variation with distance while keeping the current constant at 0A was analysed. This allowed for a comparison of the magnetic strength of the system. Figures 6.7a and 6.7b present the plotted results, showcasing a decrease in force with an increase in distance.

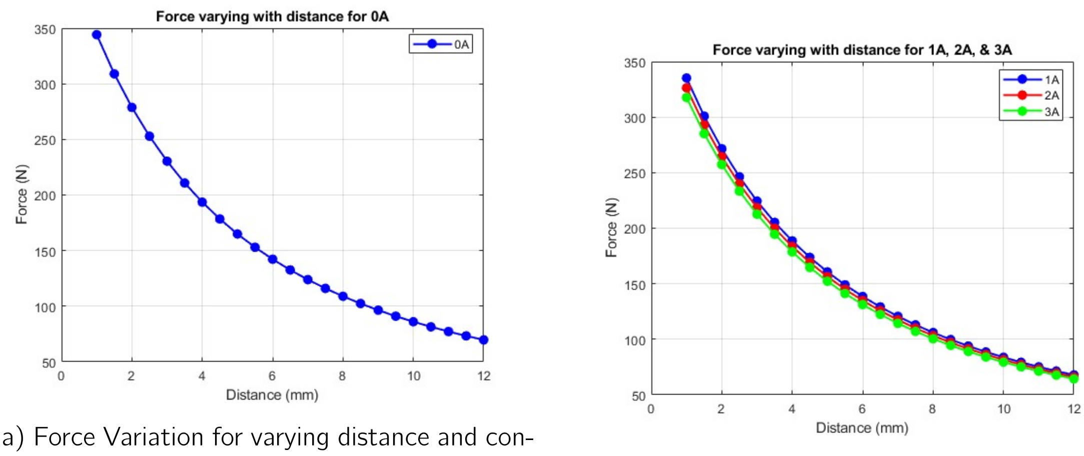

(a) Force Variation for varying distance and constant current at 0A

(b) RN - 1A, 2A, 3A

Figure 6.7: Force Variation for Varying Distance and Constant Current at 0A and 1A, 2A, 3A

Force Variation for Varying Current and Constant Distance

The force variation with current for specified distances was examined, providing insight into the effect of current on the electromagnet and the overall force exerted. Figures 6.8a and 6.8b illustrate this variation, demonstrating the influence of current on the force produced by the electromagnet.

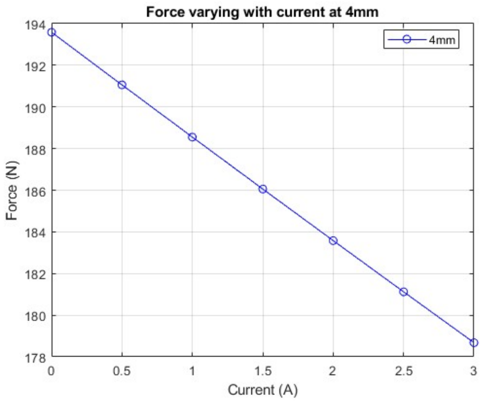

(a) RN - 4mm

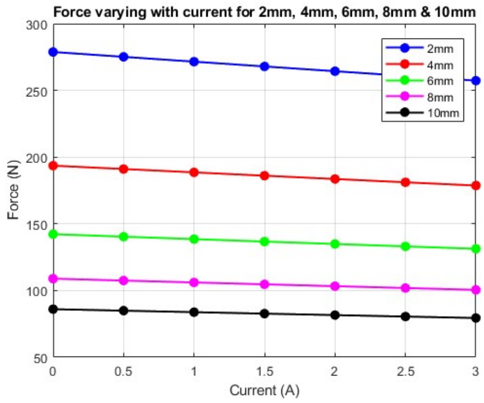

(b) RN - 2, 4, 6, 8, 10mm

Figure 6.8: Force Variation for Varying Current and Constant Distance at 4mm and 2, 4, 6, 8, 10mm

The gradients of force variation with current were examined to assess the effectiveness of the electromagnet across varying distances. Figures 6.9a and 6.9b depict these gradients plotted against distance, showcasing the expected decrease in gradient as distance increases.

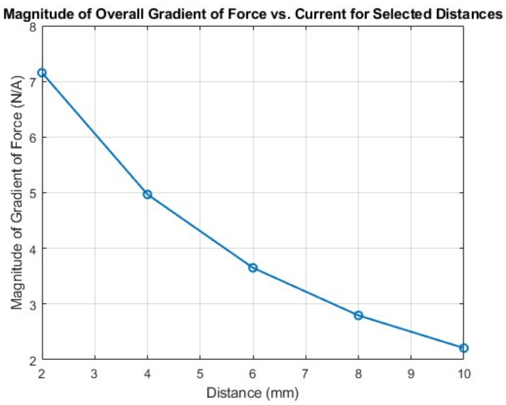

(a) RN - 2, 4, 6, 8 & 10mm

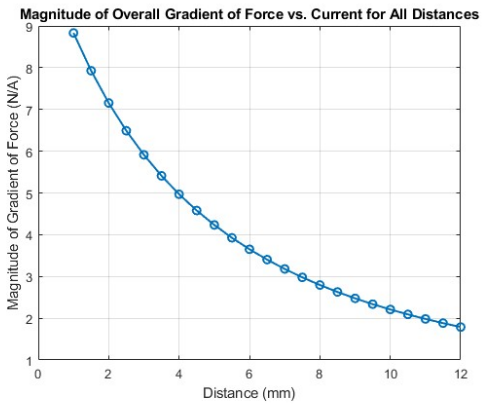

(b) RN - all distances

Figure 6.9: Gradients of Force Variation with Current

6.1.3 Theoretical Comparison

A comparison between FEMM and RN theoretical results provides valuable insights into the model's accuracy and performance across different scenarios.

Force Variation for Varying Distance and Constant Current at 0A

Figure 6.10 illustrates the comparison between FEMM and RN theoretical results for force variation with distance while keeping the current constant at 0A.

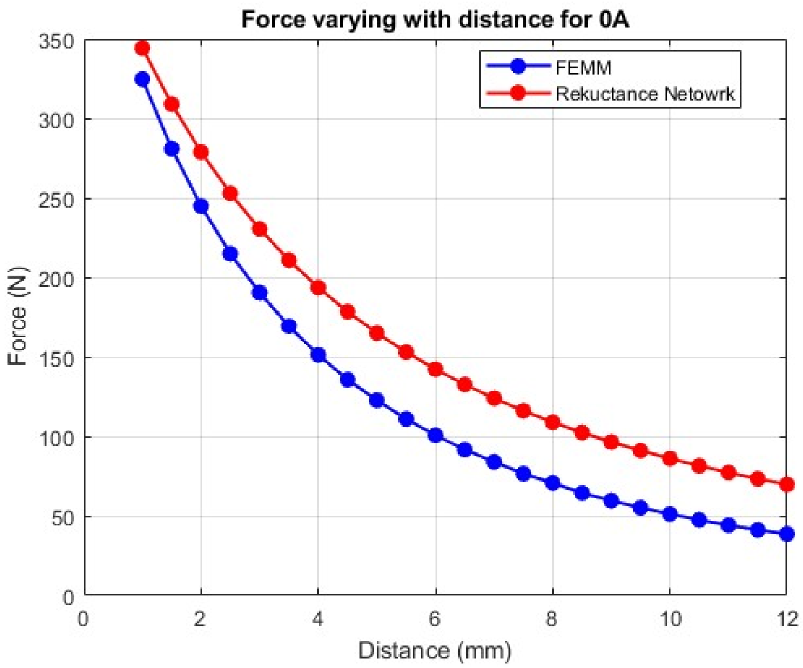

Figure 6.10: Comparison of Force Variation for Varying Distance and Constant Current at 0A

RN theoretical values exhibit higher force magnitudes compared to FEMM across all distances, indicating that the magnets are considered stronger in the RN model. This is due mainly to the simplification of the reluctance of the steel as it was assumed to be infinitely permeable. Further testing could be done to determine a value for the steel reluctance and then a more accurate model could be prepared.

Force Variation for Varying Current and Constant Distance

Figure 6.11 presents the comparison between FEMM and RN theoretical results for force variation with current for constant distances.

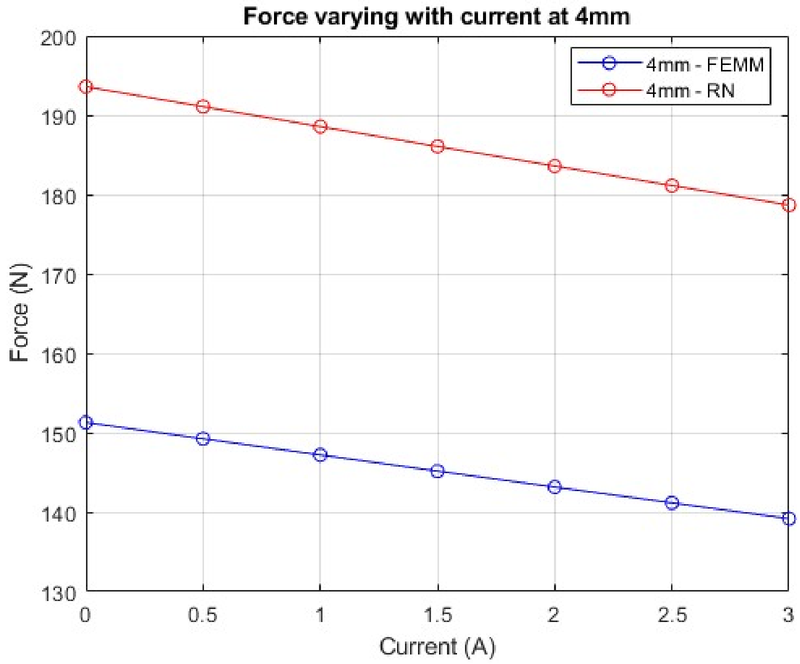

Figure 6.11: Comparison of Force Variation for Varying Current and Constant Distance

RN theoretical values again exhibit higher force magnitudes compared to FEMM for all current values, indicating a stronger effect from the electromagnet in the RN model. Again this is due to simplification for the reluctance of the steel as it was assumed to be infinitely permeable for the RN.

Gradients of Force Variation with Current

Figure 6.13 illustrates the comparison between FEMM and RN theoretical results for gradients of force against current for select distances.

RN theoretical values depict lines of greater gradients that start at higher values compared to FEMM, indicating a stronger effect from the electromagnet in the RN model.

Figure 6.14 illustrates the comparison between FEMM and RN theoretical results for gradients of force against current for all distances. RN theoretical values depict higher gradients compared to FEMM across all distances, further indicating a stronger effect from the electromagnet in the RN model due to modeling less reluctance.

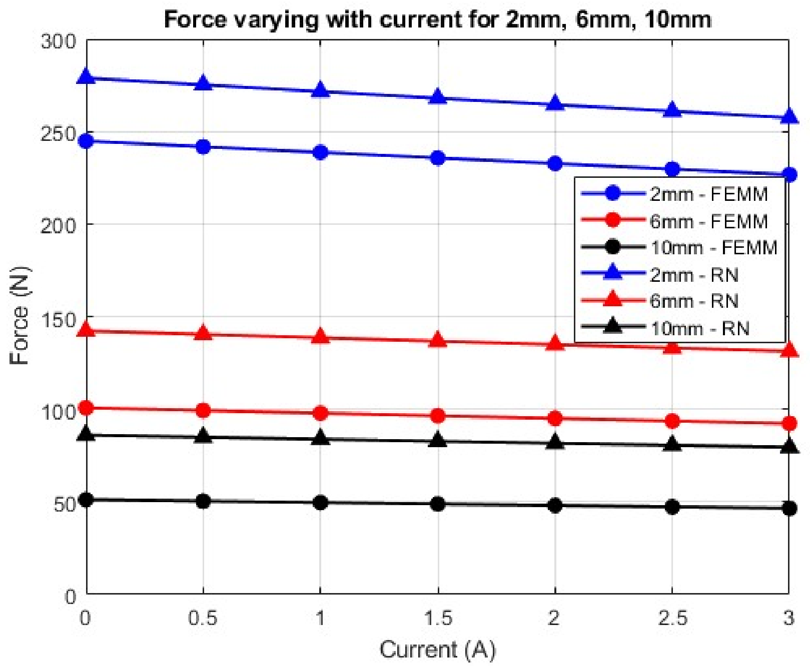

Figure 6.12: Comparison of Force Variation for Varying Current and Constant Distance

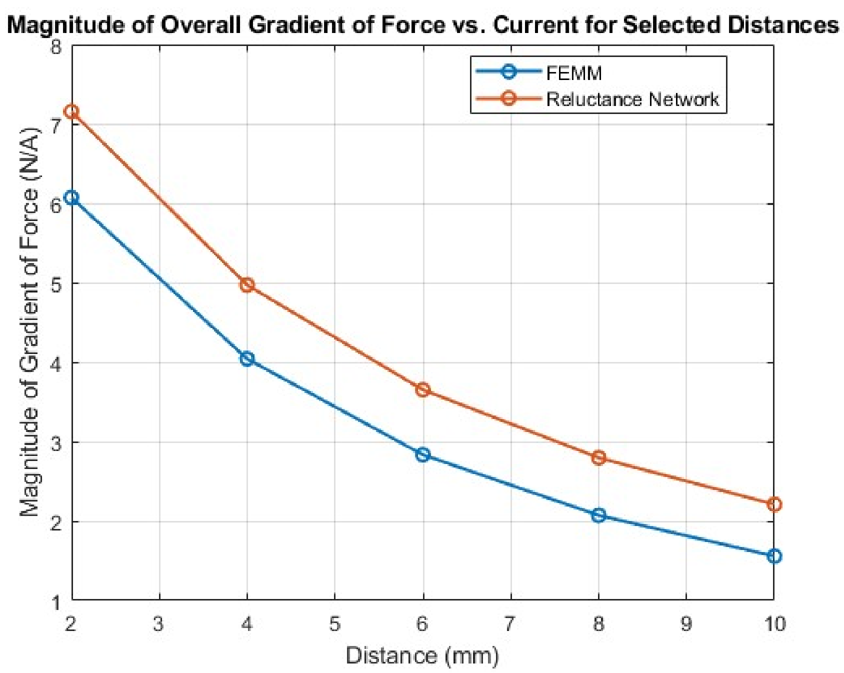

Figure 6.13: Comparison of Gradients of Force Variation with Current

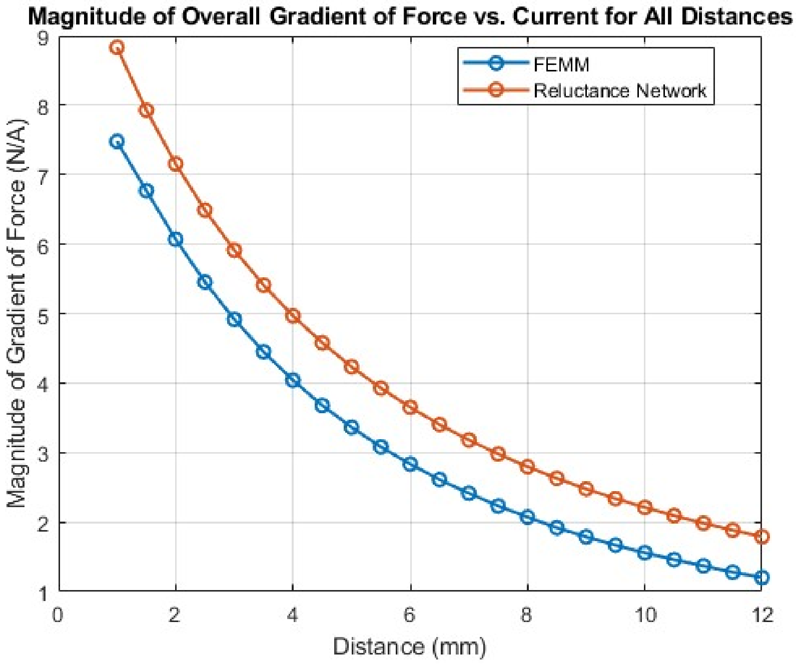

Figure 6.14: Comparison of Gradients of Force Variation with Distance

6.2 Experimental Results

The experimental results were gathered and formatted for a comprehensive analysis alongside theoretical predictions. This section compares the experimental outcomes and theoretical models, focusing on the force variations observed at zero current and the dynamic interactions due to varying currents.

6.2.1 Zero Current Values

The experimental forces recorded were consistently weaker than those anticipated by theoretical models.

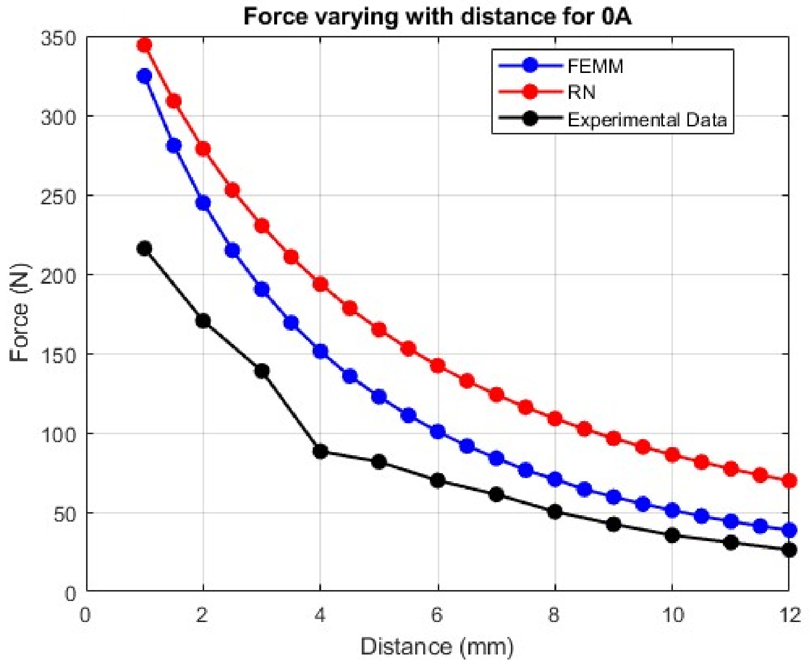

Figure 6.15: Experimental Force Variation with Distance at 0A

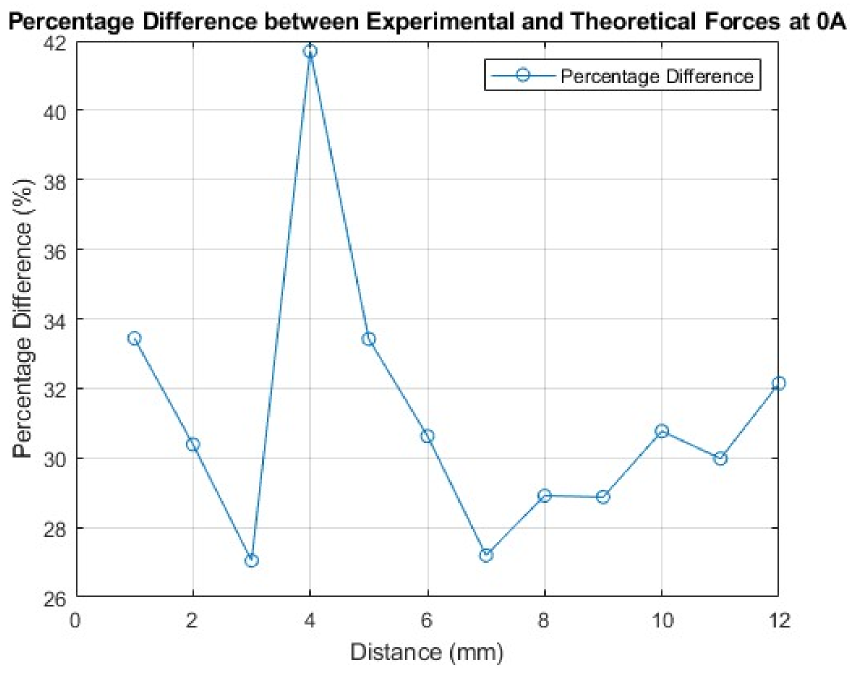

Figure 6.16: Experimental Force Variation for Varying Distance at Constant Currents

This variance can be attributed to several overlooked factors in the theoretical modeling. Most notably, the presence of an epoxy layer used to affix the magnets introduces an unaccounted air gap, significantly adding reluctance to the magnetic circuit. The exact measurement of this epoxy layer, is difficult to obtain and was absent in the theoretical considerations. However is explored in greater detail in the discussion.

Force Variation with Current

The experimental force variations across different current values were plotted. Figures 6.17 and 6.18 showcase these variations for predetermined distances, underscoring the behavior of the system under the influence of electrical currents.

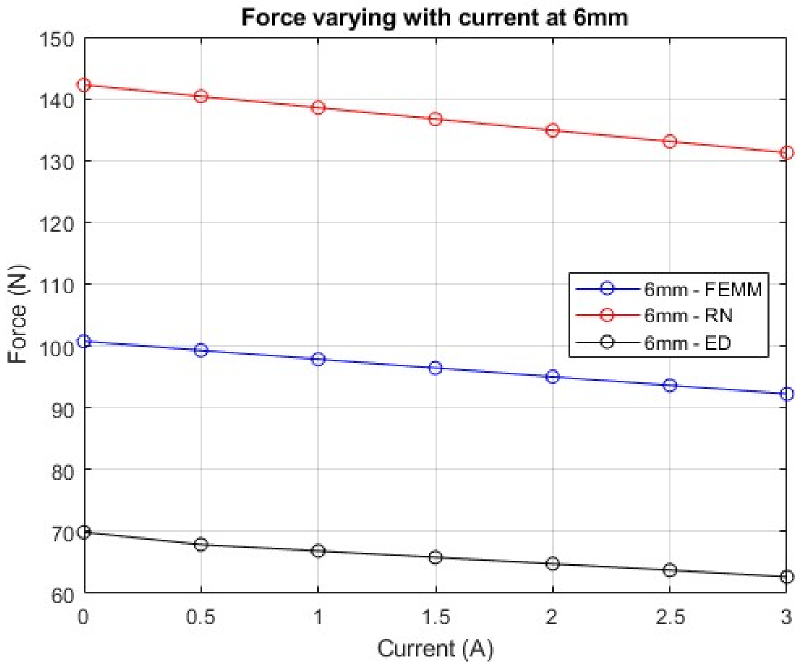

Figure 6.17: Experimental Force Variation for Varying Current at a Constant Distance

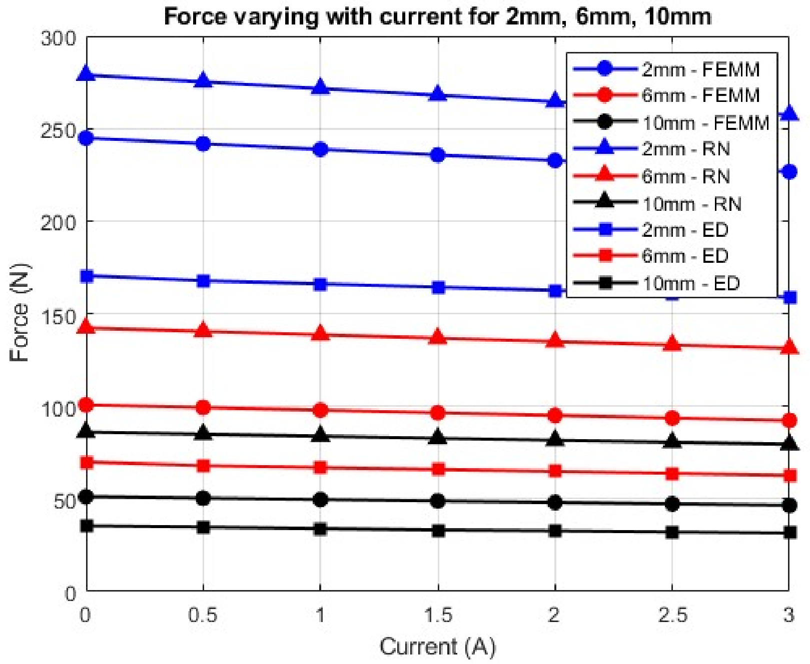

Figure 6.18: Further Experimental Force Variation for Varying Current at Constant Distances

Gradient Analysis

The gradient analysis again offers insight into the effectiveness of the electromagnet system across various operational scenarios. Figures 6.19 and 6.20 compare these gradients.

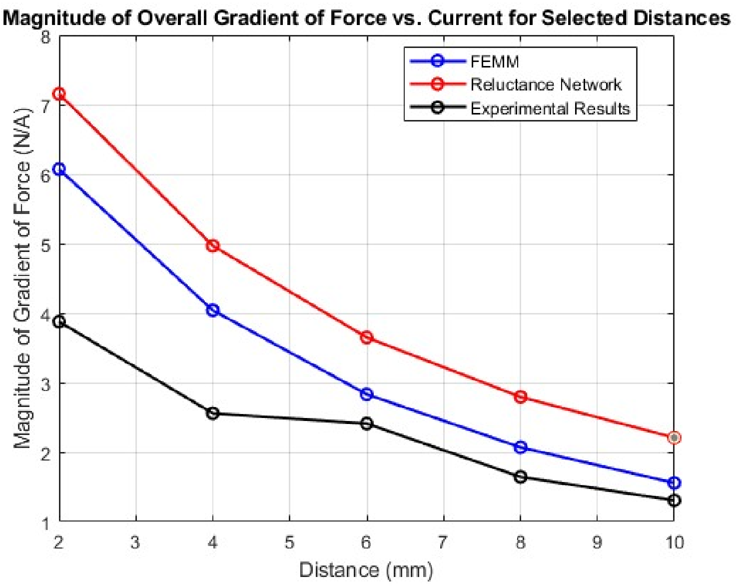

Figure 6.19: Gradients of Experimental Force Variation with Varying Current

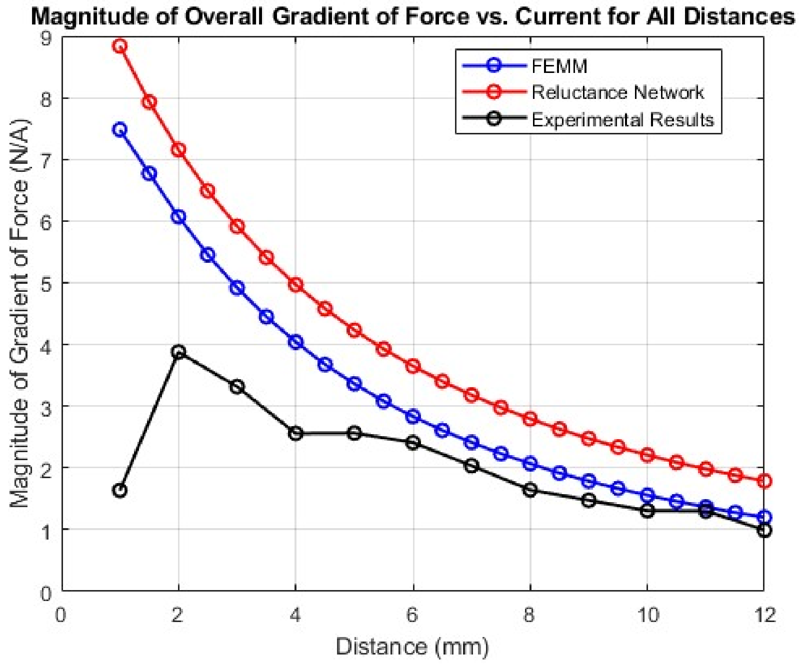

Figure 6.20: Gradients of Experimental Force Variation with Varying Current at Different Distances

The analysis indicates a weaker response in the experimental setup compared to theoretical models. Specifically, at 1mm, the force gradient significantly deviates, likely due to the load cell's calibration for forces below 200N. Since the results at 1mm all exceed 200N, this discrepancy could distort the scaling and, consequently, the gradient among the results.

6.2.2 3D Visualisation

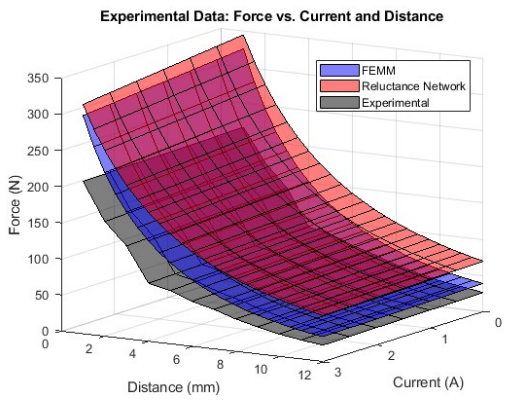

(a) View 1

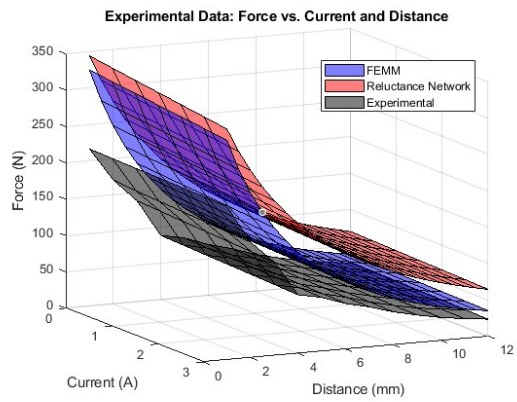

(b) View 2

Figure 6.21: 3D Visualisation of data

6.3 Discussion of Results

6.3.1 Additional Reluctance / Air-gap

It is clear that both the lines for the strength of the magnets and the effectiveness of the electromagnet fall beneath their expected values from the theoretical. This discrepancy can be better visualised by incorporating a shift in values. Adding 1.5mm to all measured distances brings the experimental results for both the permanent magnet strength and electromagnet effectiveness significantly closer to their expected theoretical values.

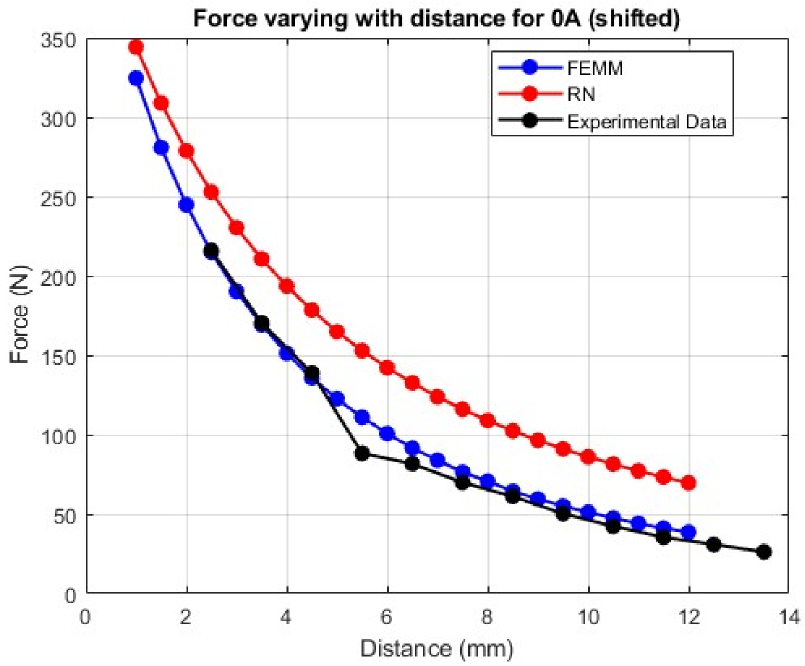

Figure 6.22: Experimental Force Variation with Distance at 0A (Shifted Values)

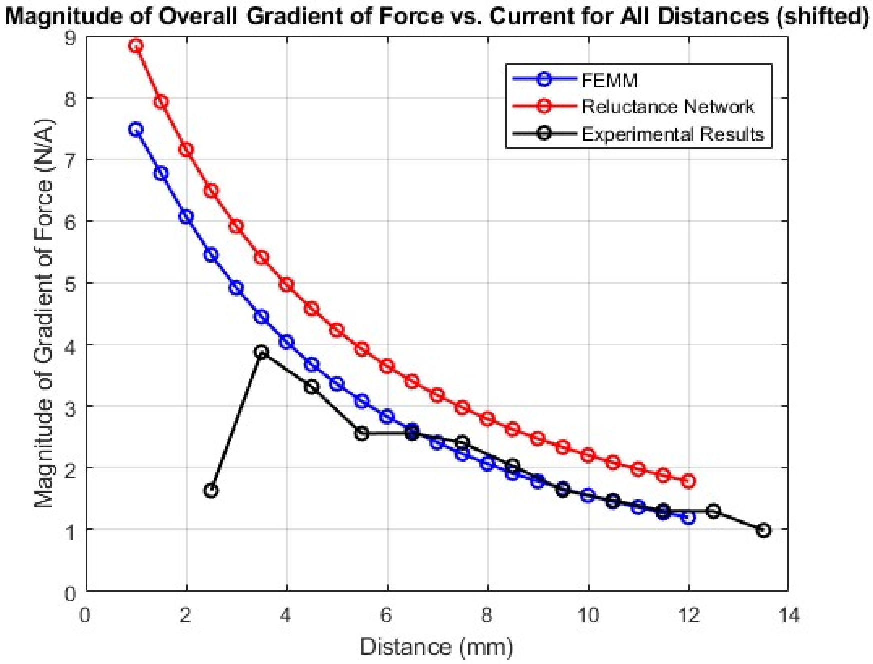

Figure 6.23: Experimental (Shifted Values)

Additional variations from the shifted values can be accounted for with uncertainties for measurements. The reluctance network appears has been simplified too much for accurate results and a permeability of the steel could be determined and then utilised in the model in order to improve it. Thus for creating the final design FEMM will be utilised along with an appropriate modification in order to take into account the new values. One way will be the shifted values as seen. Additionally a multiplication factor could be utilised which would be approximately 0.75 of every force value.

Figure 6.24 shows the 3d representation of the shifted values but this time shifting by 2mm (to more closely reflect the amount of epoxy required for the final design due to repulsive forces between each magnet), then figure 6.25 shows the FEMM values multiplied by a factor of 0.75.

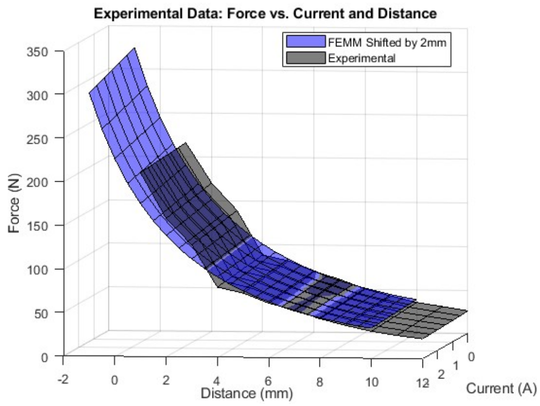

(a) View 1

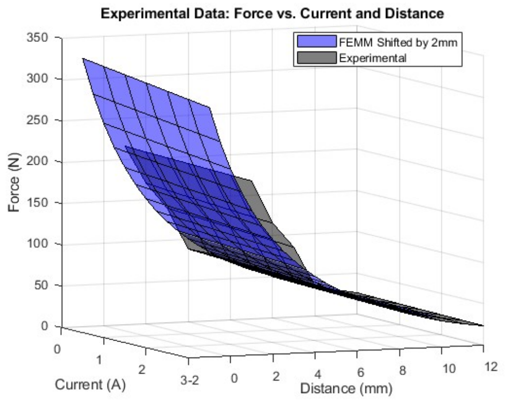

(b) View 2

Figure 6.24: Values shifted by 2mm

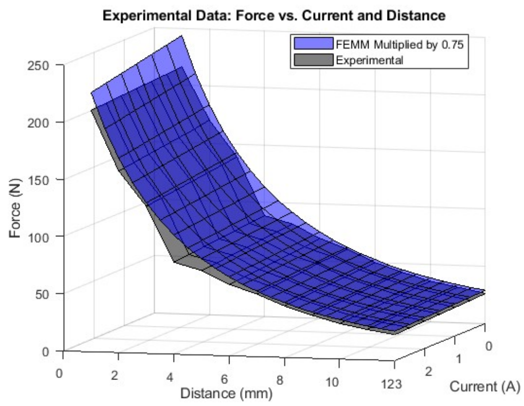

(a) View 1

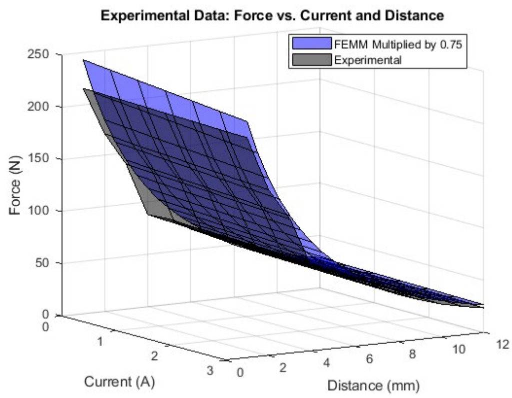

(b) View 2

Figure 6.25: Multiplication factor of 0.75

6.3.2 Concluding remarks

The experiment and the analysis helpfully concluded how the simulations translate into experimental results and thus how the final design will act. Using the information from the discussion, a successful adaption from FEMM can be done for the final design by multiplying by a factor of 0.75 or shifting the values by approximately 1.5 - 2mm depending on the amount of epoxy applied.

Chapter 7

Final Design

7.1 Updates to design

7.1.1 Magnetic force strength

Based on the experimental results the main conclusion drawn is that there will be an additional reluctance / air-gap due to the epoxy that will result in a less effective electromagnet at each distance and a less effective permanent magnet. The final configuration then is going to use larger magnets to ensure there will be a big enough air gap for the stating point (Vertical suspension constraint requires the start distance of the magnets from the track to be at least 7mm). Simulations can be done to verify that the starting displacement is greater than 7mm and to find forces at all levels. This can be plotted in 3d (figure 7.3).

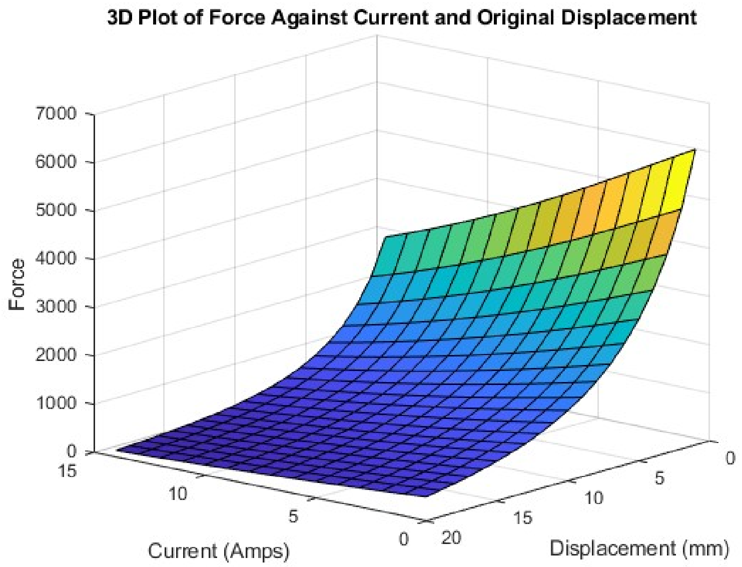

(a) FEMM Forces for Final Design

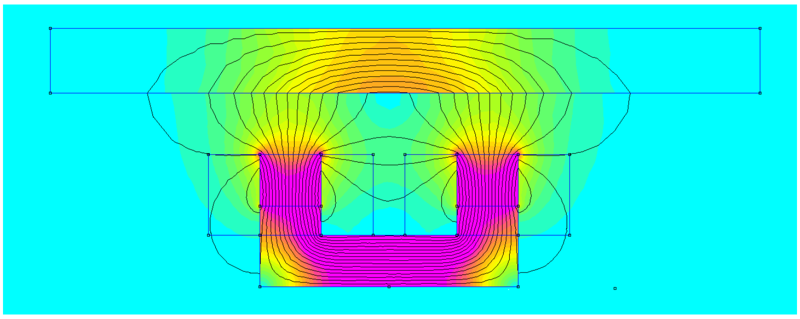

(b) Image of simulation

Figure 7.1: Final Estimate of Forces

Two methods of estimates can be used for the new values, both are plotted on figure 7.2 which shows the FEMM with a multiplication factor (MF) of 0.75 and with a shift in value of approximately 2mm. The reason for using the 2mm shift instead of the 1.5mm is that it guarantees that even if the epoxy layer is slightly larger for the final design, it will still have a starting point of at least 7mm from the track.

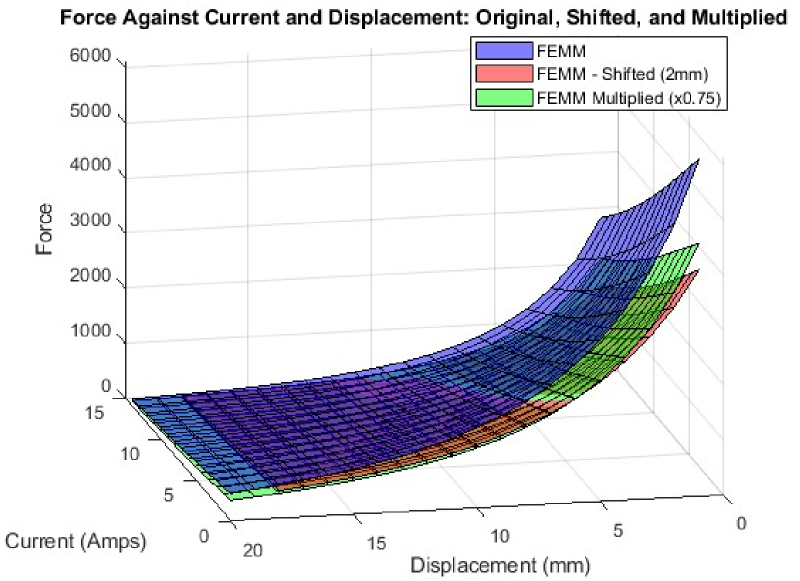

(a) Angle 1

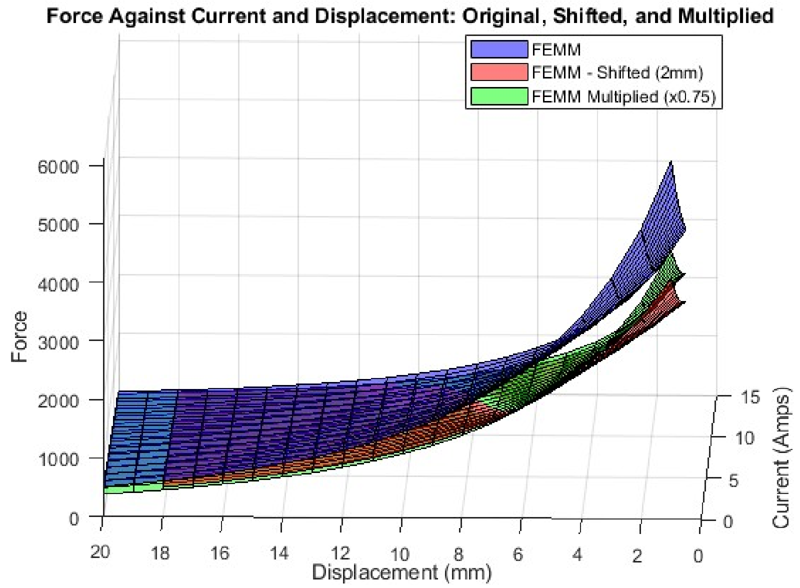

(b) Angle 2

Figure 7.2: Final Estimate of Forces

With these simulations the starting point with the 2mm shift comes to 8mm guaranteeing the 7mm distance. This alongside knowledge of the weight of the pod means we know the balance force and thus current and distance to ensure it remains balanced. The pod is estimated to weigh 250kg so the 625N (quarter of the weight due to there being 4 modules) can be viewed.

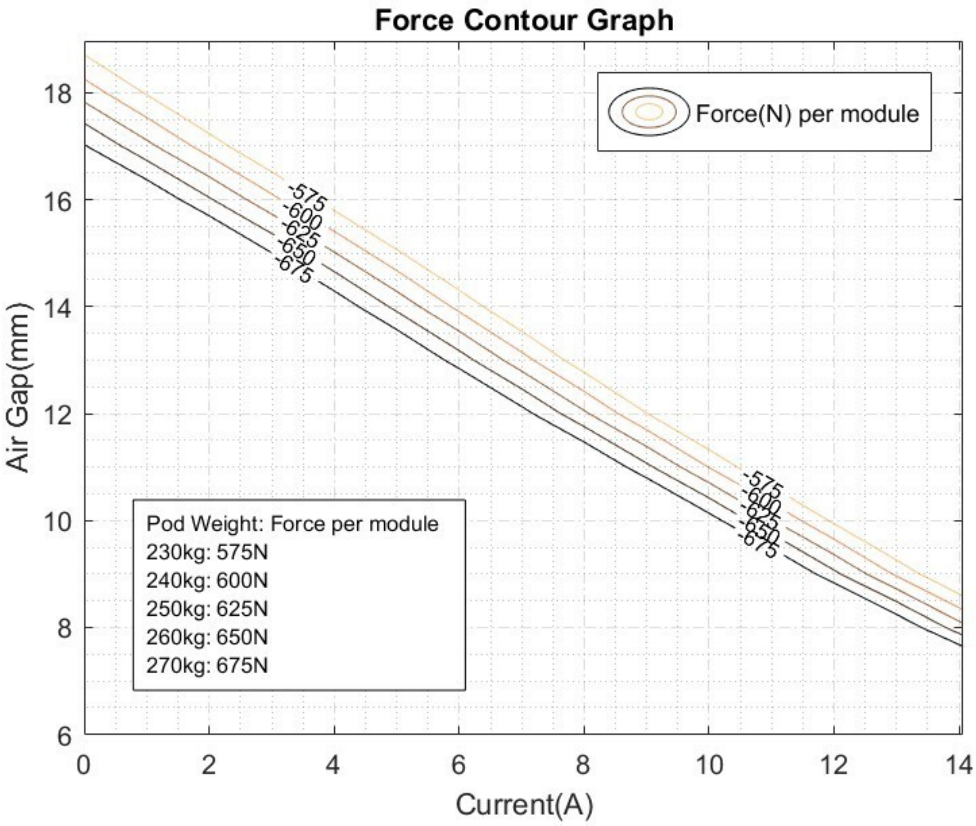

Figure 7.3: Final Force plot

If the displacement of the HEMS is greater than the target displacement then the force value will be need to be in the region below the force line (by changing the current) and if the displacement is less than the target displacement then it will need to be above this line.

7.1.2 Final CAD

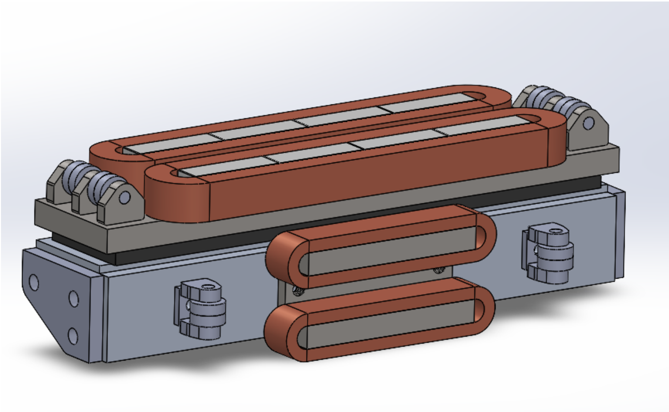

(a) Isometric View

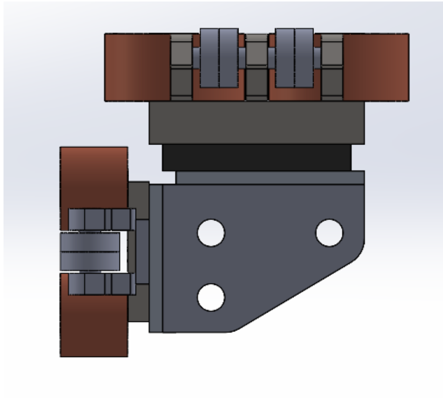

(b) Side View

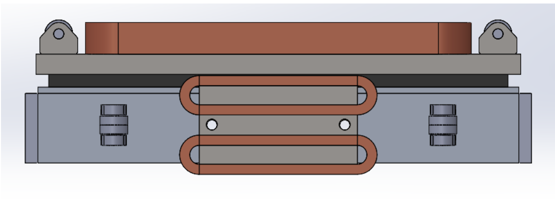

(c) Front View

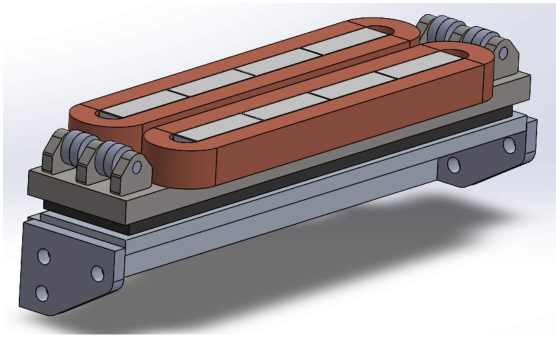

(d) Reversed Isometric View

Figure 7.4: Final CAD of Levitation Module

7.2 Safety Components

7.2.1 Structural

All components have been checked with a safety factor of 2 to ensure adequate strength in the structure. This is especially prevalent in the bracket which holds the other components together and attaches to the main pod.

7.2.2 Wheels

Safety wheels are included in the case of the vertical suspension failing. These are designed to stop the magnets colliding with the track. This is a crucial component to have to ensure the cannot collide causing them to break and scatter. additionally a layer is added on top of the magnets.

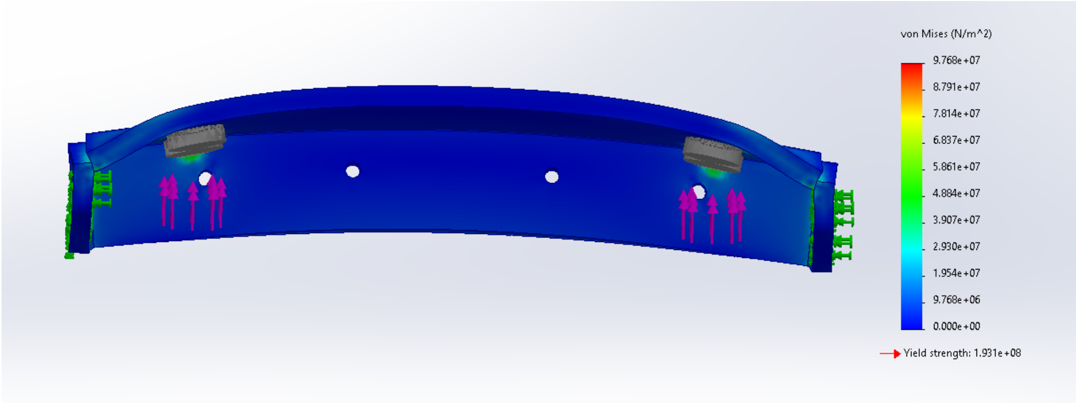

Figure 7.5: Bracket FEA Results

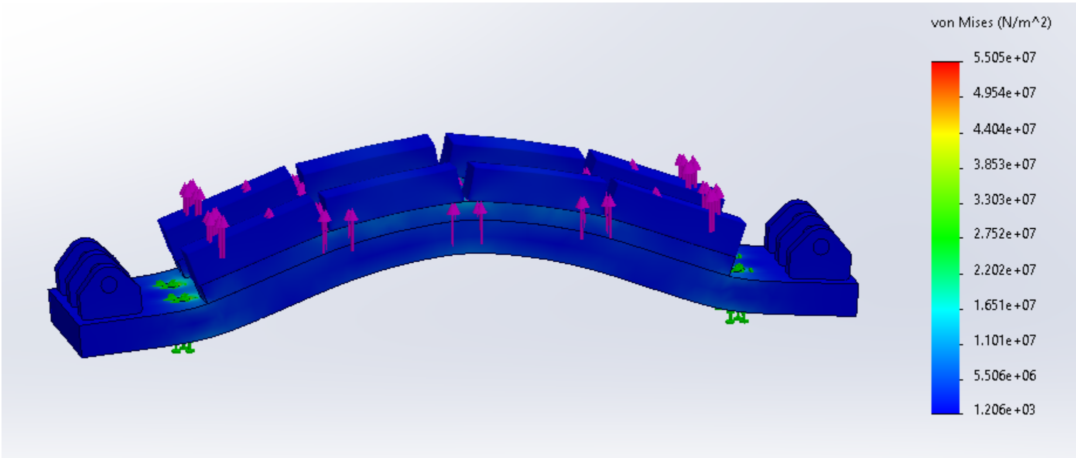

Figure 7.6: HEMS Core FEA Results

7.2.3 HEMS Core

The HEMS core is the critical component having the permanent magnets and safety wheels attached. After testing to ensure there was no yielding and the structural stability with the forces it undergoes it was also crucial to check the bending imposed. From previous results it is clear the difference a mm makes and if the middle of the HEMS core with the magnets attached bends to become closer than calculated for, then the force will increase causing a failure.

Bending was checked for worst case scenario where the HEMS detaches from the bracket and slams up into the track. With a safety factor of 2 for a 3400N force so a 6800N load applied in simulations, the bracket would bend the greatest in the middle with a displacement of 0.12mm. A maximum of 0.3mm was determined so the 0.12mm was deemed acceptable.

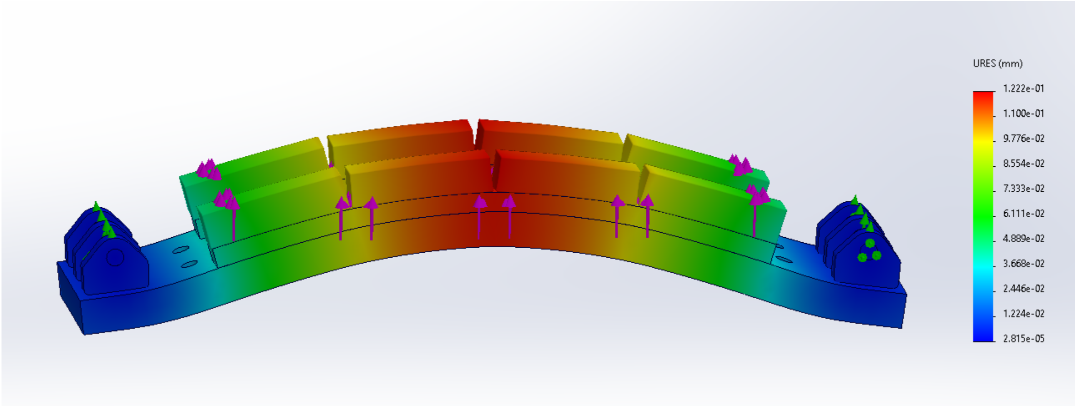

Figure 7.7: Displacement Results for the HEMS Core

7.3 Manufacturing

The process for creating each of the 4 components:

- Machining of individual pieces eg holes
- Welding to create each of the four modules
- For EMS and HEMS, both require coil winding and then placing this onto the welded core
- Using threaded rods and nuts to attach all the components to the bracket

From here it can be attached onto the main pod. Drawings for the components are included in Appendix C.

Chapter 8

Conclusion

Based on the comprehensive work undertaken in this project aimed at designing a levitation system for HYPED's hyperloop pod, significant progress has been made towards achieving the outlined objectives. The project successfully developed a final design for the levitation module, incorporating both permanent magnets and electromagnets. This approach aimed to optimise the levitation module for power efficiency, a key objective of the project which was primarily achieved in the choice of the levitation method and determining an appropriate air gap to maintain. Though it can be improved by altering controls for using the zero current air gap to take full advantage of the magnetic force from the permanent magnets.

The mathematical modeling and simulations, using Finite Element Method Magnetics (FEMM) and reluctance network analysis, have been important for understanding the interactions between the magnetic fields and the levitation dynamics. This rigorous analysis has informed the design process, leading to the development of the final design that aligns with the pod's specifications and the constraints of the track, chassis and other sub-systems.

Experimental designs and testing have provided valuable data, validating the theoretical models and highlighting areas for improvement. The iterative design process, informed by both theoretical and experimental insights, has led to the refinement of the levitation module. Adjustments to magnet size have been made to account for unforeseen factors such as the epoxy layer's impact on magnetic field strength, ensuring the final design meets the performance criteria.

While the objectives have been fully met, the project has encountered challenges, notably in delays for testing. These challenges have provided learning opportunities. There is currently still the difficulty with controlling the system which aimed to be achieved before July for EHW and without these delays this would have been easier to achieve.

Future work will concentrate on controls and further adapting these to make use of the zero current air gap and preparing for the demonstration at the EHW.

This project has demonstrated the feasibility of integrating a levitation system into HYPED's hyperloop pod, marking a significant step forward for the society and the development of sustainable and efficient transportation solutions. The experiences and knowledge gained from this project will undoubtedly contribute to the ongoing advancement of high - speed transportation technology.

References

[1] J. Jaimon, "Design and testing of the suspension system for high speed transportation," Ph.D. dissertation, The University of Edinburgh, 4 2020, phD thesis.

[2] Y. Feng, C. Zhao, D. Wu, H. Xie, and L. Tong, "Effect of levitation gap feedback time delay on the ems maglev vehicle system dynamic response," *Nonlinear Dynamics*, vol. 111, no. 8, pp. 7137–7156, 2023.

[3] Z. Long, G. He, and S. Xue, "Study of eds ems hybrid suspension system with permanent-magnet halbach array," *IEEE Trans Magn*, vol. 47, no. 12, pp. 4717–4724, Dec 2011.

[4] H.-W. Lee, k.-c. Kim, and j. Lee, "Review of maglev train technologies," *Magnetics, IEEE Transactions on*, vol. 42, pp. 1917 – 1925, 08 2006.

[5] C. Lee, J. Jo, B. Kang, Y. Han, D. Bae, Y.-S. Yoon, Y. D. Chung, S. Chu, Y. J. Hwang, and T. Ko, "Conceptual design for hts coil in superconducting electromagnet for maglev," *Applied Superconductivity, IEEE Transactions on*, vol. 21, pp. 1560 – 1563, 07 2011.

[6] M. Mueller, "Reluctance networks," Lecture Presentation at The University of Edinburgh, 2024, accessed: 2023-10-30.

[7] E. Musk, "Hyperloop alpha," 2013.

[8] "European hyperloop week," accessed: 2024.

[9] D. J. Griffiths, *Introduction to Electrodynamics*, 4th ed. Harlow: Pearson Education UK, 2013.

[10] B. D. Cullity and C. D. Graham, *Introduction to magnetic materials*, 2nd ed. Hoboken, N.J: IEEE/Wiley, 2009.

[11] R. C. O'Handley, *Modern magnetic materials: principles and applications*. New York: Wiley, 2000.

[12] A. Aharoni, *Introduction to the theory of ferromagnetism*, 2nd ed., ser. Oxford science publications. Oxford: Clarendon, 2000.

[13] H. Kronmüller and S. S. P. Parkin, Eds., *Handbook of magnetism and advanced magnetic materials*. Chichester: John Wiley, 2007.

[14] G. Bertotti, *Hysteresis in magnetism: for physicists, materials scientists, and engineers*, ser. Academic Press series in electromagnetism. San Diego: Academic Press, 1998.

[15] A. N. Conejo, J.-P. Birat, and A. Dutta, "A review of the current environmental challenges of the steel industry and its value chain," *J Environ Manage*, vol. 259, p. 109782, 2020.

[16] W. Ko and C. Ham, "A novel approach to analyze the transient dynamics of an electrodynamics suspension maglev," *IEEE Trans Magn*, vol. 43, no. 6, pp. 2603–2605, 2007.

[17] P. K. Tripathy, K. Mondal, and A. R. Khanolkar, "One-step manufacturing process for neodymium-iron (magnet-grade) master alloy," *Mater Sci Energy Technol*, vol. 4, pp. 249–255, 2021.

[18] R. Zeng, V. Murashov, T. P. Beales, H. K. Liu, and S. X. Dou, "High temperature superconducting magnetic levitation train," *Applied Superconductivity*, vol. 5, no. 1, pp. 201–204, 1997.

[19] D. Zhai, X. Lai, J. Meng, G. Liu, J. Wu, and S. Xiao, "The hybrid suspension system for middle-to-low-speed maglev trains considering the prevention of firm absorption," *IEEE Transactions on Transportation Electrification*, vol. 8, no. 1, pp. 1482–1492, 2022.

[20] J. Bardeen, L. N. Cooper, and J. R. Schrieffer, "Theory of superconductivity," *Physical Review*, vol. 108, no. 5, pp. 1175–1204, Dec 1957.

[21] C. Yao and Y. Ma, "Superconducting materials: Challenges and opportunities for large-scale applications," 2021.

[22] C. C. Chow, M. D. Ainslie, and K. Chau, "High temperature superconducting rotating electrical machines: An overview," *Energy Reports*, vol. 9, pp. 1124–1156, 2023. [Online]. Available: https://www.sciencedirect.com/science/article/pii/S2352484722025628

[23] H. Tiegna, Y. Amara, and G. Barakat, "Overview of analytical models of permanent magnet electrical machines for analysis and design purposes," *Mathematics and Computers in Simulation*, vol. 90, pp. 162–177, 2013. [Online]. Available: https://www.sciencedirect.com/science/article/pii/S0378475413000049

[24] Y. Hane, K. Sugahara, and K. Nakamura, "A novel reluctance network model applicable for open magnetic circuits," *Journal of the Magnetics Society of Japan*, vol. 45, pp. 112–117, 06 2021.

[25] Z. Bi, "Chapter 8 - applications—solid mechanics problems," in *Finite Element Analysis Applications*, Z. Bi, Ed. Academic Press, 2018, pp. 281–339. [Online]. Available: https://www.sciencedirect.com/science/article/pii/B978012809952000008X

[26] ——, "Chapter 10 - applications—fluid mechanics," in *Finite Element Analysis Applications*, Z. Bi, Ed. Academic Press, 2018, pp. 379–405. [Online]. Available: https://www.sciencedirect.com/science/article/pii/B9780128099520000108

[27] ——, "Chapter 9 - applications—heat transfer problems," in *Finite Element Analysis Applications*, Z. Bi, Ed. Academic Press, 2018, pp. 341–377. [Online]. Available: https://www.sciencedirect.com/science/article/pii/B9780128099520000091

[28] ——, "Chapter 2 - decomposition," in *Finite Element Analysis Applications*, Z. Bi, Ed. Academic Press, 2018, pp. 31–60. [Online]. Available: https://www.sciencedirect.com/science/article/pii/B9780128099520000029

[29] ——, "Chapter 3 - description of elements," in *Finite Element Analysis Applications*, Z. Bi, Ed. Academic Press, 2018, pp. 61–111. [Online]. Available: https://www.sciencedirect.com/science/article/pii/B9780128099520000030

Appendix A

Data Tables

A1 - Experimental Data for Test Setup

Test - Experimental Data

Current (A)	0.0	0.5	1.0	1.5	2.0	2.5	3.0
Air Gap (mm)	Force (N)						
1.0	216.09	215.16	214.40	213.61	212.78	211.90	211.19
2.0	170.43	167.75	166.02	164.27	162.51	160.62	158.80
3.0	138.87	137.15	135.44	133.76	132.07	130.39	128.63
4.0	88.21	86.96	85.69	84.45	83.12	81.82	80.53
5.0	81.67	80.21	79.01	77.79	76.49	75.14	73.98
6.0	69.88	67.89	66.85	65.81	64.77	63.74	62.65
7.0	61.10	60.15	59.29	57.45	56.57	55.80	54.99
8.0	50.24	49.30	48.53	47.71	46.91	46.15	45.31
9.0	42.34	41.70	40.97	40.28	39.42	38.63	37.92
10.0	35.41	34.75	33.96	33.18	32.71	32.12	31.49
11.0	30.88	30.13	29.59	28.99	28.32	27.68	26.98
12.0	26.22	25.61	25.12	24.65	24.19	23.72	23.24

A2 - FEMM Data for Test Setup

Test - FEMM Data

Current (A)	0.0	0.5	1.0	1.5	2.0	2.5	3.0
Air Gap (mm)	Force (N)						
1.0	-324.65	-320.92	-317.17	-313.42	-309.67	-305.93	-302.21
1.5	-280.84	-277.41	-274.00	-270.60	-267.23	-263.87	-260.53
2.0	-244.82	-241.74	-238.68	-235.63	-232.61	-229.60	-226.61
2.5	-214.89	-212.12	-209.36	-206.63	-203.91	-201.21	-198.53
3.0	-190.35	-187.85	-185.36	-182.89	-180.44	-178.01	-175.60
3.5	-169.26	-166.99	-164.74	-162.51	-160.29	-158.09	-155.91
4.0	-151.29	-149.23	-147.19	-145.16	-143.15	-141.15	-139.17
4.5	-135.63	-133.76	-131.90	-130.05	-128.22	-126.40	-124.60
5.0	-122.66	-120.95	-119.25	-117.56	-115.88	-114.22	-112.57
5.5	-110.92	-109.35	-107.79	-106.24	-104.71	-103.19	-101.68
6.0	-100.74	-99.29	-97.86	-96.44	-95.03	-93.63	-92.24
6.5	-91.59	-90.26	-88.94	-87.63	-86.33	-85.04	-83.76
7.0	-83.92	-82.69	-81.47	-80.26	-79.06	-77.86	-76.68
7.5	-76.47	-75.33	-74.20	-73.08	-71.97	-70.87	-69.78
8.0	-70.68	-69.62	-68.57	-67.53	-66.50	-65.48	-64.47
8.5	-64.34	-63.37	-62.39	-61.43	-60.48	-59.53	-58.59
9.0	-59.53	-58.61	-57.71	-56.81	-55.92	-55.04	-54.17
9.5	-55.06	-54.21	-53.36	-52.53	-51.70	-50.88	-50.06
10.0	-51.15	-50.36	-49.57	-48.79	-48.01	-47.24	-46.48
10.5	-47.44	-46.69	-45.96	-45.22	-44.50	-43.78	-43.07
11.0	-44.10	-43.40	-42.71	-42.02	-41.34	-40.67	-40.00
11.5	-41.10	-40.45	-39.80	-39.16	-38.52	-37.89	-37.27
12.0	-38.64	-38.03	-37.42	-36.81	-36.22	-35.62	-35.04

A3 - Reluctance Network Data for Test Setup

Test - Reluctance Network Data

Current (A)	0.0	0.5	1.0	1.5	2.0	2.5	3.0
Air Gap (mm)	Force (N)						
1.0	344.15	339.66	335.20	330.77	326.36	321.99	317.65
1.5	308.88	304.85	300.84	296.86	292.91	288.99	285.09
2.0	278.76	275.12	271.51	267.92	264.36	260.81	257.30
2.5	252.84	249.54	246.27	243.01	239.78	236.57	233.38
3.0	230.38	227.37	224.39	221.42	218.48	215.55	212.64
3.5	210.78	208.03	205.30	202.59	199.89	197.21	194.55
4.0	193.58	191.06	188.55	186.06	183.58	181.12	178.68
4.5	178.41	176.08	173.77	171.47	169.19	166.92	164.67
5.0	164.95	162.79	160.66	158.53	156.42	154.33	152.25
5.5	152.95	150.96	148.98	147.01	145.05	143.11	141.18
6.0	142.22	140.37	138.53	136.69	134.88	133.07	131.27
6.5	132.59	130.86	129.14	127.43	125.73	124.05	122.38
7.0	123.89	122.28	120.67	119.08	117.49	115.92	114.35
7.5	116.03	114.52	113.01	111.52	110.03	108.56	107.10
8.0	108.89	107.47	106.06	104.66	103.26	101.88	100.51
8.5	102.39	101.06	99.73	98.41	97.10	95.80	94.51
9.0	96.46	95.20	93.95	92.71	91.47	90.25	89.03
9.5	91.02	89.84	88.66	87.48	86.32	85.16	84.02
10.0	86.04	84.91	83.80	82.69	81.59	80.50	79.41
10.5	81.45	80.39	79.33	78.28	77.24	76.21	75.18
11.0	77.22	76.21	75.21	74.22	73.23	72.25	71.27
11.5	73.31	72.35	71.40	70.46	69.52	68.59	67.67
12.0	69.69	68.78	67.88	66.98	66.09	65.20	64.32

A4 - FEMM Data for Final Design

Design - FEMM Data

Current (A)	0	1	2	3	4	5	6	7	8	9	10	11	12	13	14	15	16	17	18	19	20
Airgap (mm)	Force (N)																				
1	-6129.67	-5872.36	-5613.04	-5355.89	-5101.75	-4850.75	-4607.11	-4371.98	-4145.70	-3928.38	-3720.11	-3520.94	-3330.88	-3149.97	-2978.22	-2815.64	-2662.25	-2518.06	-2383.08	-2257.32	-2140.79
2	-4971.02	-4738.95	-4509.46	-4282.54	-4058.93	-3841.92	-3632.35	-3430.48	-3236.42	-3050.23	-2871.95	-2701.60	-2539.19	-2384.75	-2238.28	-2099.79	-1969.30	-1846.80	-1732.30	-1625.82	-1527.36
3	-4119.72	-3914.06	-3710.73	-3510.50	-3316.08	-3128.17	-2946.98	-2772.62	-2605.13	-2444.55	-2290.89	-2144.18	-2004.42	-1871.62	-1745.80	-1626.95	-1515.08	-1410.20	-1312.32	-1221.43	-1137.56
4	-3460.57	-3277.47	-3097.12	-2921.86	-2752.30	-2588.66	-2431.02	-2279.42	-2133.91	-1994.49	-1861.18	-1733.98	-1612.92	-1497.98	-1389.18	-1286.53	-1190.03	-1099.68	-1015.49	-937.46	-865.60
5	-2940.22	-2777.03	-2618.27	-2464.54	-2316.02	-2172.80	-2034.92	-1902.40	-1775.28	-1653.55	-1537.22	-1426.31	-1320.81	-1220.74	-1126.09	-1036.88	-953.10	-874.76	-801.87	-734.43	-672.43
6	-2523.03	-2378.61	-2238.60	-2103.19	-1972.47	-1846.48	-1725.26	-1608.81	-1497.15	-1390.28	-1288.21	-1190.95	-1098.51	-1010.87	-928.06	-850.06	-776.90	-708.56	-645.06	-586.39	-532.56
7	-2173.63	-2045.83	-1922.11	-1802.55	-1687.19	-1576.07	-1469.20	-1366.59	-1268.25	-1174.17	-1084.38	-998.87	-917.64	-840.71	-768.06	-699.71	-635.66	-575.91	-520.46	-469.32	-422.50
8	-1892.75	-1779.06	-1669.08	-1562.86	-1460.43	-1361.79	-1266.96	-1175.95	-1088.76	-1005.40	-925.87	-850.18	-778.32	-710.31	-646.14	-585.81	-529.33	-476.70	-427.93	-383.02	-341.96
9	-1653.78	-1552.46	-1454.50	-1359.93	-1268.76	-1181.01	-1096.68	-1015.78	-938.31	-864.28	-793.69	-726.54	-662.83	-602.58	-545.77	-492.41	-442.50	-396.06	-353.07	-313.54	-277.48
10	-1463.78	-1372.97	-1285.21	-1200.50	-1118.87	-1040.32	-964.86	-892.48	-823.20	-757.01	-693.93	-633.94	-577.05	-523.27	-472.60	-425.04	-380.59	-339.25	-301.03	-265.92	-233.94
11	-1293.05	-1211.60	-1132.92	-1057.00	-983.86	-913.50	-845.93	-781.14	-719.16	-659.96	-603.57	-549.97	-499.17	-451.18	-405.99	-363.61	-324.03	-287.27	-253.32	-222.18	-193.86
12	-1147.77	-1074.52	-1003.78	-935.54	-869.81	-806.61	-745.93	-687.77	-632.15	-579.05	-528.48	-480.45	-434.95	-391.99	-351.57	-313.69	-278.34	-245.55	-215.29	-187.58	-162.43
13	-1021.08	-955.10	-891.39	-829.95	-770.80	-713.93	-659.34	-607.04	-557.04	-509.32	-463.90	-420.77	-379.94	-341.41	-305.17	-271.24	-239.61	-210.28	-183.25	-158.54	-136.13
14	-921.73	-861.91	-804.15	-748.46	-694.86	-643.32	-593.87	-546.50	-501.22	-458.02	-416.90	-377.87	-340.93	-306.08	-273.32	-242.66	-214.09	-187.61	-163.23	-140.94	-120.76
15	-827.70	-773.48	-721.14	-670.69	-622.13	-575.46	-530.68	-487.80	-446.81	-407.73	-370.54	-335.25	-301.86	-270.38	-240.80	-213.12	-187.35	-163.48	-141.52	-121.48	-103.34
16	-746.97	-697.65	-650.06	-604.18	-560.04	-517.62	-476.94	-437.98	-400.76	-365.28	-331.52	-299.50	-269.22	-240.68	-213.88	-188.81	-165.49	-143.91	-124.07	-105.97	-89.63
17	-675.14	-630.25	-586.93	-545.20	-505.05	-466.48	-429.49	-394.08	-360.26	-328.03	-297.38	-268.32	-240.85	-214.97	-190.68	-167.98	-146.87	-127.35	-109.43	-93.11	-78.38
18	-613.96	-572.92	-533.33	-495.18	-458.47	-423.22	-389.42	-357.06	-326.16	-296.71	-268.72	-242.18	-217.09	-193.46	-171.29	-150.57	-131.31	-113.51	-97.17	-82.30	-68.88
19	-557.78	-520.38	-484.30	-449.54	-416.10	-383.99	-353.20	-323.73	-295.59	-268.78	-243.30	-219.14	-196.31	-174.82	-154.65	-135.81	-118.31	-102.13	-87.29	-73.79	-61.62
20	-505.62	-471.41	-438.41	-406.63	-376.07	-346.72	-318.60	-291.69	-266.00	-241.54	-218.30	-196.28	-175.48	-155.91	-137.56	-120.43	-104.54	-89.86	-76.42	-64.21	-53.22

Appendix B

Risk Assessment, SSOW & COSHH

THE UNIVERSITY of EDINBURGH
School of Engineering

RISK ASSESSMENT

Risk Ref No:	EMS_RA035_B26
Date:	16/01/2024
Review Date:	16/01/2025

LOCATION:	B26	SUPERVISOR / MANAGER:	Chris Sturgeon	HAZARD LEVEL[1]:	2
ACTIVITY:	Hybrid Magnet Force Testing (Construction and Testing)	COMPLETED BY:	Paul Dewhurst	LAB MANAGER:	Amer Syed

"UID (DYNA, ELE, POW, PROP, SIMS, SOFT, STAT)"	HAZARD	People at Risk[2]	Initial Level of Risk			CONTROL MEASURES	Revised Level of Risk			Controls Implemented By:
			H ✓	M ✓	L ✓		H ✓	M ✓	L ✓	
PROP_001	Fingers getting caught in between magnet and ferromagnetic objects	S,T				Keep ferromagnetic objects a safe distance away from permanent magnets and employ proper handling. These magnets are rated strong enough to bruise a nail if caught but gloves should widen the gap and cushion the collision to make this near impossible.				S,T
PROP_002	Magnets colliding with themselves	S,T				Always keep permanent magnets away from other permanent magnets and employ proper handling.				S,T
PROP_003	Plate colliding with Permanent Magnets	S,T				Rubber tape added to both the permanent magnets to cushion a possible collision. Additionally, the structure itself will have and bar fixed so that the plate can never get closer than 5mm.				S,T
PROP_004	Shards from collisions	S,T				Though the magnets should not be able to do this, using the methods outlined above will decrease the possibility of a collision of an object with the magnet resulting in it splitting. This with an additional protective				S,T

[1] 1=Low power hand and small bench tools; 2= Low to medium power tools; 3= Powerful portable and light industrial tools; 4= Large industrial tools. ISAM.xps (yale.edu)
[2] E= Employee/student; C= Contractor; P= Member of the public/visitor

THE UNIVERSITY of EDINBURGH
School of Engineering

RISK ASSESSMENT

"UID (DYNA, ELE, POW, PROP, SIMS, SOFT, STAT)"	HAZARD	People at Risk[2]	Initial Level of Risk			CONTROL MEASURES	Revised Level of Risk			Controls Implemented By:
			H ✓	M ✓	L ✓		H ✓	M ✓	L ✓	
						case around the testing structure to catch possible debris. Always wear PPE.				
PROP_005	Wire Overheating	S,T				Ensure not to exceed 5A. Test parameters should only require 0 to 3A.				S,T
PROP_006	Short circuit	S,T,P				Appropriate insulated cables of the correct power rating were used. Temperature of the power supply was monitored and wasn't left on over long period of time.				S,T
PROP_007	Direct skin contact with epoxy may cause irritation.	S,T				Use disposable gloves. Wash hands after using the material. See COSHH at the end.				S,T
PROP_008	Live wires	S,T				Ensure power supply is off and wires are disconnected before use				S,T

[1] 1=Low power hand and small bench tools; 2= Low to medium power tools; 3= Powerful portable and light industrial tools; 4= Large industrial tools. [ISAM.xps (yale.edu)]

[2] E= Employee/student; C= Contractor; P= Member of the public/visitor

Safe System of Work (SSOW):

Hybrid Magnet Force Testing (Construction and Testing)

Overview	
Purpose: To test the force of magnets **Equipment:** **Power Supply** **Load Sensor**	
Key Watchpoints	
	• Permanent Magnets • Coils • Steel Plate
Required PPE (delete as appropriate and add any special PPE required as text)	
	
Pre-Work Considerations	
Locate Emergency Stop Buttons	Know the location of all the system **Emergency Stop** buttons so that you can stop the system quickly in an emergency. Ensure that an **Emergency Stop** button is located within 2 metres of the operator at all times.
Know potential crush and pinch points	• Be aware of potential crush and pinch points on your system and keep personnel and equipment clear of these areas.
Wear proper clothing	Do not wear neckties, shop aprons, loose clothing or jewellery, or long hair that could get caught in equipment and result in an injury. Remove loose clothing or jewellery and restrain long hair. Make sure that your footwear is appropriate to a work environment.

Know facility safe procedures	• Most facilities have internal procedures and rules regarding safe practices within the facility. Be aware of these safe practices and incorporate them into your daily operation of the system.
Practice good housekeeping	Keep the floors in the work area clean. Do not leave tools, fixtures, or other items not specific to the test, lying about on the floor or system. • Ensure that nothing is placed on the crosshead before you operate the load frame
Give self-ample time	• Turn all electricity off if there is any sign of risk.
Stay alert	• Avoid long periods of work without adequate rest. In addition, avoid long periods of repetitious, unvarying, or monotonous work because these conditions can contribute to accidents and hazardous situations. If you are too familiar with the work environment, it is easy to overlook potential hazards that exist in that environment.

Hybrid Magnet Force Testing (Construction and Testing)

Overview

Purpose:

To make the test rig and see force variance depending on distance and current for the electromagnet.

Outcome:

The construction of the test rig and multiple values for the force at different distance and varying the current.

Procedure:

These steps are then put into the instructions section and labelled with the corresponding risk.

1. The magnets will be attached to the U bar using the correct handling conditions outlined. This will include putting the epoxy putty between them and letting it set.
2. The wire will then be wrapped around the U bar and additional wiring necessary to create the parallel circuit ready to be plugged in (do not plug in yet)
3. The U bar will then be fixed to the top of the structure using an aluminium plate. Additionally, the rubber tape will be added to the permanent magnets.
4. The plate will then be fixed at the correct distance along with the load cell for the specified iteration. Metal sheet possibly borrowed to ensure correct placement.
5. Put case around test rig. Connect to power supply and apply designated voltage for the specified iteration. Use Amp meter to check current is accurate. Note values. Turn off supply and disconnect wires.
6. Repeat 4 and 5 for all iterations.

Equipment:

- Power Supply
- Load Sensor

	Material Scope (Materials or consumables used)	Associated risk and mitigation
1	Magnet	**PROP_001** **PROP_002** **PROP_003** **PROP_004**
2	Wire	**PROP_005** **PROP_006**
3	Epoxy	**PROP_007**
4	Steel Plate and U bar	**PROP_003**

	Work Equipment Scope (Tools etc)	Associated risk and mitigation
1	Power supply	**PROP_006**
2	Load Sensor	No risks associated.

	Safe System of Work Instructions	Associated risk and mitigation
1	Construction of Testing Structure (Bosch already assembled)	No risks associated.
2	Attaching Magnets to U bar with epoxy	**PROP_001** **PROP_002** **PROP_003** **PROP_004** **PROP_007**
3	Adding the coil to the U bar	**PROP_005** **PROP_006** **PROP_008**
4	Fixing U bar and adding rubber tape	**PROP_001** **PROP_002** **PROP_003** **PROP_004**
5	Handling Plate and fixing it in place	**PROP_001** **PROP_002** **PROP_003** **PROP_004**
6	Wires and power supply	**PROP_005** **PROP_006** **PROP_008**
7		

8		
9		
10		
11		
12		
13		
14		
15		
16		
17		
18		
19		

Prepared by

Name: Paul Dewhurst	
Signature: Paul Dewhurst	Date: 27/11/2023

Approved by

Supervisor: Chris Sturgeon	
Signature:	Date: 19/1/24

Lab Manager:	Amer Syed
Signature:	Date: 18 Jan 24

Review Required Every 12 months

Name	Review Date	Signature

Verification by Users

Sign below to indicate you have:

1. Read and understood the Safe System of Work: Hybrid Magnet Force Testing (Construction and Testing)
2. Reviewed relevant Risk Assessment: EMS_RA035_Unsure of Location_Hybrid magnet testing
3. Been issued or have acquired the relevant PPE as per the SSOW and RA.

If you have any questions, concerns or doubts undergoing this activity STOP and ASK

Name	Signature	Date	Approved
Paul Dewhurst	[signature]	18/1/2024	
FADZRUL KAMARUDZAMAN	[signature]	18/1/2024	
Sam Tsai	[signature]	18/1/2024	

Supporting Information

COSHH FORM

Always follow good laboratory practice, full guidance at http://www.docs.csg.ed.ac.uk/Safety/Policy/Chem/CS_CoP002GLP.pdf

Each section has corresponding in depth guidance (section 2) for completion – please ensure you follow this guidance when completing this assessment (http://www.docs.csg.ed.ac.uk/Safety/ra/COSHH_notes.pdf).

This form can be used to evaluate the hazards of a single substance, group of related substances or a process/procedure as well as any proprietary purchased materials.

School/Management Unit	Engineering	Assess. No.	1
Title of Activity	Hybrid Magnet Force testing		
Location(s) of Work	Makerspace		

Outline of task/method: Epoxy put between steel U bar and magnets. Leave to set for 1 hour

A. Hazards including any substances produced during the procedure

Hazard(s) – state name of substance(s) and classify hazard (see guidance notes)	**Present Risk Evaluation** Low/Med/High	**Control Measures** (i.e., alternative work methods / mechanical aids / engineering controls, etc.)	**Risk Evaluation after control** Low/Med/High
Applying Epoxy	Med	Wear gloves, keep away from mouth.	Low

Risk evaluation should be based on hazard classification and hazard statements – if control methods stated above reduce the risk to low at this point, the risk assessment is complete. If any medium to high hazards remain, please continue to complete the rest of the form.

B. Exposure route(s) by which harm may occur

Skin Contact	Skin Absorption	Eye Contact	Inhalation	Ingestion	Injection via sharps

Irritable Chance with gloves is low	Irritable Chance with gloves is low	Irritable Chance with safety goggles is low	Can wear a mask. Making chance low. Substance is also a putty.	Can wear a mask. Making chance low	Very low chance

C. Engineering Control Measures (Fume cupboards/LEV etc.)

State any engineering controls required for this task/method; None just PPE

D. Personal Protective Equipment (PPE)

State any PPE required for this task/method. Include which type and when they are to be worn; Eye protection: Yes, standard safety glasses. Hand protection: Yes, plastic gloves. Special clothing: No Face protection: No Respiratory protection: Potential use of Mask

E. Health Monitoring

Is **health surveillance** required for the protection of the health of employees?	**Yes**	**No**
Health surveillance may be required if working with animals or other skin or respiratory sensitisers, please see http://www.ed.ac.uk/schools-departments/health-safety/guidance/hazardous-substances/sensitisers for further guidance		No
Is **biological monitoring** required to ensure that the control of exposure to the hazardous substance(s) is adequate? http://www.hse.gov.uk/pubns/books/hsg167.htm for guidance If yes for health monitoring, contact the Health and Safety Department for further guidance on obtaining biological monitoring (health.safety@ed.ac.uk)		No

F. Training

State any health and safety training required for this task/method; None

G. Supervision

State what supervision (if any) is required for persons undertaking this task/method: None

H. Implications for persons not involved in the work activity

Persons identified may require to be informed, in part or in full, of the information contained in the Safe System of Work. None

I. Emergency procedures

State all emergency procedures including contact names and numbers; Firs Aid: Get Tom, or other member of staff and call 999 if necessary Fire fighting: Get Tom, or other member of staff and call 999 if necessary Spill Management: Get Tom (is putty though so can't really spill) Any others:

J. Waste disposal

State waste disposal routes for all hazardous substances in this task/method; Waste disposal bin

If in doubt contact the University Waste and Environmental Manager Ext. 514287.

	Yes	No
Are you satisfied that the control measures outlined above are adequate to control the risks to health from the hazardous substances used in the work activity described to the lowest level reasonably practicable? **If no, work can not continue until safe to do so**		

K. Accreditation and verification of COSHH risk assessment

When this assessment is complete it should be signed and dated by the assessor and then checked and signed by the person responsible for operations in that section of the School/Unit where the work is being carried out. You must ensure that the person undertaking the task is competent to do so and has received sufficient information, instruction and training and has seen and signed the Safe System of Work.

Assessed by:	Paul Dewhurst	Checked by:	
Signature:	Paul Dewhurst	Signature:	
Date:	27/11/2023	Date:	

L. Review of Assessment

This assessment should be reviewed at regular intervals and immediately if there is reason to suspect that it is no longer valid (for example after any accidents or incidents) or if there is a significant change in the work to which it relates.

When the assessment is reviewed, add below the signature of the assessor and the person responsible for work in that area of the School/Unit. If the activity has materially changed in any way then a new assessment should be undertaken and a new assessment form completed. Any original signatories covered by the modified assessment should sign again.

Assessed by:		Checked by:	
Signature:		Signature:	
Date:		Date:	

Annexe A

Annexe A can be used instead of Sections A-J above. It covers the same areas but in a table format, (http://www.docs.csg.ed.ac.uk/Safety/ra/COSHH_Annexe_A.docx).

Safe System of Work

Now formulate a Safe System of Work (form SSW, http://www.docs.csg.ed.ac.uk/Safety/ra/SSW_form.pdf or http://www.docs.csg.ed.ac.uk/Safety/ra/SSW_form.doc) (also known as Standard Operating Procedure or SoP) and ensure all laboratory users countersign to verify they understand it.

Setup

1. U-bar made from 3 bars with square sections of steel.
2. Permanent magnets
3. Coils
4. Test structure attachment
5. The test structure
6. Plate with load cell

1.

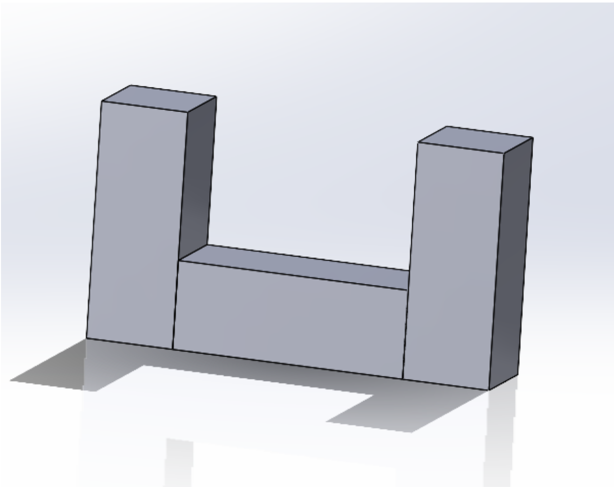

Needs to be welded. Each section 40mm long and 16 square section.

2.

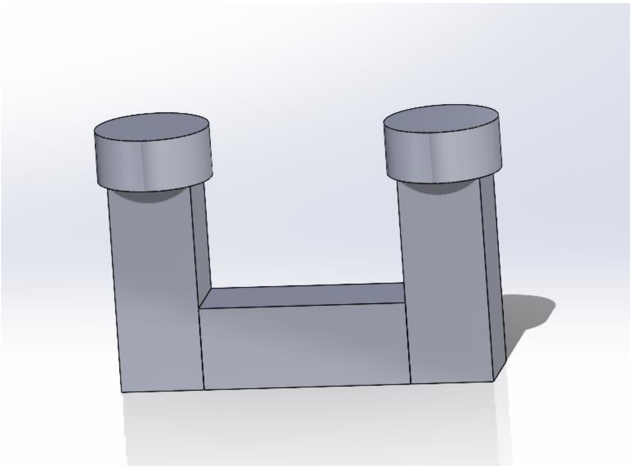

Magnets fitted onto U-bar. Fixed using epoxy putty.

3.

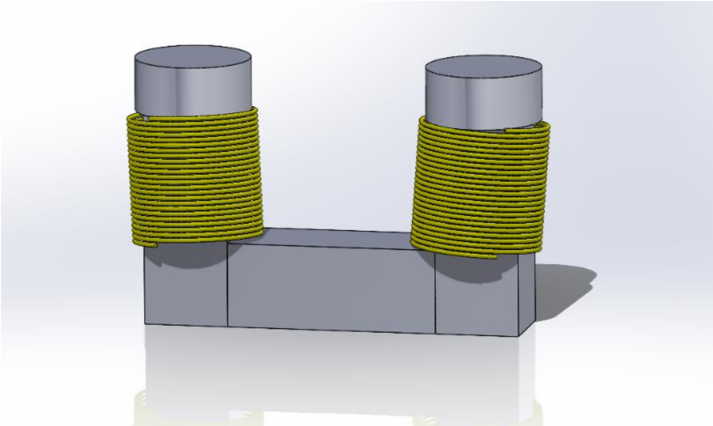

Wire around both sides of the U bar and then each coil will be connected in parallel. This will be done after the U bar has been attached to the main structure.
This will be connected toa power supply for testing.

4.

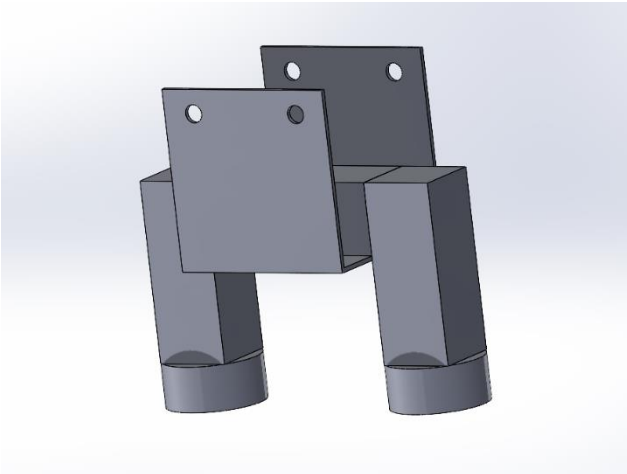

A plate that is bent will be used to secure the magnet to the main structure along with more epoxy.

5.

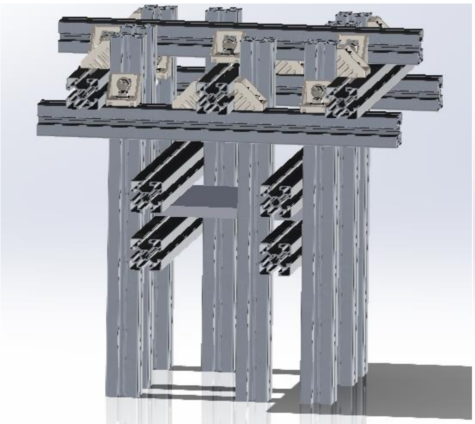

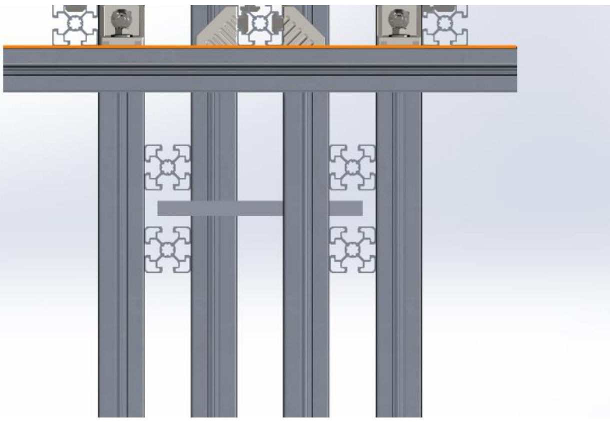

Basically, a main structure made of Bosch where the permanent magnet will be attached to the underside of the top. This will exert a force on the plate. The main structure has already been made.

6.

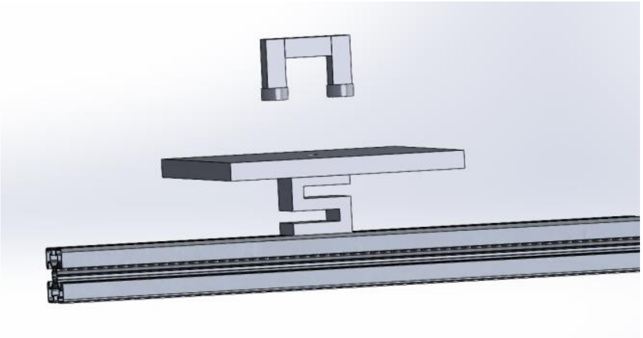

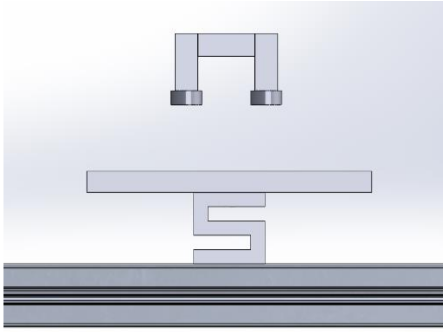

So the magnet is attached to the main structure at the top. The Bosch bar connected to the load cell is also going to be connected to the main structure.

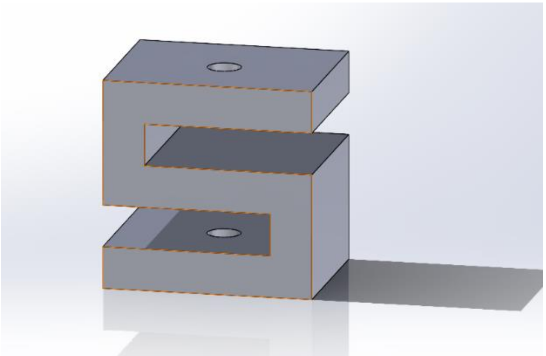

Load cell looks something like this so s type. Roughly 5cm tall and can be attached using an 8mm (rough guess for now) bolt.

Appendix C

Drawings for Components

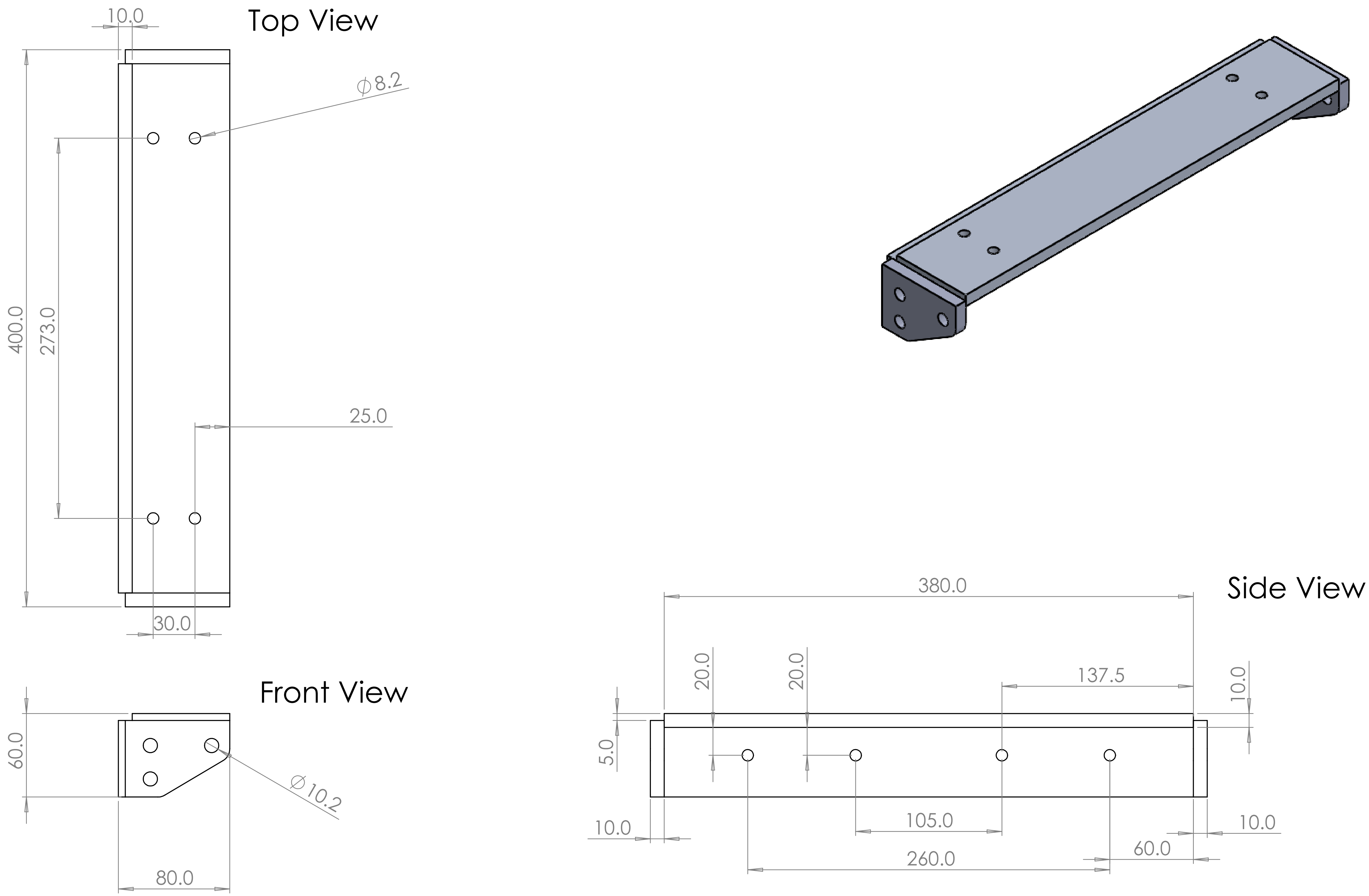

UNLESS OTHERWISE SPECIFIED: DIMENSIONS ARE IN MILLIMETERS SURFACE FINISH: TOLERANCES: ±0.1 LINEAR: ANGULAR:		FINISH:		DEBURR AND BREAK SHARP EDGES		DO NOT SCALE DRAWING	REVISION: 4
						Quantity: 4	
	NAME	SIGNATURE	DATE			TITLE: LEV-BRACKET-ASSEM	
DRAWN							
CHK'D							
APPV'D							
MFG							
Q.A				MATERIAL: Aluminium 5083		DWG NO.	A3
				WEIGHT:		SCALE:1:5	SHEET 1 OF 4

Top View

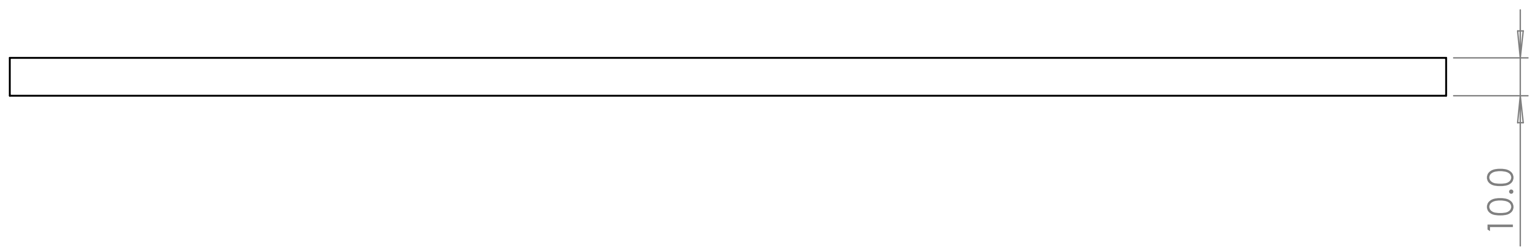

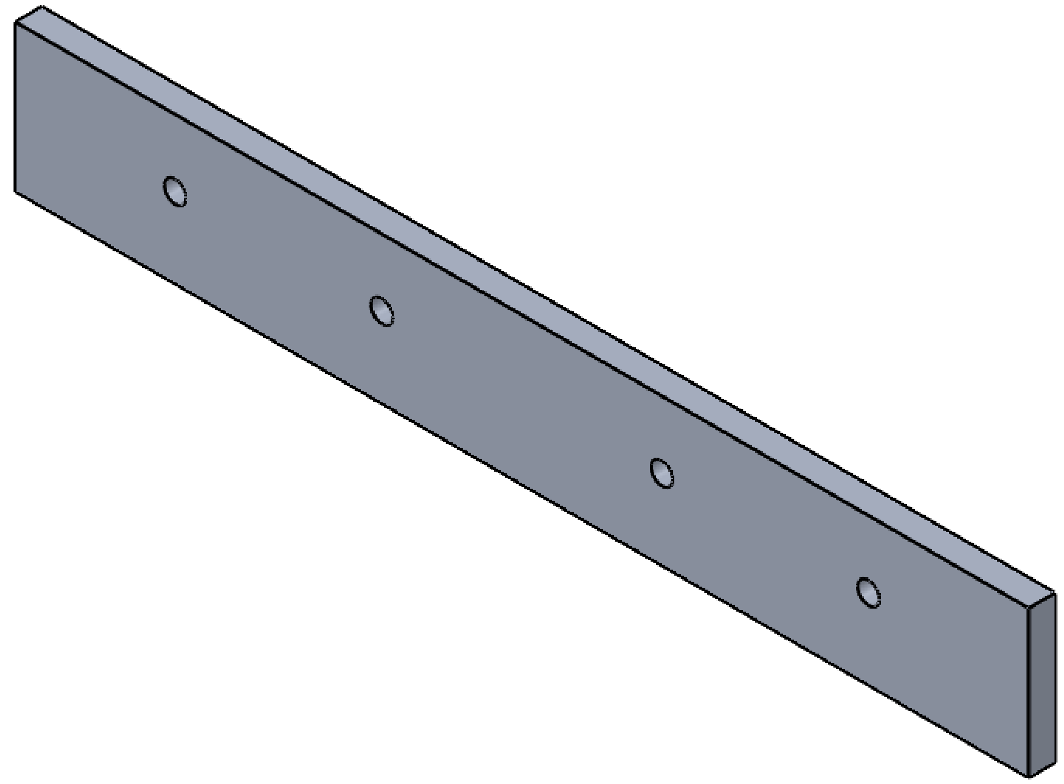

Front View

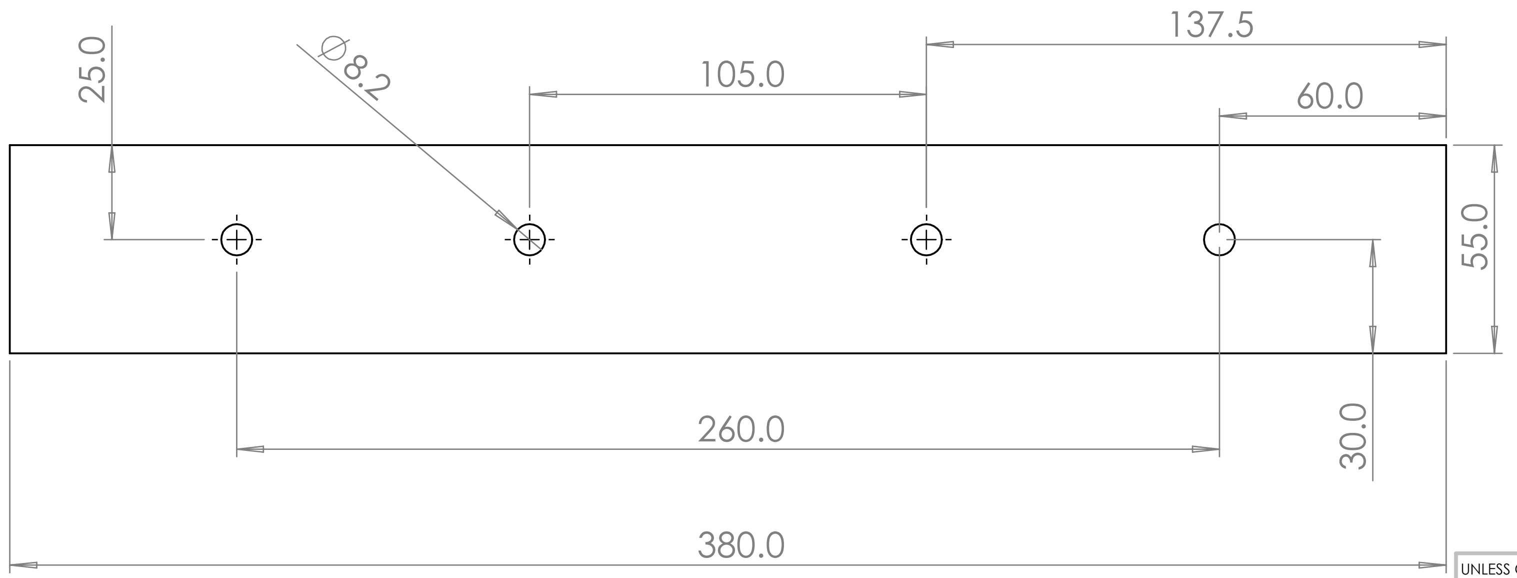

Side View

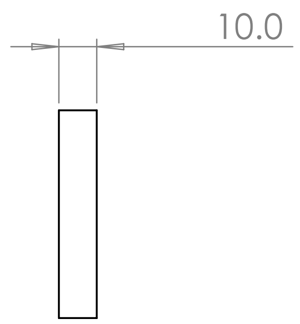

UNLESS OTHERWISE SPECIFIED: DIMENSIONS ARE IN MILLIMETERS SURFACE FINISH: TOLERANCES: ±0.1 LINEAR: ANGULAR:	FINISH:			DEBURR AND BREAK SHARP EDGES	DO NOT SCALE DRAWING	REVISION: 4
					Quantity: 4	
	NAME	SIGNATURE	DATE		TITLE:	
DRAWN					LEV-BRACKET-EMS PLATE	
CHK'D						
APPV'D						
MFG						
Q.A			MATERIAL: Aluminium 5083		DWG NO.	A3
			WEIGHT:		SCALE:1:5	SHEET 2 OF 4

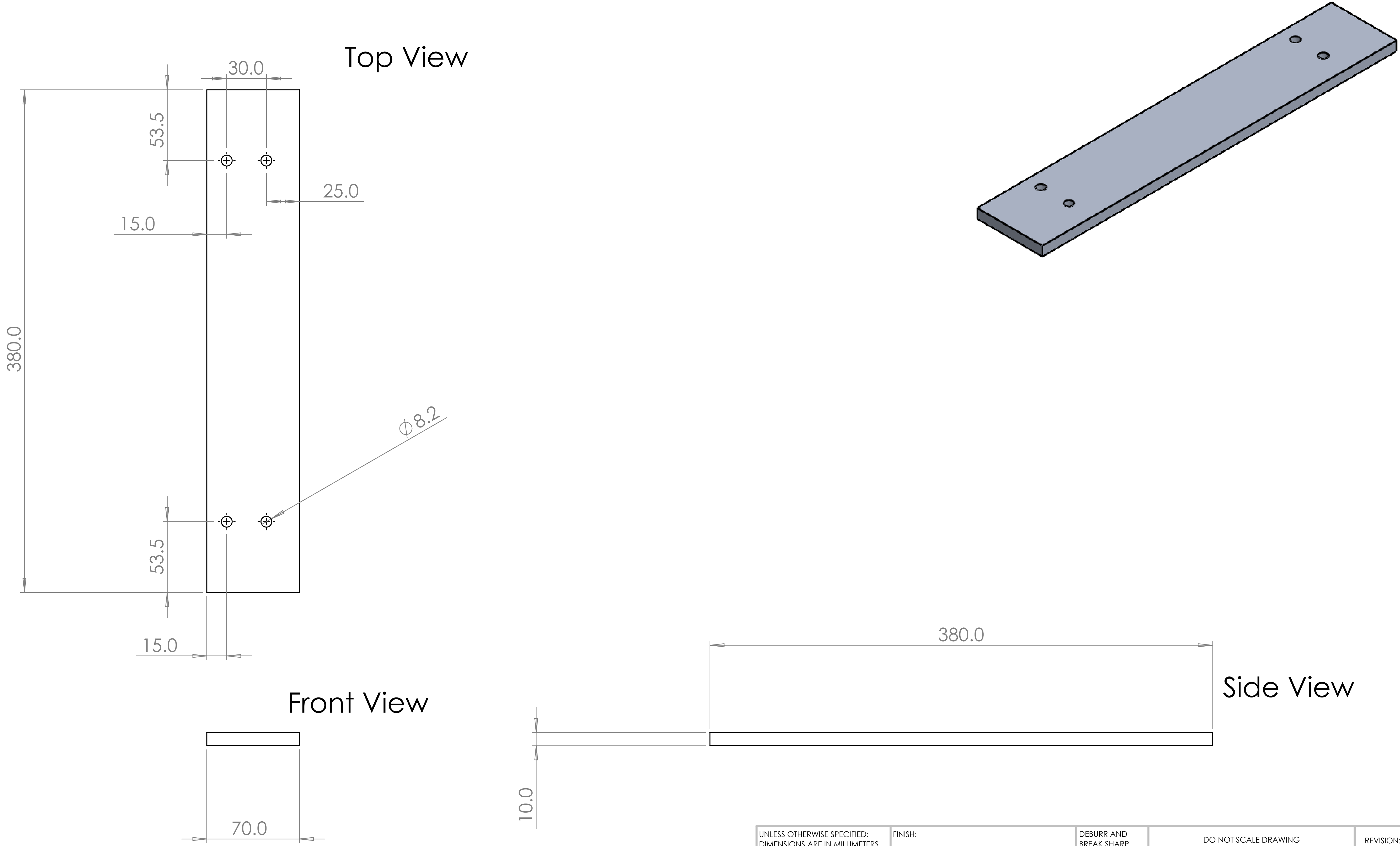

UNLESS OTHERWISE SPECIFIED: DIMENSIONS ARE IN MILLIMETERS SURFACE FINISH: TOLERANCES: ±0.1 LINEAR: ANGULAR:		FINISH:			DEBURR AND BREAK SHARP EDGES	DO NOT SCALE DRAWING	REVISION: 4
						Quantity: 4	
	NAME	SIGNATURE	DATE			TITLE:	
DRAWN						LEV-BRACKET-HEMS PLATE	
CHK'D							
APPV'D							
MFG							
Q.A				MATERIAL: Aluminium 5083		DWG NO.	A3
				WEIGHT:		SCALE:1:5	SHEET 3 OF 4

Top View

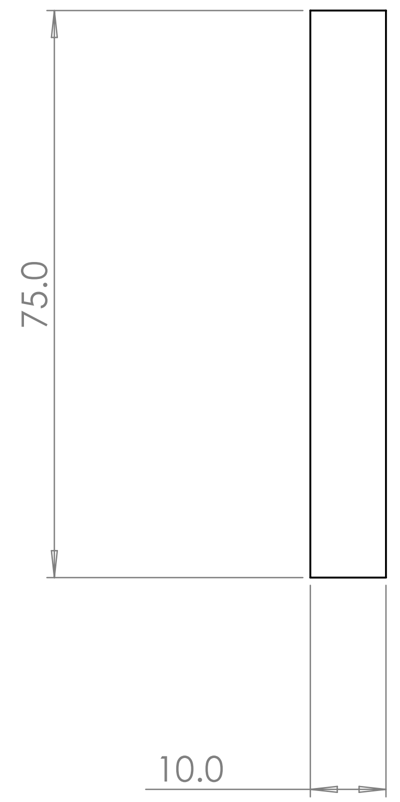

Front View

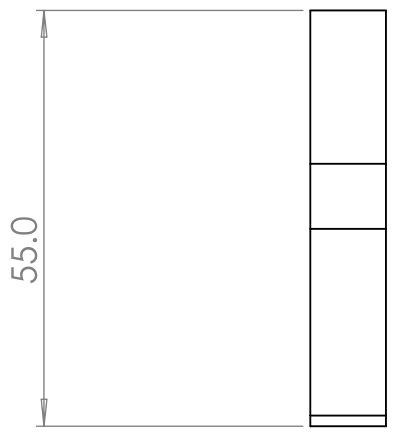

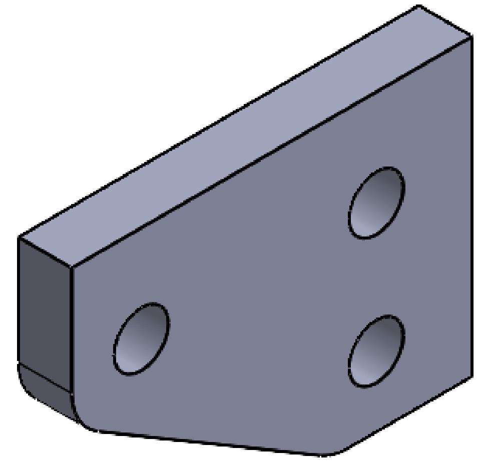

Side View

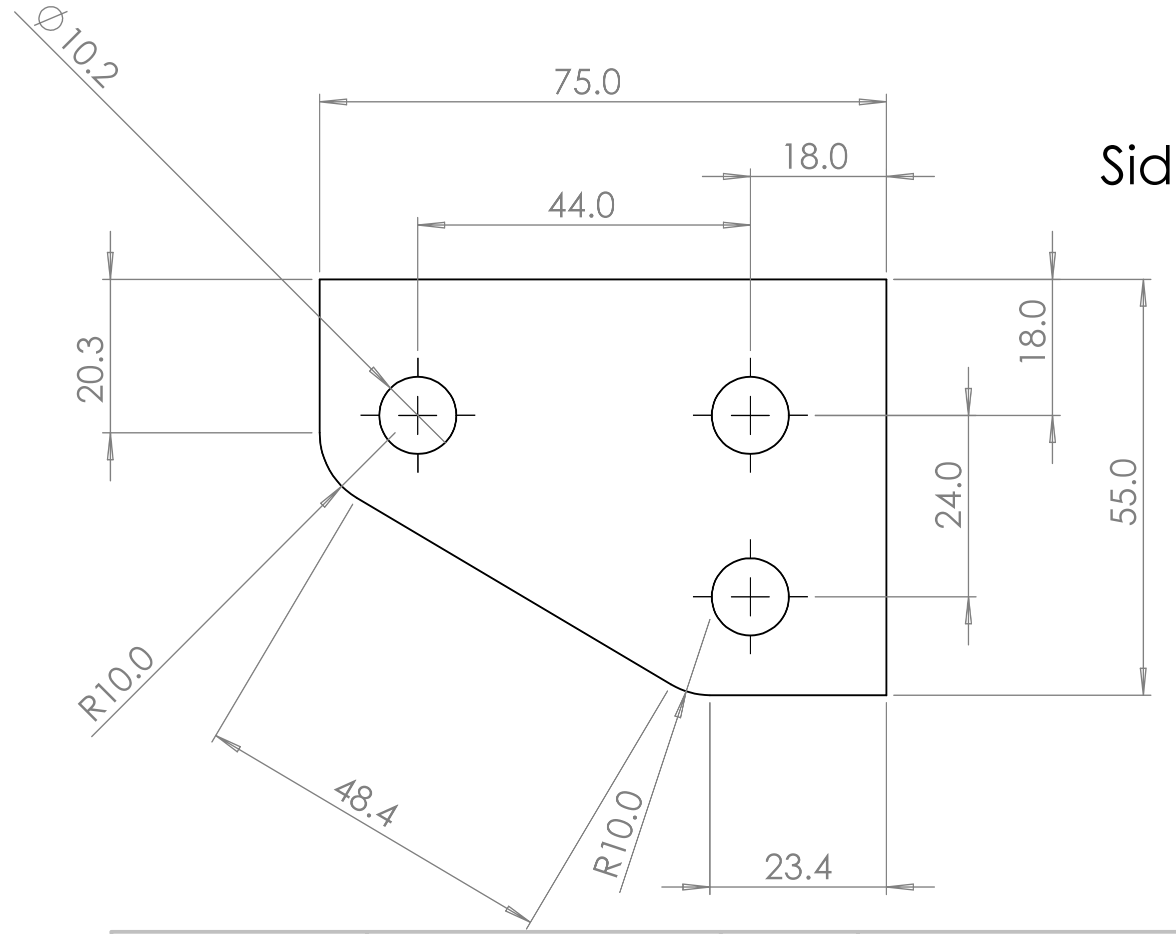

UNLESS OTHERWISE SPECIFIED:
DIMENSIONS ARE IN MILLIMETERS
SURFACE FINISH:
TOLERANCES: ±0.1
LINEAR:
ANGULAR:

FINISH:

DEBURR AND BREAK SHARP EDGES

DO NOT SCALE DRAWING

REVISION: 4

Quantity: 8

	NAME	SIGNATURE	DATE
DRAWN			
CHK'D			
APPV'D			
MFG			
Q.A			

TITLE:

LEV-BRACKET-SIDE PLATE

MATERIAL:

Aluminium 5083

DWG NO.

A3

WEIGHT:

SCALE:1:1

SHEET 4 OF 4

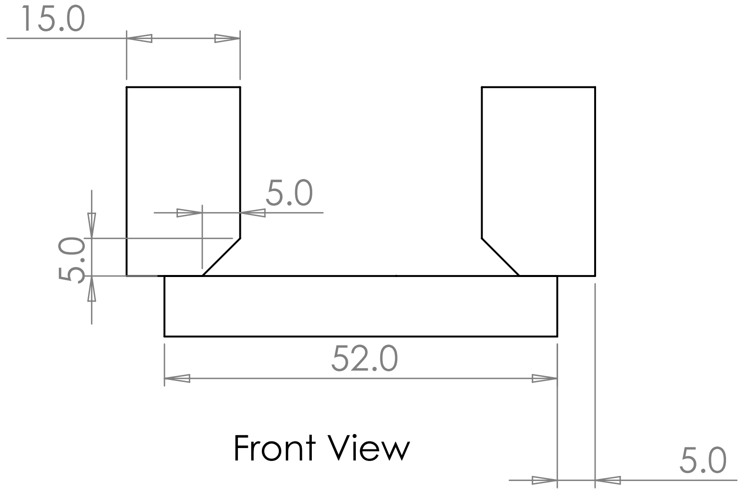

Front View

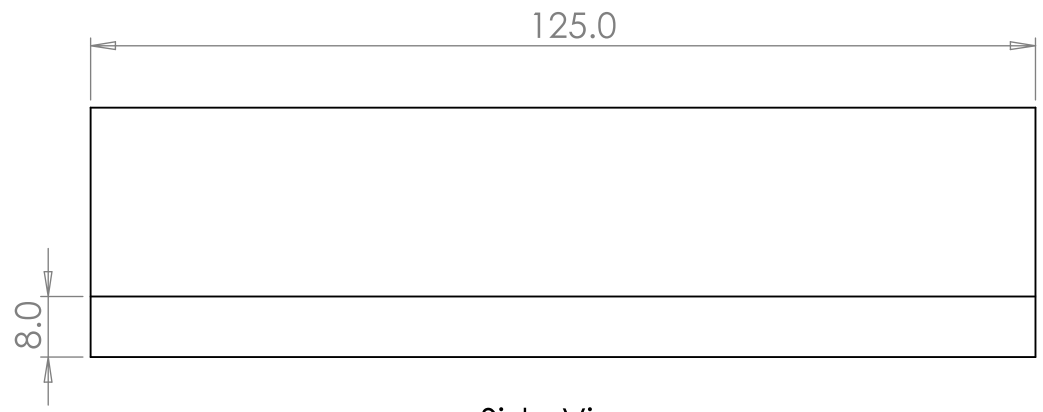

Side View

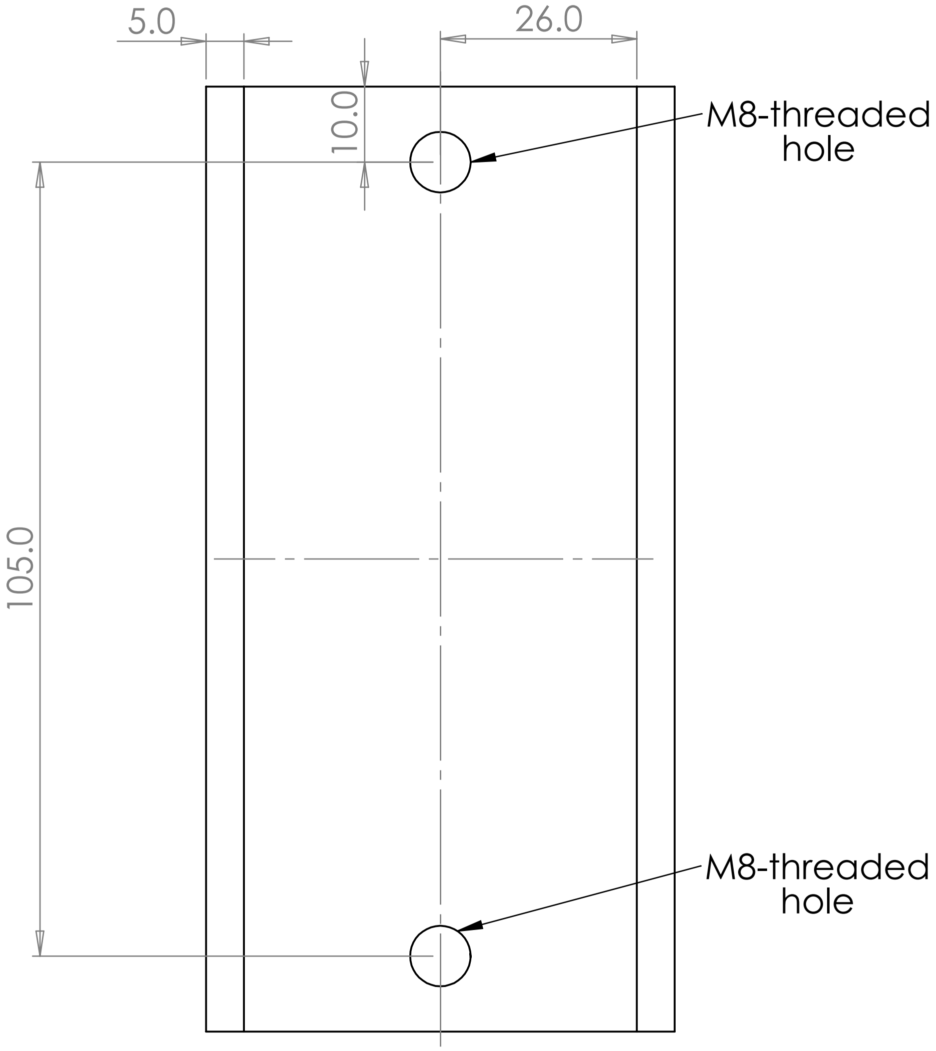

Bottom View

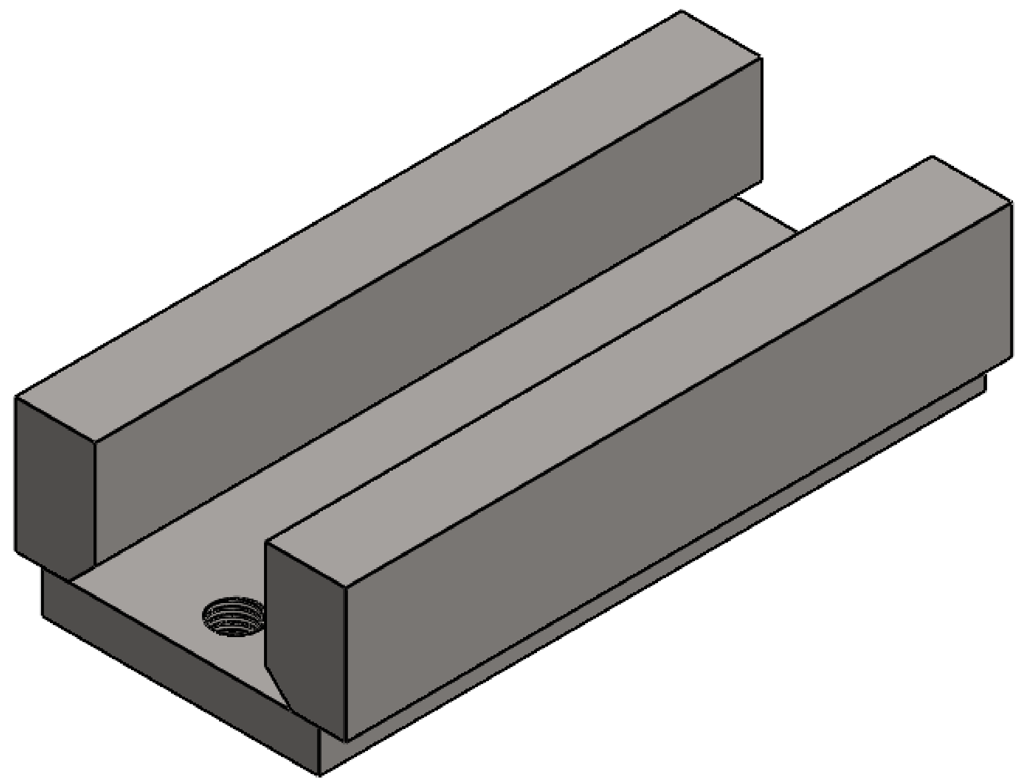

Isometric View

UNLESS OTHERWISE SPECIFIED: DIMENSIONS ARE IN MILLIMETERS SURFACE FINISH: TOLERANCES: ±0.1 LINEAR: ANGULAR:	FINISH:	DEBURR AND BREAK SHARP EDGES	DO NOT SCALE DRAWING	REVISION: 4
			Quantity: 4	
NAME / SIGNATURE / DATE			TITLE: LEV-EMS-CORE	
DRAWN				
CHK'D				
APPV'D				
MFG				
Q.A		MATERIAL: EN3B Mild Steel	DWG NO.	A3
		WEIGHT:	SCALE:1:2	SHEET 1 OF 1

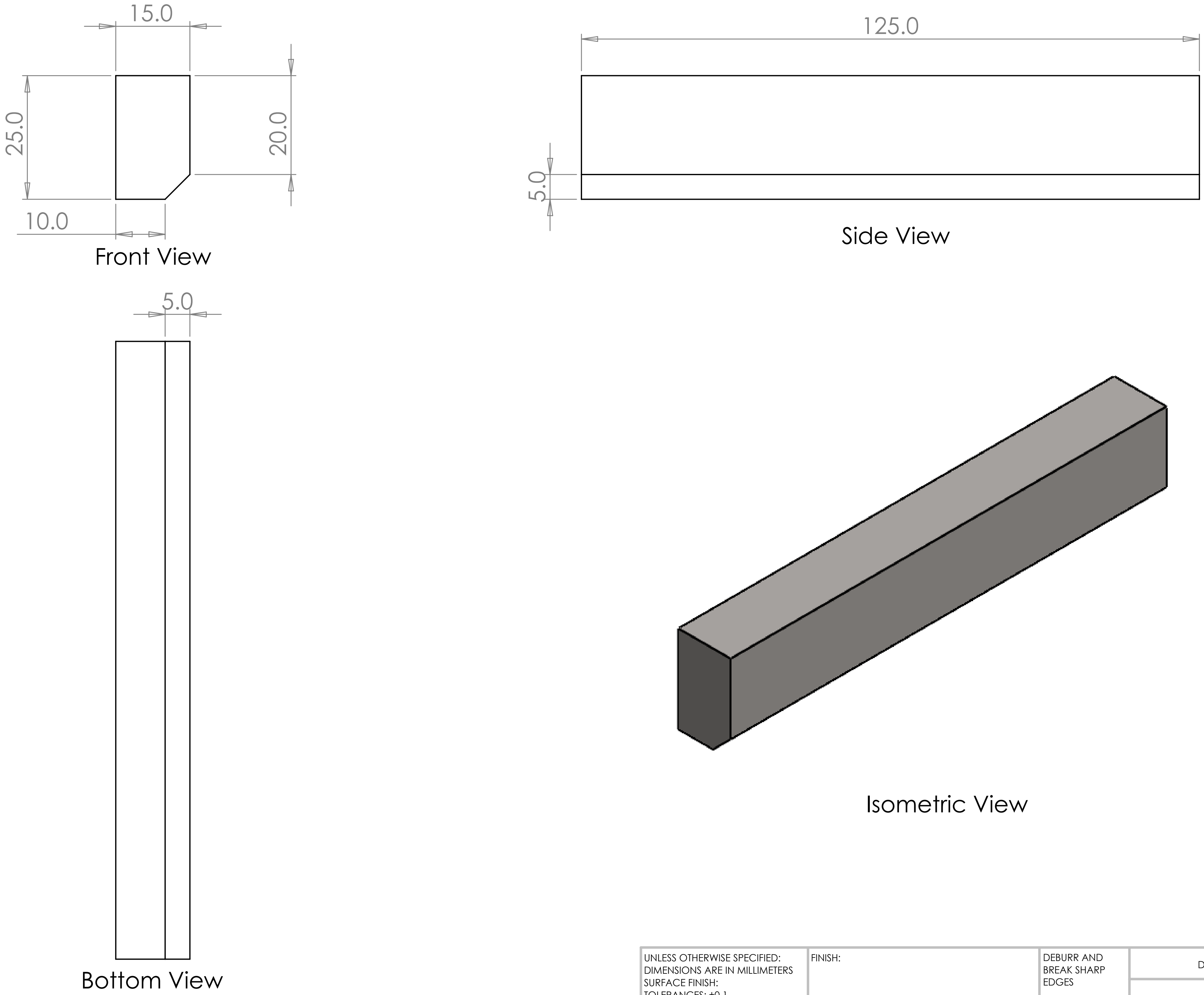

UNLESS OTHERWISE SPECIFIED: DIMENSIONS ARE IN MILLIMETERS SURFACE FINISH: TOLERANCES: ±0.1 LINEAR: ANGULAR:	FINISH:	DEBURR AND BREAK SHARP EDGES

DO NOT SCALE DRAWING | REVISION: 4

Quantity: 8

	NAME	SIGNATURE	DATE
DRAWN			
CHK'D			
APPV'D			
MFG			
Q.A			

TITLE:

LEV-EMS-CORE ARM

MATERIAL: EN3B Mild Steel

DWG NO.

A3

WEIGHT:

SCALE:1:1

SHEET 1 OF 1

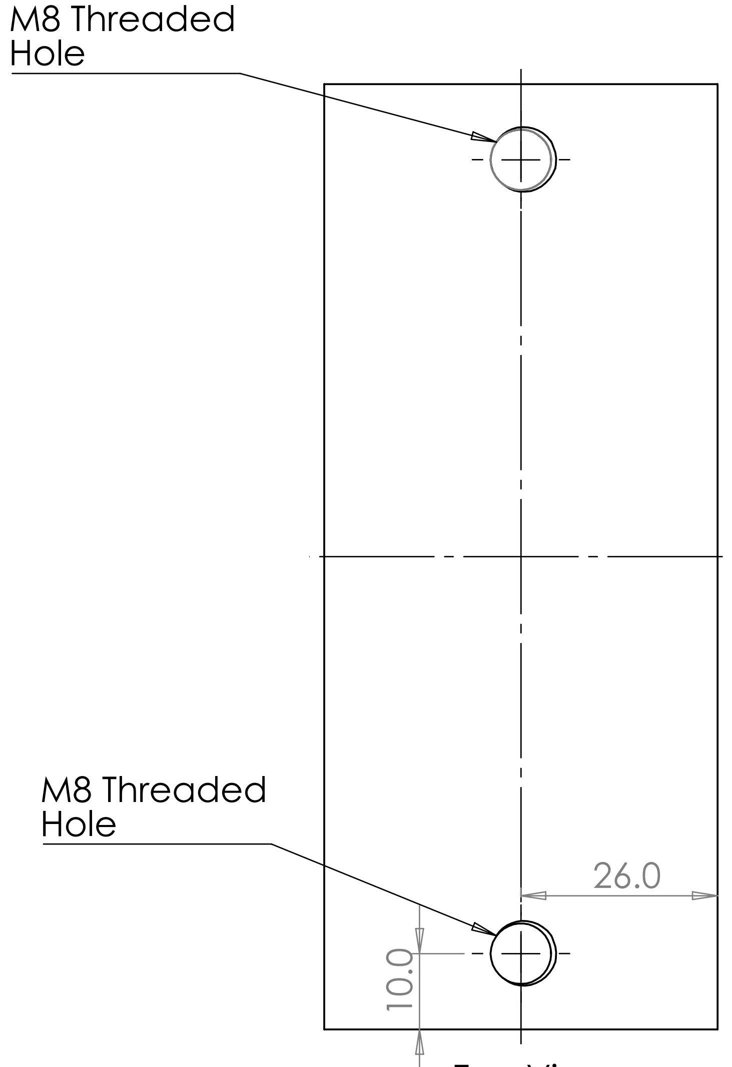

Top View

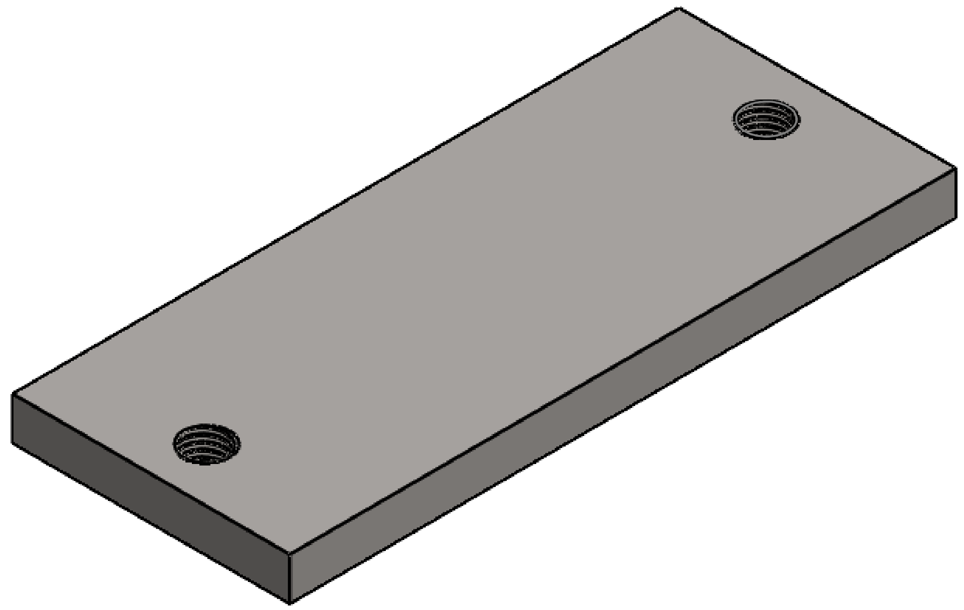

Isometric View

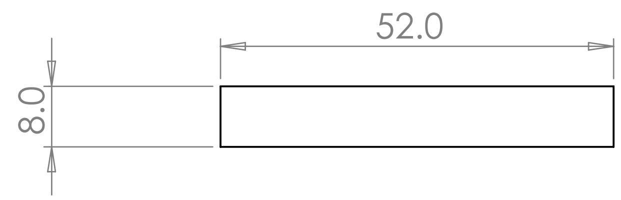

Front View

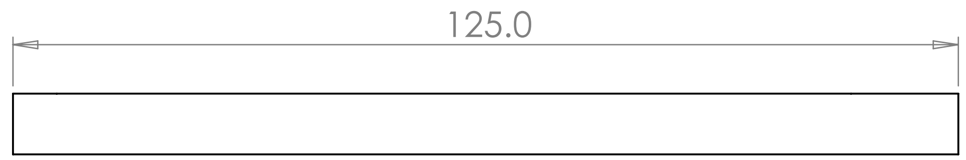

Side View

UNLESS OTHERWISE SPECIFIED: DIMENSIONS ARE IN MILLIMETERS SURFACE FINISH: TOLERANCES: ±0.1 LINEAR: ANGULAR:	FINISH:		DEBURR AND BREAK SHARP EDGES	DO NOT SCALE DRAWING	REVISION: 4
				Quantity: 4	
	NAME	SIGNATURE	DATE	TITLE:	
DRAWN				LEV-EMS-CORE BASE	
CHK'D					
APPV'D					
MFG					
Q.A			MATERIAL: EN3B Mild Steel	DWG NO.	A3
			WEIGHT:	SCALE:1:1	SHEET 1 OF 1

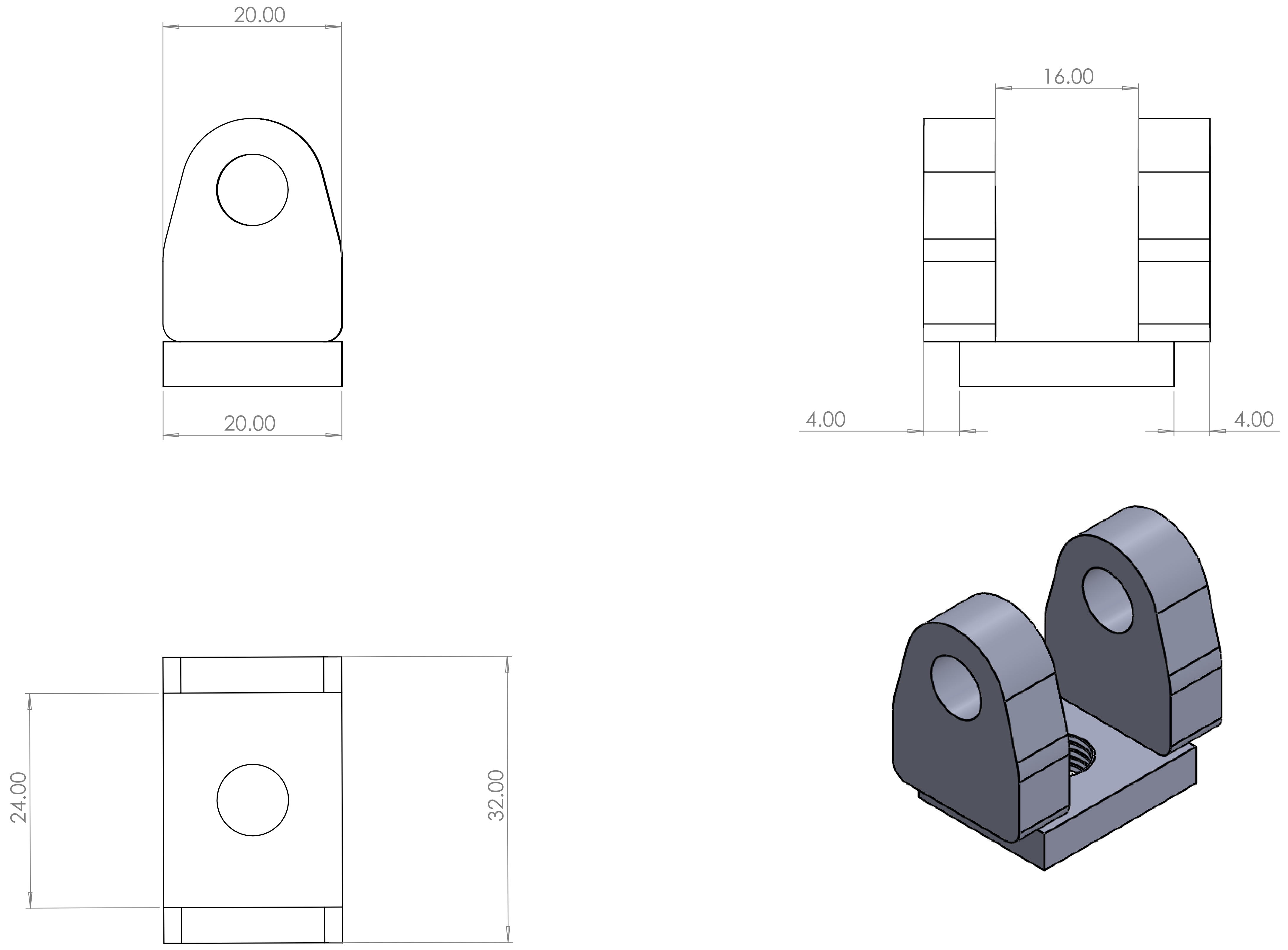

UNLESS OTHERWISE SPECIFIED:
DIMENSIONS ARE IN MILLIMETERS
SURFACE FINISH:
TOLERANCES:
LINEAR:
ANGULAR:

FINISH:

DEBURR AND BREAK SHARP EDGES

DO NOT SCALE DRAWING

REVISION: 4

Quantity: 8

	NAME	SIGNATURE	DATE
DRAWN			
CHK'D			
APPV'D			
MFG			
Q.A			

TITLE: LEV-EMS-WHEEL ASSEM

MATERIAL: EN3B Mild Steel

DWG NO.

A3

WEIGHT:

SCALE:2:1

SHEET 1 OF 1

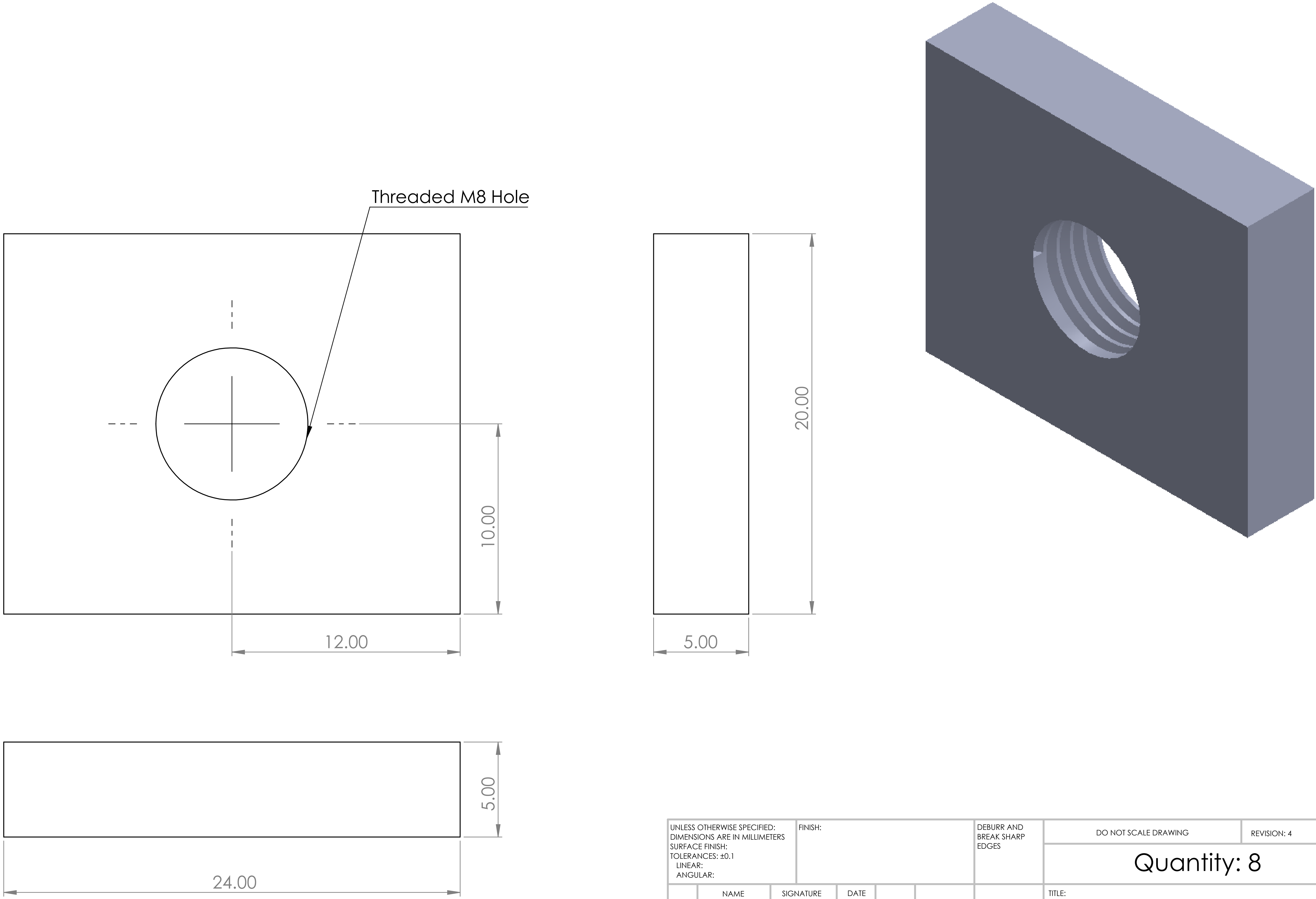

UNLESS OTHERWISE SPECIFIED: DIMENSIONS ARE IN MILLIMETERS SURFACE FINISH: TOLERANCES: ±0.1 LINEAR: ANGULAR:	FINISH:		DEBURR AND BREAK SHARP EDGES		DO NOT SCALE DRAWING	REVISION: 4
					Quantity: 8	
	NAME	SIGNATURE	DATE		TITLE: LEV-EMS-WHEEL PLATE	
DRAWN						
CHK'D						
APPV'D						
MFG						
Q.A				MATERIAL: EN3B Mild Steel	DWG NO.	A3
				WEIGHT:	SCALE:5:1	SHEET 1 OF 1

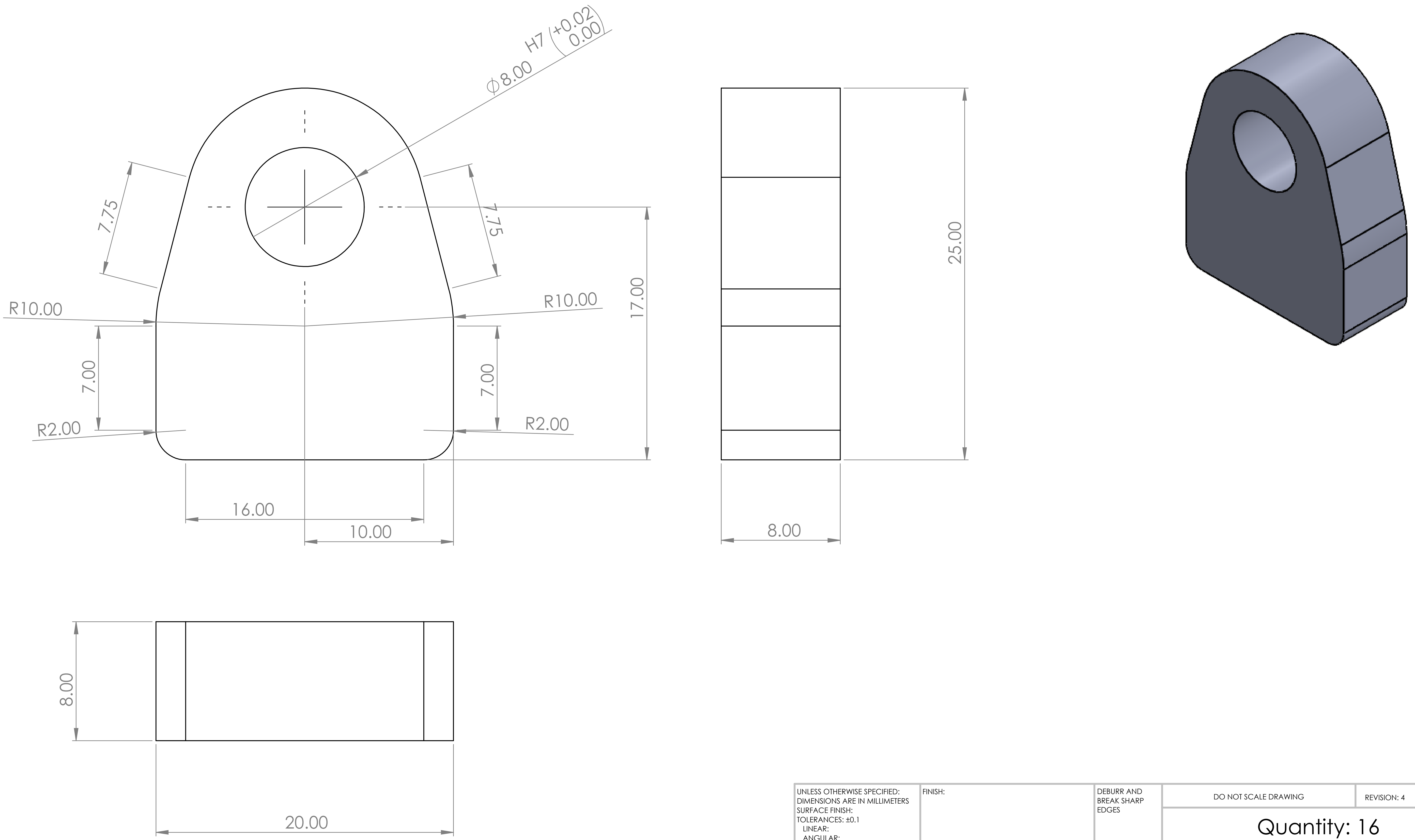

UNLESS OTHERWISE SPECIFIED:
DIMENSIONS ARE IN MILLIMETERS
SURFACE FINISH:
TOLERANCES: ±0.1
LINEAR:
ANGULAR:

FINISH:

DEBURR AND BREAK SHARP EDGES

DO NOT SCALE DRAWING

REVISION: 4

Quantity: 16

	NAME	SIGNATURE	DATE
DRAWN			
CHK'D			
APPV'D			
MFG			
Q.A			

TITLE:

LEV-EMS-Wheel Stand

MATERIAL:

EN3B Mild Steel

DWG NO.

A3

WEIGHT:

SCALE:2:1

SHEET 1 OF 1

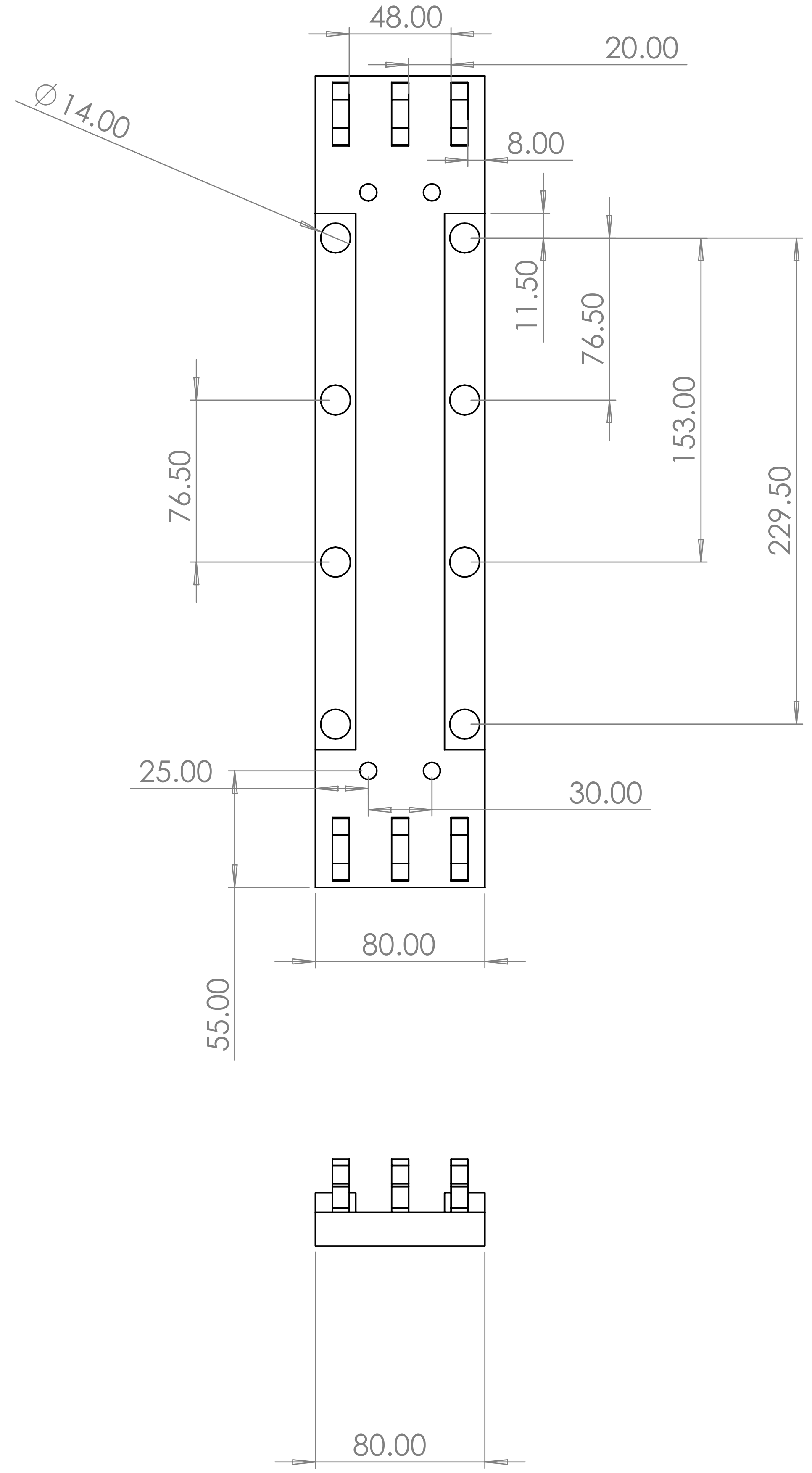

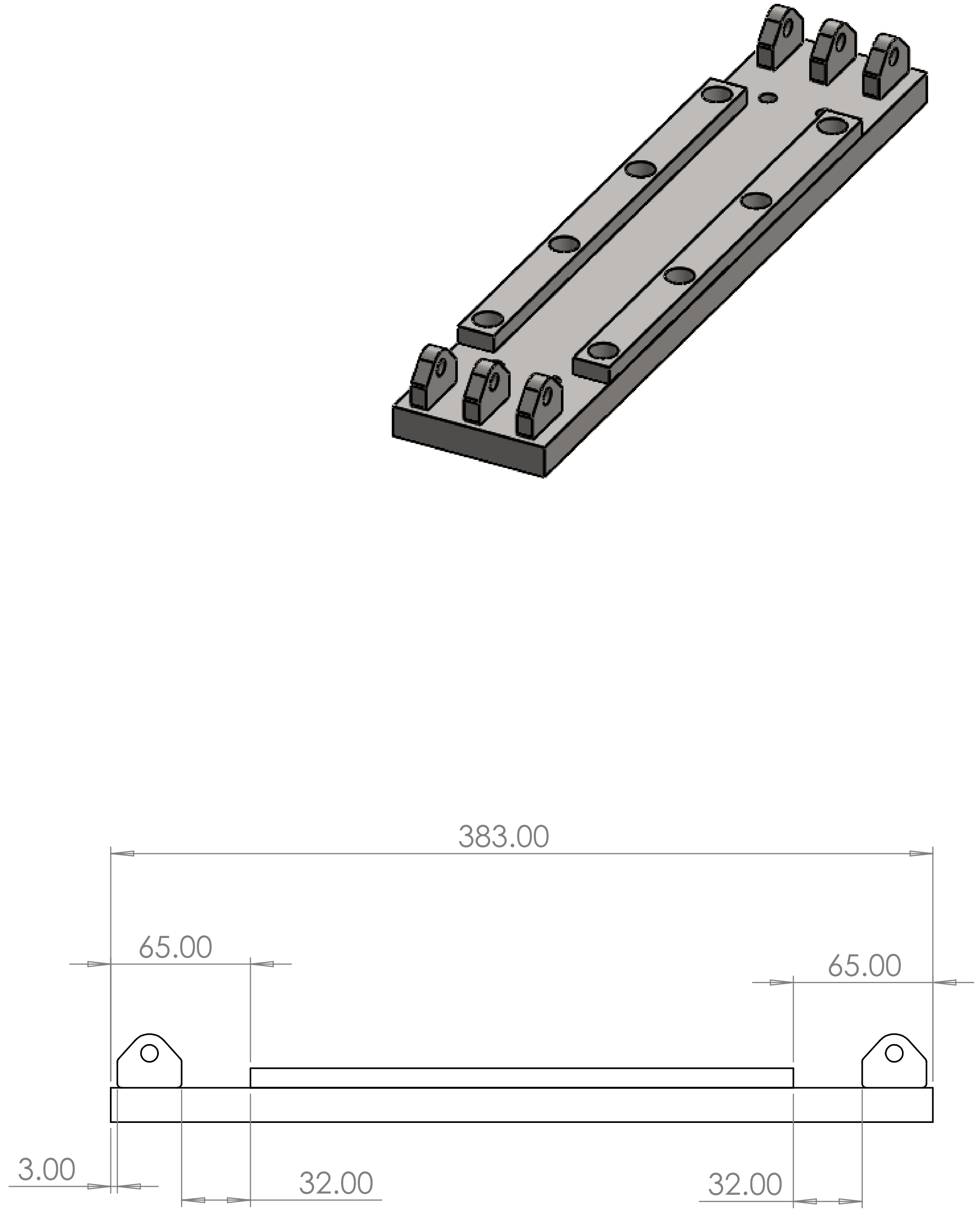

UNLESS OTHERWISE SPECIFIED: DIMENSIONS ARE IN MILLIMETERS SURFACE FINISH: TOLERANCES: ±0.1 LINEAR: ANGULAR:	FINISH:	DEBURR AND BREAK SHARP EDGES	DO NOT SCALE DRAWING	REVISION: 4
			Quantity: 4	

	NAME	SIGNATURE	DATE	
DRAWN				
CHK'D				
APPV'D				
MFG				
Q.A				MATERIAL: EN3B Mild Steel
				WEIGHT:

TITLE: LEV-HEMS-ASSEM

DWG NO. | A3

SCALE:1:5 | SHEET 1 OF 1

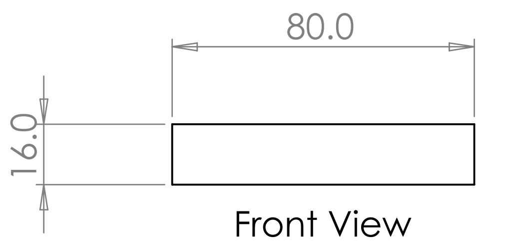

Front View

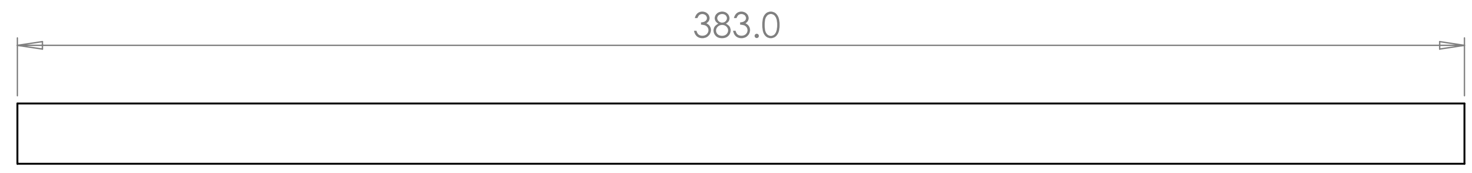

Side View

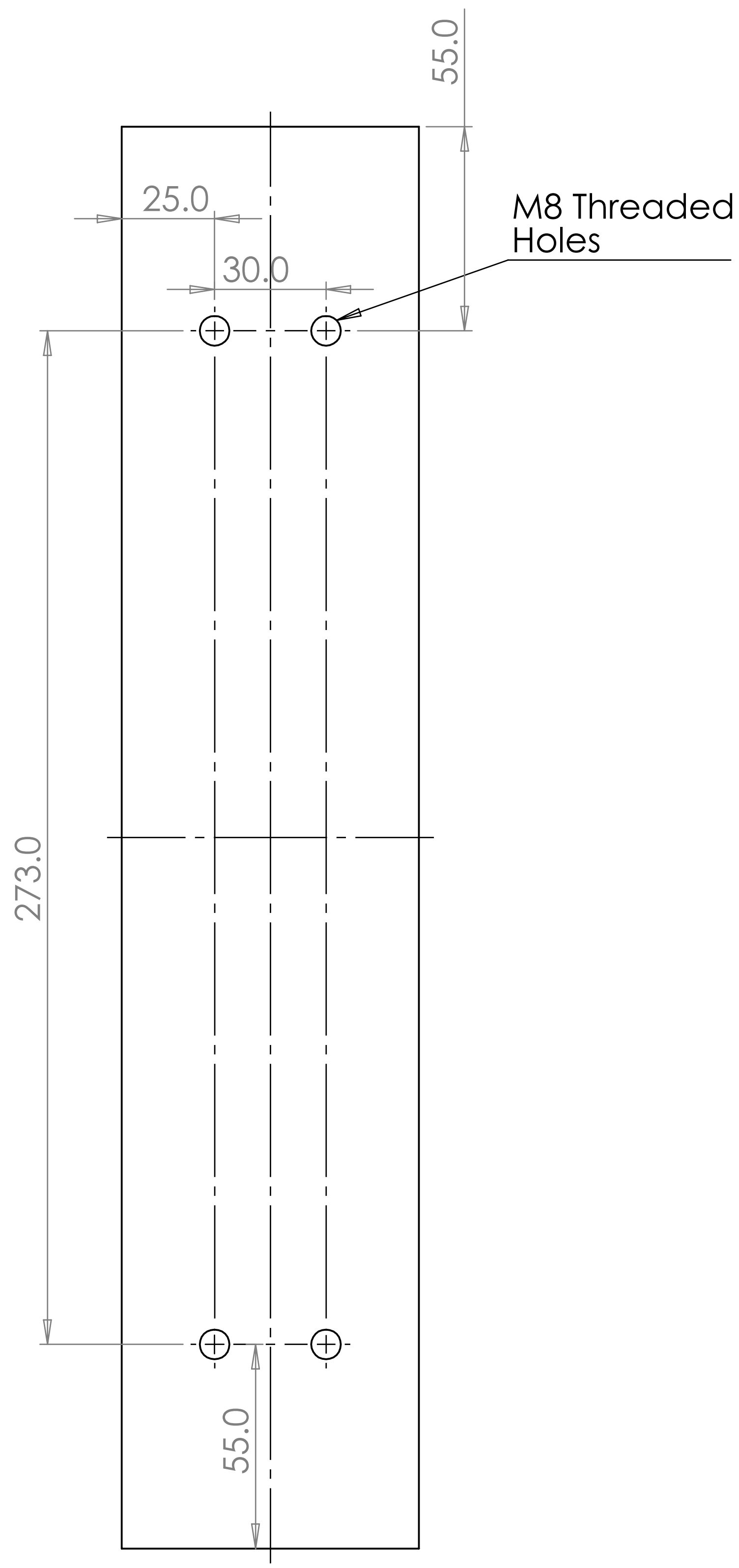

Bottom View

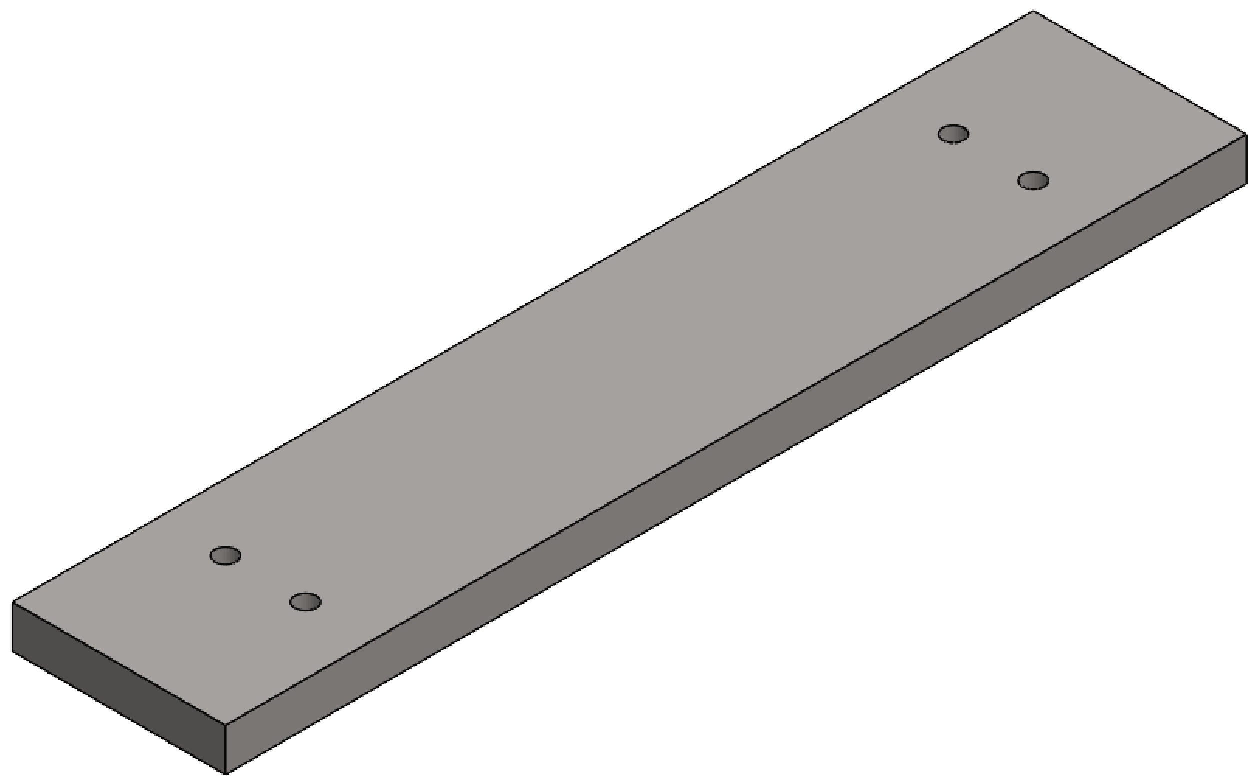

Isometric View

UNLESS OTHERWISE SPECIFIED: DIMENSIONS ARE IN MILLIMETERS SURFACE FINISH: TOLERANCES: ±0.1 LINEAR: ANGULAR:	FINISH:			DEBURR AND BREAK SHARP EDGES	DO NOT SCALE DRAWING	REVISION
					Quantity: 4	
	NAME	SIGNATURE	DATE		TITLE:	
DRAWN					LEV-HEMS-CORE BASE	
CHK'D						
APPV'D						
MFG						
Q.A				MATERIAL: EN3B Mild Steel	DWG NO.	A3
				WEIGHT:	SCALE:1:5	SHEET 1 OF 1

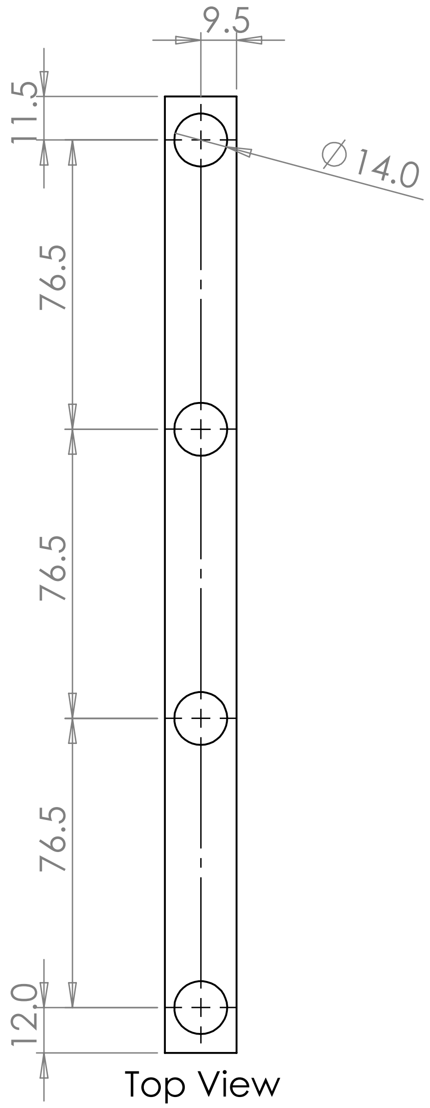

Top View

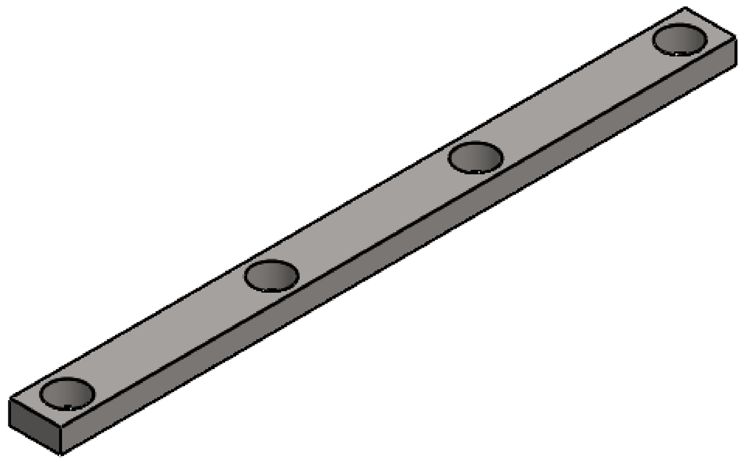

Isometric View

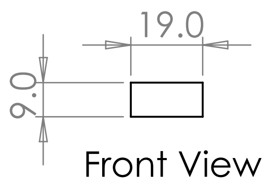

Front View

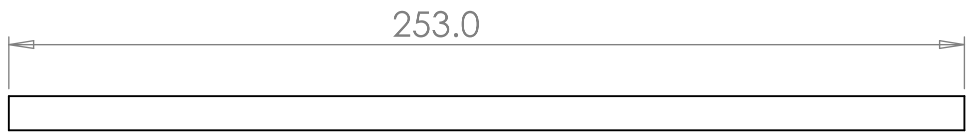

Side View

UNLESS OTHERWISE SPECIFIED: DIMENSIONS ARE IN MILLIMETERS SURFACE FINISH: TOLERANCES: ±0.1 LINEAR: ANGULAR:	FINISH:	DEBURR AND BREAK SHARP EDGES	DO NOT SCALE DRAWING	REVISION
			Quantity: 8	
	NAME / SIGNATURE / DATE		TITLE:	
DRAWN			LEV-HEMS-CORE ARM	
CHK'D				
APPV'D				
MFG				
Q.A		MATERIAL: EN3B Mild Steel	DWG NO.	A3
		WEIGHT:	SCALE:1:2	SHEET 1 OF 1

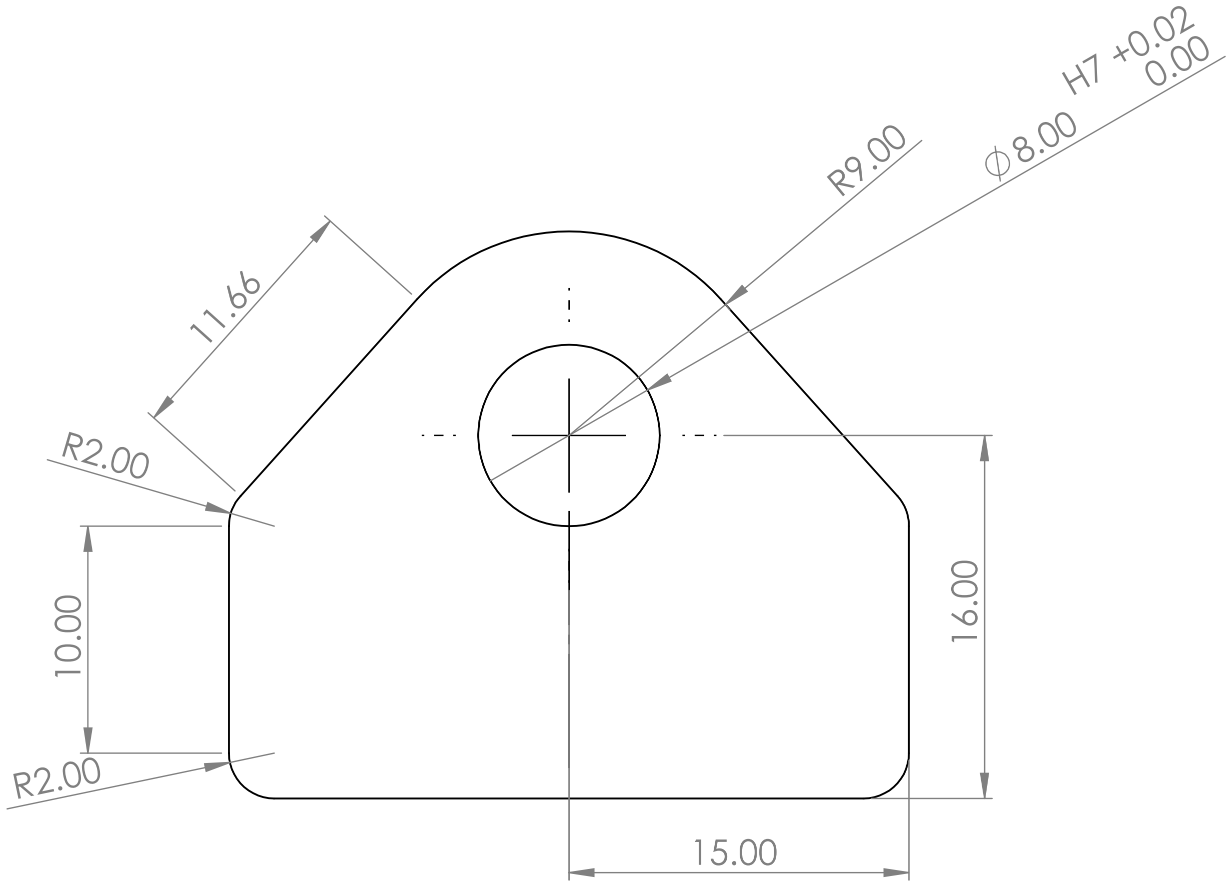

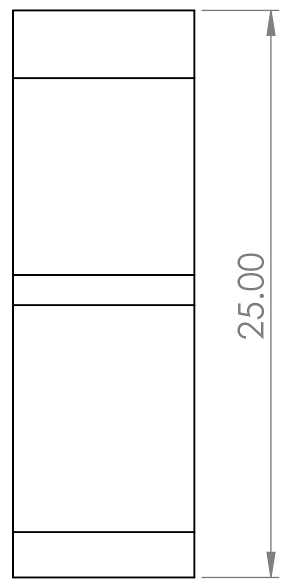

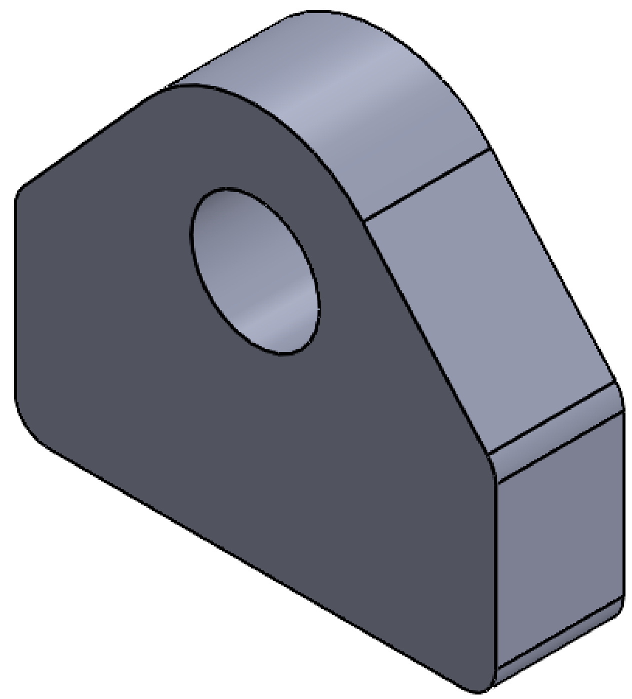

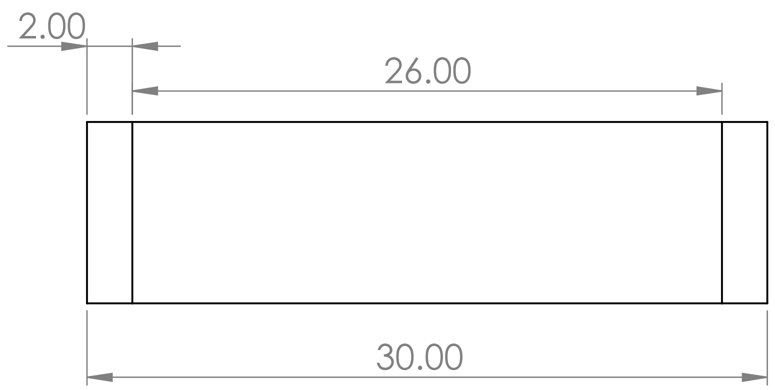

UNLESS OTHERWISE SPECIFIED: DIMENSIONS ARE IN MILLIMETERS SURFACE FINISH: TOLERANCES: ±0.1 LINEAR: ANGULAR:	FINISH:	DEBURR AND BREAK SHARP EDGES	DO NOT SCALE DRAWING	REVISION
			Quantity: 24	

	NAME	SIGNATURE	DATE	
DRAWN				
CHK'D				
APPV'D				
MFG				
Q.A				

TITLE: LEV-HEMS-WHEEL STAND

MATERIAL: EN3B Mild Steel

DWG NO.

A3

WEIGHT:

SCALE:2:1

SHEET 1 OF 1